Genetic and Epigenetic Mechanisms Controlling Flower Color and Pattern Diversity in *Dahlia*

Sho OHNO

2016

Contents

Introduction 1

Chapter 1.

Analysis of the key factors for flower color patterning in *Dahlia*

1.1 A basic helix-loop-helix transcription factor *DvIVS* regulates anthocyanin synthesis in *Dahlia* 3

1.2 A basic helix-loop-helix transcription factor *DvIVS* determines flower color intensity in cyanic *Dahlia* cultivars 37

1.3 Simultaneous post-transcriptional gene silencing of multiple chalcone synthase genes resulting in pure white area formation in bicolor flowering *Dahlia* 66

Chapter 2.

Analysis of petal color lability in a bicolor flowering *Dahlia* 93

Abstract 125

Acknowledgements 129

References 130

Introduction

Dahlias (*Dahlia variabilis*) are popular Asteraceae ornamental plants cultivated in many countries due to huge variation in flower shapes, sizes and colors. This wide variation is based onto complicated genetic background, namely dahlia is believed to be an autoallooctaploid with chromosome number 2n = 8x = 64 (Lawrence, 1929; Lawrence, 1931a; Lawrence and Scott-Honcrieff, 1935; Gatt et al., 1998) having a large genome size (2C value = 8.27–9.62 pg; Temsch et al., 2008), and more than 50,000 cultivars have been bred during the last century (McClaren, 2009). In addition to propagation from tuberous roots, dahlias are easily propagated vegetatively; cuttings are typically used for winter cut flower production (Konishi and Inaba, 1964; Naka et al., 2007).

Especially striking are the flower color variations. Dahlias exhibit a wide range of petal colors, such as ivory, yellow, pink, red, purple and black. In addition to huge color variation, there are flower color patterns such as variegation and bicolor. Pigments contributing to wide range of flower color in dahlia are flavonoids, mainly anthocyanin, butein, and flavone derivatives (Price, 1939; Bate-Smith and Swain, 1953; Nordström and Swain, 1953; Bate-Smith et al., 1955; Nordström and Swain, 1956; Nordström and Swain, 1958; Harborne et al., 1990; Yamaguchi et al., 1999). It was identified that the pigments in dahlia petals of some cultivars are pelargonidin 3-(6”-malonylglucoside-5-glucoside), cyanidin 3-(6”-malonylglucoside)-5-glucoside, butein 4′-malonylsophoroside, butein 4′-malonylglucoside, apigenin 4′, 7-glucoside and luteolin 7-diglucoside (Takeda et al., 1986; Harborne et al., 1990; Nordström and Swain, 1953). There are a few studies for molecular analysis of flavonoid biosynthesis in dahlia (Fischer et al., 1988; Wimmer et al., 1998; Yamaguchi et al., 1999; Ogata et al., 2001; Suzuki et al., 2002; Schlangen et al., 2009; Schlangen et al., 2010a), but flavonoid biosynthetic genes have been largely unknown, and it remained only to propose four elements explaining the inheritance of petal colors in dahlia: A (pale anthocyanin), B (deep anthocyanin), I (flavone), and Y (yellow) (Lawrence, 1931b; Lawrence and Scott-Honcrieff, 1935; Bate-Smith et al.,

1955; Broertjes and Ballego, 1967; Singh et al., 1970).

Polyploids are very common among plants. Polyploidy can be evolutionally advantageous in three points including heterosis, asexual reproduction and gene redundancy (Comai, 2005). In polyploids, complicated combination of alleles and/or loci can make for enormously huge variations in phenotype. However, at the same time, it might be difficult that single loss of function mutation in biosynthetic pathway genes exhibit a phenotypic change, because of gene redundancy. Many horticultural plants are also polyploids, therefore, how they diverse and regulate phenotypic characteristics is fascinating from the horticultural aspect.

In this study, I investigated the mechanisms controlling flower color and pattern diversity in dahlia. Using transposon tagging to two lateral mutants from a variegated cultivar 'Michael J', I revealed that a basic helix-loop-helix (bHLH) transcription factor *DvIVS* regulates anthocyanin synthesis in dahlia (Chapter1, 1.1). Moreover, I identified that *DvIVS* regulates flower color intensity in dahlia (Chapter1, 1.2). Further, I demonstrated that post-transcriptional gene silencing (PTGS) of two different chalcone synthase (CHS) genes is involved in bicolor pattering in bicolor flowering cultivars (Chapter1, 1.3). I also revealed that petal color lability in bicolor flowering dahlia is associated with PTGS of *CHS* in leaves, and proposed a model for phenotypic lability of bicolor cultivars (Chapter 2). Understanding the roles of genetic and epigenetic mechanisms controlling flower color and pattern diversity in dahlias provides information about not only the future breeding of dahlias, but also the regulation scheme of redundant genes in polyploid species.

Chapter 1

Analysis of the key factor for anthocyanin synthesis in *Dahlia*

1.1 A basic helix-loop-helix transcription factor *DvIVS* regulates anthocyanin synthesis in *Dahlia*

Introduction

The flavonoid biosynthetic pathway is the most well-studied secondary metabolite synthesis pathway in plants. In particular, anthocyanins are found in the flowers of many species and have many functions, such as recruiting pollinators and scavenging active oxygen species (Yamasaki et al., 1996; Winkel-Shirley, 2001). Anthocyanidin, aglycone of anthocyanin, is formed in the anthocyanin biosynthetic pathway by the condensation of three molecules of malonyl-CoA with one molecule of 4-coumaroyl-CoA; the enzymes involved in this pathway are as follows: CHS, chalcone isomerase (CHI), flavanone 3-hydroxylase (F3H), dihydroflavonol 4-reductase (DFR), and anthocyanidin synthase (ANS). In the anthocyanidin synthetic pathway, cyanidin is synthesized when flavonoid 3'-hydroxylase (F3'H) is active, delphinidin is synthesized when flavonoid 3' 5'-hydroxylase (F3'5'H) is active, and pelargonidin is synthesized when both F3'H and F3'5'H are inactive. The synthesized anthocyanidins are glycosylated by glucosyltransferase (3GT, 5GT) and modified through processes such as acylation (Grotewold, 2006). In dahlia, the malonyl group(s) is linked to the 3-glucosyl moiety of anthocyanins by anthocyanidin 3-*O*-glucoside-6"-*O*-malonyltransferase (Suzuki et al., 2002). Finally, they are transported to vacuoles by glutathione S-transferase (GST) and multidrug and toxic compound extrusion (MATE) transporter family proteins (Tanaka et al., 2008: Fig. 1-1). Flavones are synthesized by flavone synthase, and butein is

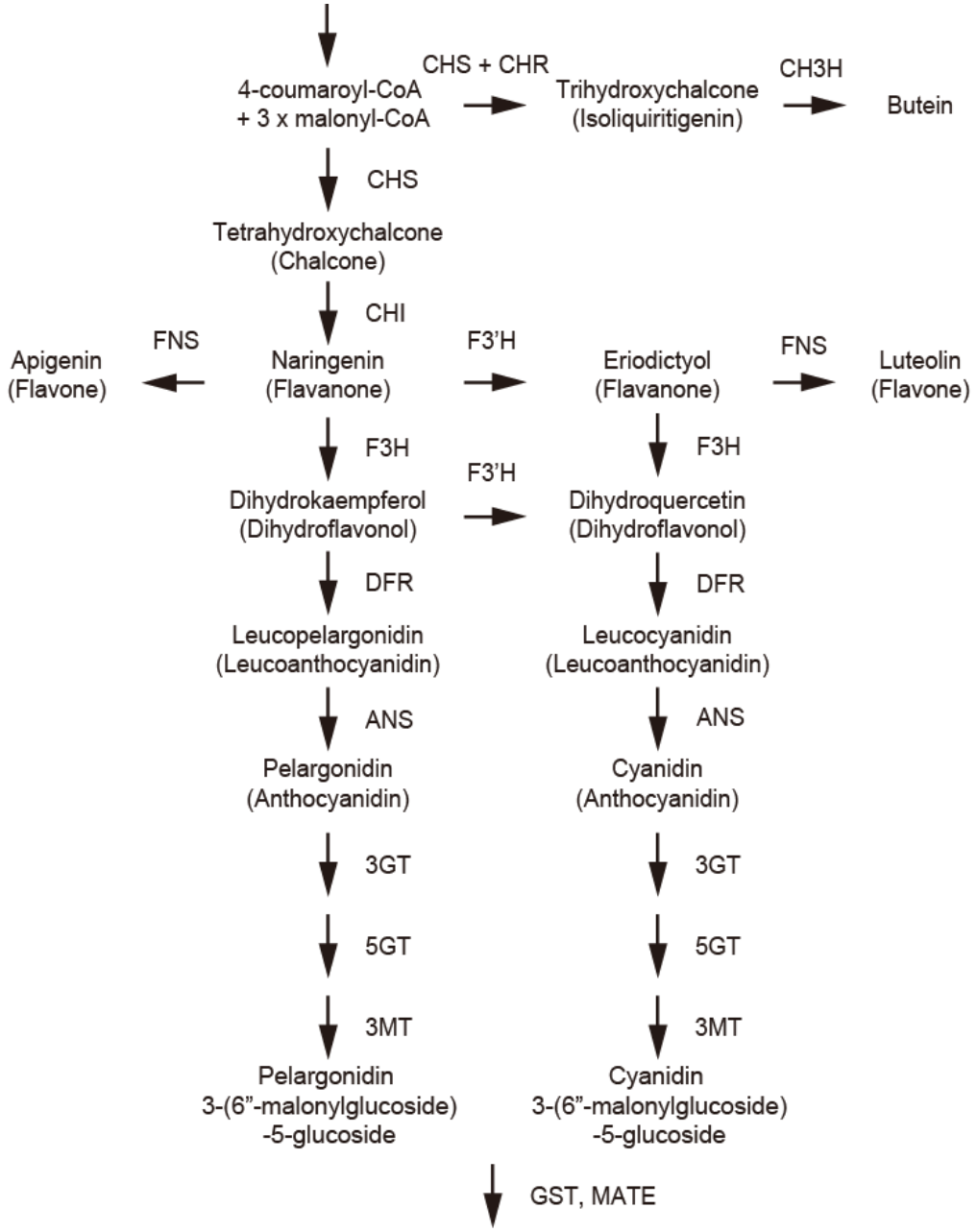

Fig. 1-1. Simplified flavonoid synthesis pathways. Only compounds detected in 'Michael J' are shown. Abbreviations: ANS, anthocyanidin synthase; CH3H, chalcone 3-hydroxylase; CHI, chalcone isomerase; CHR, chalcone reductase; CHS, chalcone synthase; DFR, dihydroflavonol 4-reductase; F3H, flavanone 3-hydroxylase; F3′H, flavonoid 3′-hydroxylase; FNS, flavone synthase; GST, glutathione S-transferase; GT, glucosyltransferase; MATE, multidrug and toxic compound extrusion; MT, malonyl transferase.

synthesized by chalcone reductase concerted with CHS and chalcone 3-hydroxylase (Martens and Mithöfer, 2005; Bomati et al., 2005; Schlangen et al., 2010b). The genes encoding the abovementioned enzymes involved in the anthocyanin synthesis pathway are regulated by transcription factors such as bHLH, R2R3-MYB, and WD40 repeats (WDR); these three proteins function as transcription factors by forming complexes or acting alone (Koes et al., 2005; Gonzalez et al., 2008; Hichri et al., 2011).

To isolate the genes that impart color to flowers, mutants formed by transposable elements have been widely used. This method of gene isolation, called transposon tagging, was used to isolate *pallida* (*DFR*) in *Antirrhinum majus* (Martin et al., 1985), *bronze* (*UDP-glucose flavonoid 3-O-glucosyltransferase*) in *Zea mays* (Fedoroff et al., 1984) and *ph6* (*An1*) in *Petunia hybrida* (Chuck et al., 1993). This method is very useful because it is applicable to high polyploidy plants such as dahlia.

In this chapter, the regulation factor of anthocyanin synthesis in dahlia was clarified. Two lateral mutants spontaneously occurred in 'Michael J' (Fig. 1-2A), which has yellow petals with orange variegation were used as materials. One mutant is MJOr (Fig. 1-2B), a bud mutant producing orange petals accumulating anthocyanins, flavones, and butein. The other is MJY (Fig. 1-2C), a bud mutant producing yellow petals accumulating flavones and butein. In this section, anthocyanin synthesis pathway genes and transcription factors were isolated, and showed that DvIVS, belonging to the An1 subgroup of bHLH transcription factor family, regulates anthocyanin synthesis in petals of dahlia.

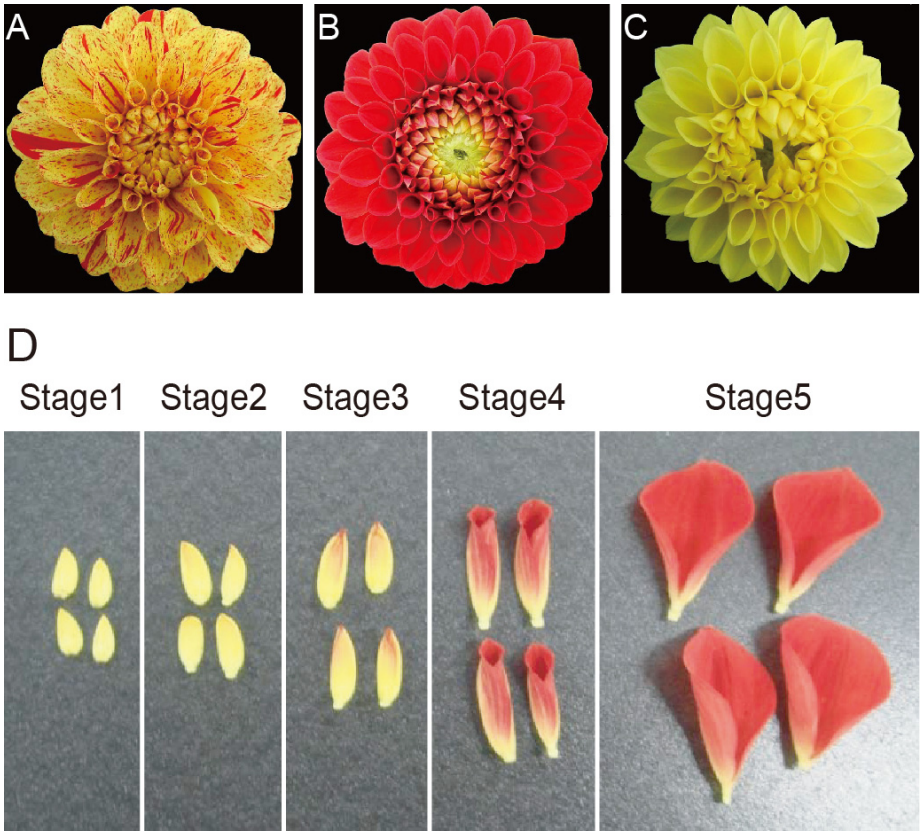

Fig. 1-2. Inflorescence phenotypes of 'Michael J' (MJW) and its bud mutants; A, MJW; B, MJOr and C, MJY. A, MJW petals are bright yellow with a small number of brilliant orange markings; B, MJOr petals are brilliant orange; this color is mainly derived from anthocyanins and butein; C, MJY petals are bright yellow; this color is mainly derived from butein; D, Developmental stages of MJOr petals. Developmental stages were defined on the basis of the degree of coloration.

Materials and methods

Plant materials and developmental stages

D. variabilis 'Michael J' (MJW) was obtained from a grower, Yukihiro Fukuda (Haibara, Nara, Japan). MJW has bright yellow petals with a small number of brilliant orange markings (Fig. 1-2A). It rarely produces completely orange (Fig. 1-2B) or completely yellow (Fig. 1-2C) petals as a bud mutation. A completely orange mutant line (MJOr) and a completely yellow petal mutant line (MJY) were isolated and obtained from personal connection. The two lines and wild-type plants were grown under standard greenhouse conditions or in the experimental field of Kyoto University (Kyoto, Japan). To analyze temporal gene expression, MJOr petals were classified into 5 stages on the basis of the degree of coloration (Fig. 1-2D): stage 1: an uncolored petal; stage 2: the tip of a petal is colored; stage 3: a petal colored in the center; stage 4: coloring is completed and petal starts to unfold; and stage 5: a completely unfolded petal. The size and stage of MJY petals used were almost same.

HPLC analysis

Petals were soaked overnight in 5 mL of MAW solution (methanol: acetic acid: water, 4:1:5 v/v) to extract the pigments. For pigment hydrolysis, extracted solutions were evaporated, redissolved in 2 mL of 20% hydrochloric acid, boiled, and used as crude aglycones. HPLC analysis was performed using an LC10A system (Shimadzu, Kyoto, Japan) with a C18 column (Nihon Waters K.K., Tokyo, Japan) maintained at 40°C and a photodiode array detector. The detection wavelength was 350 nm for flavones, 380 nm for chalcones, and 530 nm for anthocyanins. Eluent A was 1.5% phosphate dissolved in water and eluent B was 1.5% phosphate, 20% acetic acid, and 25% MeCN dissolved in water. Analysis was performed at a flow rate of 1 mL min^{-1} and column temperature of 40°C, using a mobile phase gradient starting at 20% B to 85% B over 40 min with 5 min re-equilibration at 20% B. As standards for the determination of flavonoids, commercially

available naringenin, apigenin, and luteolin (Wako Pure Chemical Industries, Osaka, Japan) as well as HPLC-separated and HPLC-purified hydrolyzed cyanidin and pelargonidin from rose petals were used. To obtain hydrolyzed standards of butein and isoliquiritigenin, extracts from orange petals of a seedling line, HywR7R, were separated by paper chromatography, and each band was eluted with methanol. Each elute was dried and redissolved in a small amount of methanol. The color, Rf value, and maximum wavelength of eluted compounds were measured, and the compounds were determined by comparing the data with those of authentic butein (kindly supplied by Dr. Norio Saito) and previously reported data (Nordström and Swain, 1956; Saito et al., 1970).

Isolation of nucleic acids and sequencing

To clone the *DvIVS* genomic region and *Tdv1* region, genomic DNA of petals was isolated using a modified cetyltrimethylammonium bromide method (Murray and Thompson, 1980) and purified with MagExtractor™-Plant Genome- (Toyobo, Osaka, Japan). Genomic DNA was also isolated using Qiagen Genomic-tip 100/G (Qiagen, Valencia, CA, USA) for genomic PCR analyses. Total RNA was isolated using the isothiocyanate/cesium chloride centrifugation method and RNeasy Plant Mini Kit (Qiagen), modified QuickGene RNA Cultured Cell Kit S (Fujifilm, Tokyo, Japan), or Get pure RNA Kit (Dojindo, Kumamoto, Japan). All sequence analyses were performed using a BigDye ® Terminator v 3.1 Cycle Sequencing Kit and a 3100 Genetic Analyzer (Applied Biosystems, Foster city, CA, USA).

Gene isolation

DvCHS1, *DvCHI*, *DvF3H*, *DvDFR*, *DvANS*, *DvFNS*, *DvIVS*, *DvDEL* and *DvActin* cDNAs were isolated using degenerate primers designed from conserved regions of each gene shown in Table 1-1. To isolate *Dv3GT*, *DvMYB1*, *DvMYB2*, *DvWDR1* and *DvWDR2* cDNAs, dahlia cDNA libraries (Suzuki et al*.,* 2002) provided by Yoshikazu Tanaka (Suntory, Osaka, Japan) were screened. *A. majus* Chalcone 4'-*O*-

Table 1-1. Degenerate primers used for isolating the cDNA fragment

Genes	Forward primer	Reverse primer	Used sequences for designing primers
DvCHS1	GTGTGCTCCGAGATYACKGC	ACGTCTTTGAGDAGATGAAA	DQ521272 (*Chrysanthemum* x *morifolium*) Z67988 (*Callistephus chinensis*) Z38096 (*Gerbera hybrida*)
DvCHI	TKICCIGTIARIGGIARDAT	AARTTYACIGBIATHGGIGT	EF094933 (*Chrysanthemum* x *morifolium*) Z67980 (*Callistephus chinensis*) AF509335 (*Saussurea medusa*) AB080768 (*Ipomoea batatas*) AB234907 (*Verbena* x *hybrida*) prf:1807331B (*Petunia* x *hybrida*) AB213651 (*Nicotiana tabacum*) DQ120521 (*Camellia sinensis*)
DvF3H	CATCGTTTCTAGCCATCTTC	TTCASCACTACYTTTTGGTC	U86837 (*Chrysanthemum* x *morifolium*) X72593 (*Callistephus chinensis*)
DvDFR	GACACAAGAAGGAAGCTTTG	GATRAAYGGACCAACTACYA	Z67981 (*Callistephus chinensis*) Z17221 (*Gerbera hybrida*)
DvANS	TACCCAAAATGCCCTCAACC	CAACTTGTGTTCCATATG	AF015885 (*Callistephus chinensis*) AY997840 (*Gerbera hybrida* cultivar Tacora) AY997841 (*Gerbera hybrida* cultivar Ansofie) AY997842 (*Gerbera hybrida* cultivar Fame) AY547342 (*Saussurea medusa*)
DvFNS	YCACATYAARGCMYTGRTTTTGGA	TDGACCAAATRTTBACRAAYAACA	AF188612 (*Callistephus chinensis*) AF156976 (*Gerbera hybrida*) EU561012 (*Hieracium pilosella*) AB221081 (*Lobelia erinus*) XM_002319530 (*Populus trichocarpa*)
DvDEL	GGTACTAYAATGGMGAYATHAARA	AATACGGAAARCAYACWACWGTCT	M84913 (*Antirrhinum majus*) AF020545(*Petunia x hybrida*) AB024050(*Perilla frutescens*) AB232774(*Ipomoea nil*) AJ007709(*Gerbera hybrid* cv. 'Terra Regina')
DvIVS	ATGGRTAYTAYAACGGYGCRATAAA	ATCACTCTCKATRATIGAHACYTCYA	AB154369(*Ipomoea purpurea*) AB154370(*Ipomoea tricolor*) AB103172(*Perilla frutescens*) AJ277509(*Arabidopsis thaliana*) AF260919(*Petunia x hybrida*)
DvActin	GCCAAYAGAGARAAGATGAC	ACCAGARTCCARCACAATAC	AY064043 (*Arabidopsis thaliana*) AB047313 (*Oryza sativa*) AY372368 (*Trifolium pratense*) AY305724 (*Gossypium hirsutum*) AF548026 (*Stevia rebaudiana*)

glucosyltransferase (AB198665), *Ipomoea nil* MYB (AB232770) and WDR (AB232779) cDNAs were used as probes and AlkPhos Direct (GE Healthcare, Piscataway, NJ, USA) was used for probe hybridization. Partial sequence of *DvCHS2*, *DvGST* and *DvR3MYB* were fortunately obtained while performing RACE of other genes. Partial sequence of *DvCHS3* was obtained from database (JN556044) and partial sequence of *DvCHS4* was obtained from RNA-seq data (Ohno et al., unpublished data). To determine the complete sequence of mRNA of all genes, 3' rapid amplified cDNA ends (RACE) and 5' RACE was performed using a GeneRacer^{TM} Kit (Invitrogen, Carlsbad, CA, USA). Primers used are shown in Table 1-2. Each end of the genes was sequenced for at least 16 clones for each gene to avoid single nucleotide polymorphisms (SNPs) because of dahlia's high polyploidy. For 5' and 3' RACE of the transcription factor genes, total RNA from *D. variabilis* 'Matsuribayashi' was used.

RT-PCR and real-time RT-PCR

The total RNA of MJOr and MJY was subjected for reverse transcription using an oligo-$(dT)_{20}$ primer and ReverTra Ace (Toyobo). The obtained cDNA products served as templates for PCR performed using Blend Taq polymerase (Toyobo). *DvActin* was used as an internal standard. The primers used are shown in Table 1-3. Primers for *Dv3MT* and *DvF3'H* were designed according to AF489108 (Suzuki et al., 2002) and GQ281058 (Schlangen et al., 2010a), respectively. The PCR program was set at 94°C for 2 min, followed by 30–35 cycles of 94°C for 30 s, 55°C for 30 s, and 72°C for 2–3 min.

Total RNA extracted from stage 1–5 petals was used. Real-time RT-PCR was performed using SYBR® Premix Ex Taq ^{TM} II (Takara, Ohtsu, Japan) according to the manufacturer's instructions. Real-Time PCR was performed using a 7900HT Fast Real-Time PCR System (Applied Biosystems). The primers used are shown in Table 1-4. The PCR program was set at 50°C for 1 s, 95°C for 30 s, followed by 40 cycles of 95°C for 5 s, 60°C for 15 s, 72°C for 20 s, and the subsequent dissociation steps. Three different infloresences were used as replicates for each stage, and *DvActin* was used as an internal

standard. Because of the low transcription level, samples that did not reach the threshold were calculated as 40 cycles.

To test partial expression of *DvIVS*, three primer sets were used for RT-PCR: IVS-Full-F and IVS-Full-R, 35S-IVS-F and IVS-611R, and IVS-725F and IVS-Full-R (Table 1-5). The first primer set amplifies from the start to stop codon. The second primer set amplifies from 30 bp after the start codon to the third exon, and the third primer set amplifies from the fifth exon to the stop codon.

Table 1-2. Primers used for RACE

Genes		First PCR primers	Nested PCR primers
DvCHS1	5′RACE	CGCGCCTCCACTATCCGGTAGAATA	
	3′RACE	GGTGACGGTGCAGCCGCGATCAT	
DvCHS2	5′RACE	GGCGGGGTTGCAGTGCCGATGGCAA	
	3′RACE	TGGCTCCGTCTTTGGACGCCCGTCA	GCTCGGTAAAGATGCGGCTGTCAAA
DvCHS3	5′RACE	GCACGCGCCTACTCGCCCTCAACTT	CAGCTCCACCTCGTCGAGTATGCGT
	3′RACE	CACGTTGATTCTTTGGTCGGCCAAG	GGTCTACGTGACTGGAATTCGATGT
DvCHS4	5′RACE	ACCGAAGGATTAAGATCCAGGAGTT	CAATATCTCTTCGGTTAAGTACATG
	3′RACE	TGGCTCGGTCCTTCGTTTGGCCAAA	TTTTGGGTTGCGCATCCGGGTGGCC
DvCHI	5′RACE	GGGACCAGTAACGATGTCCCTAAA	TGGGTCAACTCGTGGGCGGTTTT
	3′RACE	GGCAAAACCGCCCACGAGTTGAC	GGACATCGTTACTGGTCCCTTTGA
DvF3H	5′RACE	AGGGCCTCTTTTTCAAGGCCCATT	AGAGCTTGCAGGCCAGGCCCATTAA
	3′RACE	TGGGCGGTTCAAGAACGCGGATCA	ACGCGGATCACCAAGCCGTGGTCAA
DvDFR	5′RACE	GTGACTCGTCATAGACCGGAAGTT	
	3′RACE	ACTTCCTCTGCCGGAACGGTAAA	
DvANS	5′RACE	CCTTAGAAACCGTCTCCGGGAGCGGTT	CCGGGAGCGGTTTCAGGATGATCTT
	3′RACE	CCCAAAATGCCCTCAACCGGAGCTA	CCGGAGCTAGCACTCGGTGTTGAA
Dv3GT	5′RACE	CAGCAGTACATCCAAGTCGGGCTCT	CAAGTCGGGCTCTGGCGGCGGCAAA
	3′RACE	CGGAGATAGCGAAGGGGCTGGAGAA	CGAAGGGGCTGGAGAAGAGTGGGGT
DvGST	3′RACE	CCGATTAGGGCGGCTTGTCCACAAA	CCGCGTTAACTTAGACTCCGGAGAA
DvFNS	5′RACE	CTCACATTTTCATTTGACTTCCGTA	GGTGGATGAAGTCGGAAGGCTTCT
	3′RACE	GCTGGAACAGACACAACCGCAGTA	CCCTATGGTCATGGAAAAAGCAAA
DvMYB1	5′RACE	CAGATAGTGTGGGTGACGGGACTA	GGGTGACGGGACTAACCCTTGGGAAATAT
	3′RACE	GCGGGGAGAATACCAGGAAGAACT	TTCGACCCCGTCCCAAACCACAAAA
DvMYB2	5′RACE	TGGTGGTGGTGGCGGGGACGGTTGT	CCACTTGTTACCAAGAAGGCTATGGA
	3′RACE	CCGCCCTGACCTCAAATGTGGCAACT	GTGGCAACTTCTCCGAAGAAGAAGA
DvDEL	5′RACE	CCTTCTCTGGTACGCCGAACTCAA	GGTACGCCGAACTCAACTATACCTT
	3′RACE	CCACGAAGGCCTCTGGCTGCATTGT	CCTCTGGCTGCATTGTCCCCTGAAGAT
DvIVS	5′RACE	CCAAGGATCGACGCCTTGTCCATT	GTCACCAACGGCACCAACGTTCTAA
	3′RACE	TCCATCGCCTCTCGCCTCGGCAAAA	GCGCGAACCACGTCCTAGCGGAA
DvWDR1	5′RACE	AAGCCGACCACTGCACCTGGTTAAT	GGAGCCCAAGCAATCGCATTGACACT
	3′RACE	CCGTTAGGGTTTTCGACCTTCGCGATA	TCGACCTTCGCGATAAGGAACACT
DvWDR2	5′RACE	TGCGAATCATCCCCAGCCGTACAT	GCAATCGCGTTCACACTCGACTGAT
	3′RACE	GGATAGTGCGAAGGTTGTGGTGCTT	CGTTTCCCGACGTTACCTGTTGT
DvActin	3′RACE	TATGTTGCTATCCAGGCCGT	TCTCTTTATGCCAGTGGTCG

Table 1-3. Primers used for semi-quantitative RT-PCR

Genes	Forward primers	Reverse primers
DvCHS1	AATCCCGGTTTCAAGTGATTA	ATGCAATGTAAGTGACAACATA
DvCHS2	TCTTATTACTGCTCGCAATATCTT	AGTTAGGGCGAAATCGGCATGGTA
DvCHS3	ACACATTCTTCAATAGATCAAGTTA	CATTATTACATCAACCGTTACTTAT
DvCHS4	CACCACATACAAATTGTAACTTCAC	GTATGAAATTTCATATTATGTAATA
DvCHI	ATGGCTGGTCTKGAGGTCGAA	GGGCTGAGCTTATTTATTAC
DvF3H	CATCTTTGAAATGGGACGAGACTTC	GATTACTCAAAACACTTCATTATTT
DvDFR	ATCGGCTCCTGGTTAGTTAT	CCATTAATAATATGAACTTTATTAA
DvANS	TACCTTCCATCCATCATGGTCACTT	GTTCTTAGAATGACCCAAACAACAA
Dv3GT	AAGCAATAAGAAAAATGGCGACTA	AAGGCTACCACGATGCAACCAACT
Dv3MT	AAATACGAAGTTGTTTCAATC	TTGCACTTTCTAATCCATCAT
DvGST	GTCCATTTAACAAGAACTTGGAGCT	ATAAAACATTTATTTGTGAGTCACA
DvF3'H	TCGGCTTCGTTGACGTGGTG	TACGGTGCAAACACCAGATCC
DvFNS	TCTCATCTTACCATGAATACACT	GCGAAGGGAAACACACTAGATTCG
DvMYB1	CACAAACATTTTCAATAGAAAATTG	TAAGAAAGTTATACTCCGTTACATC
DvMYB2	ACAAAAAAGATATCAAAAAGAACAA	AAATCCAAATGAGAATTCATTTCAT
DvR3MYB	TTCTCAAGAATTGTATTGAGAAATT	GATTTGTTAAAAAGACTAATGATAA
DvDEL	ATCTCCTCCAATTCATCAAGATTTT	CCTTTTCTACAGATCAATCAAACAT
DvIVS	TTTGACGTAATTTTGGACCTAATTT	CATCCATTTTTAAATTGTTTGTGGT
DvWDR1	TTTCTACTTTTCCAATAATATCACA	AGATTCTGTAAAACTTAATATGACT
DvWDR2	GATACAGATTATCCCCAATTCCAAA	GTATTCCCAAACCTATATAGGCTAA
DvActin	TGCTTATGTTGGTGATGAAG	CCCTGTTAGCCTTAGGATTT

Table 1-4. Primers used for real-time RT-PCR

Genes	Forward primers	Reverse primers
DvCHS1	CATGTGCTAAGCGAATACGG	CCTCTCCGGTGGTATTGAAC
DvCHS2	TGTCCCAACTACCATGCCGATTTC	TTACACATTAAAATGACACAGTGA
DvIVS	GCATATGCAAAGCAGCAAGATCTAT	TGAAGAAAAGTTTCACATGTTGAAT
DvActin	TGCTTATGTTGGTGATGAAG	CCCTGTTAGCCTTAGGATTT

Table 1-5. Primers used for analyzing the *DvIVS* genomic region and *Tdv1* region

Genes		Primers
DvIVS	IVS-Full-F	TTTGACGTAATTTTGGACCTAATTT
	35S-IVS-F	ATGGCTGCCGCTGGTTCCGTAAACG
	IVS-474F	CGGTGAGCAACAGGTGGCGGAGAA
	IVS-611R	CCGACACCAGGAGGAAATGAGAAA
	IVS-625F	GCATATGCAAAGCAGCAAGATCTAT
	IVS-725F	CGGTGATATGCATCCCTGTACTAAA
	IVS-826R	TGAAGAAAAGTTTCACATGTTGAAT
	IVS-1082F	TGCCTCACAATAATAAAGATTCAAT
	IVS-1316F	CAGAAGAATTTGCACCGGAGTTTA
	IVS-1614R	GAGCTCTTCGTGCGACGTCGTTTT
	IVS-G1163F	TCCCAGCTCACGGTTCAGTTTTAAA
	IVS-G2241F	AAGTGCTGAGCCAGTAAGACTGTTT
	IVS-G2633F	TTGAATAAACAAGTTGATAGTAAT
	IVS-G2844F	GATTAGGGATCCTTTTCAACAACAT
	IVS-G2869R	AATGTTGTTGAAAAGGATCCCTAAT
	IVS-G3415F	ATATCTGATCGTAATTTAACAAATT
	IVS-GR3012R	CTTGGGTACATTTCATATGTAATTT
	IVS-GR3637R	GATTCACGTGTGACGTATTATTGTT
	IVS-GR4193R	AGTACTTTTATGACTTTTAGTGAAA
	IVS-Full-R	CATCCATTTTTAAATTGTTTGTGGT
Tdv1	IVS-TP1F	TAGCGGCGACAATTGTCGCCGCT
	IVS-TP2F	CGAAATATAAACAAACAAAGTTAAA
	IVS-TP3F	ATATTCAACTTTTAGTTTATTCAA
	IVS-TP4F	ACATATTAGCATTTTAAACTTGT
	IVS-TP1R	CACTACAAGAAATATAGTCAATA
	IVS-TP2R	GAGCATTTATACATTTGATAAAT
	IVS-TP3R	CATAAGTAAATGGTGGGCCTCATA
	IVS-TP4R	TGTCAAACATGTCAGTCAAACAT
	IVS-TP5R	CGTGTGCAAAATGTCAGAATACT
	IVS-TP6R	TAATGAGAGTCGGTGGGTCGATA
	IVS-TP7R	ACTCCTTCAATACGTGTAACAAA
	IVS-TP8R	AATGTTTGCATAATTAGGCATTT
	IVS-TP9R	CATTAACGTATTAGCGGCGACACTA

Cloning of the genomic DvIVS gene and the transposable element

Genomic PCR was performed with LA Taq (Takara) using 100 ng genomic DNA as a template in a 10 μl volume. The PCR program was set at 94°C for 1 min, followed by 35 cycles of 98°C for 10 s, 55°C for 10 s, and 68°C for 15 min. Amplified PCR products were electrophoresed with 1× TAE and 0.8% agarose gel and cloned into pCR®-XL-TOPO using a TOPO® XL PCR Cloning Kit (Invitrogen) according to the manufacturer's instructions. The *DvIVS* gene of MJOr was amplified using the primer set IVS-Full-F and IVS-Full-R (Table 1-5). The insertion sequence of MJY was amplified with the primers IVS-G2241F and IVS-G2869R (Table 1-5), which were designed on the basis of the upstream and downstream regions of the insertion sequence. Four plasmids with the *DvIVS* gene and six plasmids with inserted fragments were sequenced by primer walking using the primers shown in Table 1-5.

Sequence analysis of cDNAs and the genomic DvCHS1 gene

To examine regulation of redundant copies of each anthocyanin synthesis gene, sequence analyses for multiple copies of these genes were performed. Extracted total RNA of MJOr and MJY were subjected for reverse transcription with an oligo-$(dT)_{20}$ primer using ReverTra Ace (Toyobo). RT-PCR of *DvCHS1*, *DvCHI*, *DvF3H*, and *DvDFR* were performed using KOD Plus polymerase (Toyobo), and PCR products were cloned into pCR®-Blunt II-TOPO® using a Zero Blunt® TOPO® PCR Cloning Kit (Invitrogen). The PCR program was set at 94°C for 2 min, followed by 30 cycles of 94°C for 50 s, 55°C for 30 s, and 68°C for 2 min. A total of 40 cloned plasmids of both lines' with *DvCHS1*, *DvCHI*, *DvF3H*, and *DvDFR* were extracted, except for MJY *DvCHS1* (only 20 plasmids were extracted). To determine the accurate sequence, plasmids with *DvCHS1*, *DvF3H*, and *DvDFR* of both lines were sequenced twice both from the 3′ and 5′ ends. The primers used are shown in Table 1-6. To exclude misreading of sequences or misamplification in PCR, SNPs that were only observed in one clone were omitted.

To analyze the sequence of genomic region of *DvCHS1* in MJOr, MJY, and MJW,

genomic PCR was performed using the primer set shown in Table 1-3. A total of 30 clones of the *DvCHS1* gene were sequenced for each line.

GenBank accession numbers

Sequence data of these genes have been deposited at DDBJ/GenBank data libraries under accession numbers AB576129, AB576130, AB576131, AB576132 (*DvCHS1*), AB576133 (*DvCHS2*), AB591827 (*DvCHI*), AB591828 (*DvF3H*), AB591829 (*DvDFR*), AB591830 (*DvANS*), AB769840 (*DvGST*), AB769842 (*DvFNS*), AB601003 (*DvMYB1*), AB601004 (*DvMYB2*), AB621921 (*DvR3MYB*), AB601005 (*DvIVS*), AB601006 (*DvDEL*), AB601007 (*DvWDR1*), AB601008 (*DvWDR2*), AB601010 (*DvIVS* genomic region), AB601009 (*Tdv1*) , and *DvActin* (AB621922).

Table 1-6. Primers used for confirming the sequence

Genes	5' direction primers	3' direction primers
DvCHS1	TGTTGTTCTCGGCCAAGTCT	GTCGGGCTAACGTTTCATCT
DvF3H	GTGAATTATTACCCAAAGTGTCCAC	TTGGTCCATATCAACACAAGCTTTT
DvDFR	TCCAATGTGACTCGTCATAGA	TGGGATCGATGAGGATTTATC

Results

Pigment analysis

Wild type ‘Michael J’ (MJW) produces yellow petals with orange variegation, while MJOr and MJY produce completely orange and completely yellow petals, respectively, without any variegation. To clarify the difference in pigment accumulation between MJOr and MJY, aglycons were extracted from petals and analyzed them by HPLC. In both lines, peaks of chalcones (butein and isoliquiritigenin) and flavones (apigenin and luteolin) were detected (Table 1-7). In addition to these, peaks of anthocyanidins (pelargonidin and cyanidin) were detected in MJOr but not in MJY (Table 1-7). These data showed that chalcones and flavones are synthesized in both lines, while anthocyanidins are synthesized only in MJOr.

Temporal expression of anthocyanin synthesis pathway genes

Twelve flavonoid biosynthetic genes (*DvCHS1*, *DvCHS2*, *DvCHS3*, *DvCHS4*, *DvCHI*, *DvF3H*, *DvDFR*, *DvANS*, *Dv3GT*, *DvGST* and *DvFNS*) were isolated from dahlia. Expression levels of these genes and *DvF3’H* and *Dv3MT* between MJOr and MJY were compared by RT-PCR. Six genes, namely *DvCHS1*, *DvF3H*, *DvDFR*, *DvANS*, *Dv3MT* and *DvGST* were down regulated in MJY (Fig. 1-3). To examine the temporal expression pattern of some of anthocyanin synthetic genes during petal development, MJOr petals were divided into five developmental stages based on the degree of coloration and performed RT-PCR. Although expression levels of *DvCHS2* and *DvCHI* showed no difference, expression levels of *DvCHS1*, *DvF3H*, *DvDFR*, and *DvANS* were lower in MJY than in MJOr at all developmental stages (Fig. 1-4). Downregulation of multiple genes encoding the anthocyanin synthesis pathway enzymes suggested that transcription factor(s) do not function in MJY.

Seven transcription factors (*DvMYB1*, *DvMYB2*, *DvR3MYB*, *DvDEL*, *DvIVS*, *DvWDR1* and *DvWDR2*) were isolated from dahlia and expression levels were compared.

Table 1-7. Aglycons in the petals of MJOr and MJY.

Line	Anthocyanidin		Flavone		Chalcone	
	Pelargonidin	Cyanidin	Apigenin	Luteolin	Butein	Isoliquiritigenin
Orange	+	+	+	+	+	+
Yellow	−	−	+	+	+	+

+ : Abundant, − : Not detected

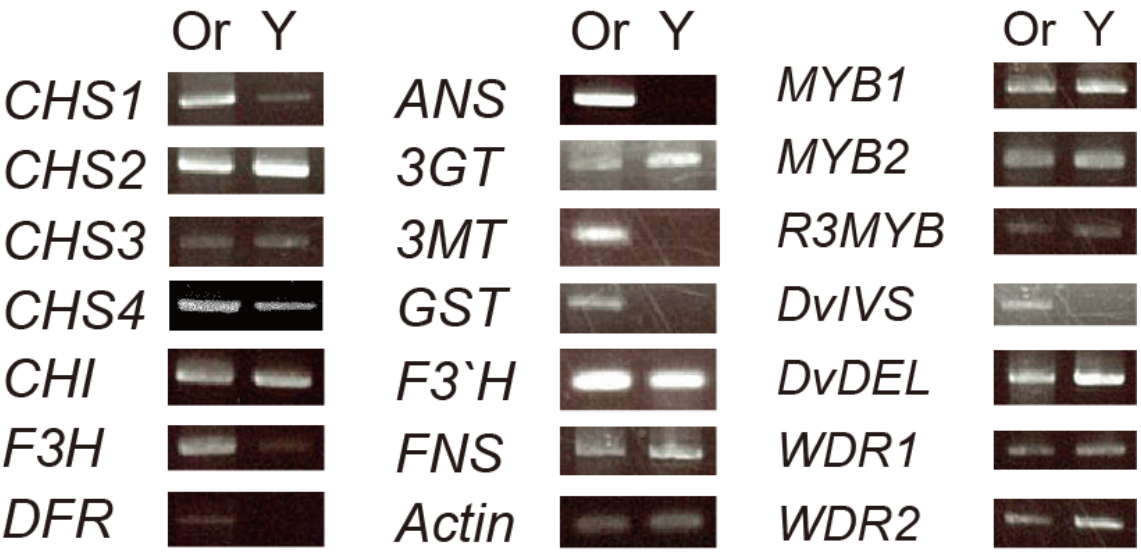

Fig. 1-3. RT-PCR analysis of flavonoid biosynthetic genes and transcription factors. Or indicates MJOr and Y indicates MJY, respectively.

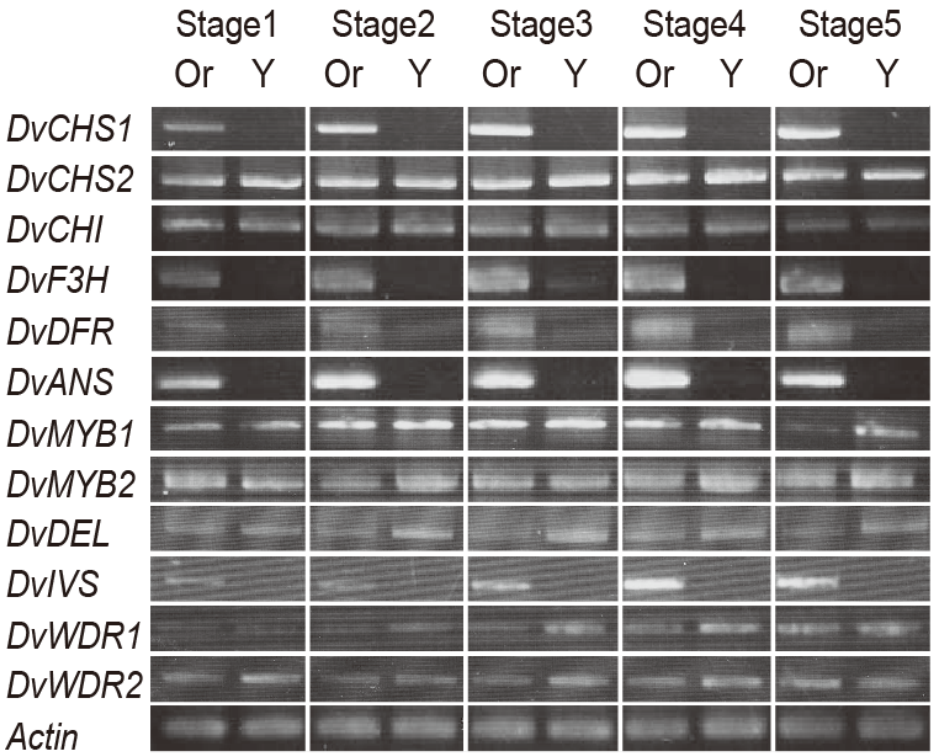

Fig. 1-4. Semi-quantitative RT-PCR analysis of temporal expression of anthocyanin synthesis genes and transcription factors in MJOr and MJY. The constitutively expressed gene for actin in *Dahlia variabilis* was used as an internal control.

Only a bHLH transcription factor *DvIVS* was down regulated (Fig. 1-3). Temporal expression analysis by RT-PCR also showed expression levels of *DvMYB1*, *DvMYB2*, *DvDEL*, *DvWDR1*, and *DvWDR2* did not differ significantly, but the expression level of *DvIVS* was lower in MJY than in MJOr, which is similar to that of *DvCHS1*, *DvF3H*, *DvDFR*, and *DvANS* (Fig. 1-4). This result suggested that *DvIVS* has a role as a transcription factor that activates anthocyanin biosynthesis genes including *DvCHS1*, *DvF3H*, *DvDFR*, *DvANS*, *Dv3MT* and *DvGST*.

To confirm these results, real-time RT-PCR of *DvCHS1* and *DvCHS2*, which seem to be regulated and unregulated by *DvIVS*, respectively, was performed using total RNA extracted from stage 1–5 petals. In MJOr, the relative expression level of *DvIVS* and *DvCHS1* compared to that of *DvActin* increased until stage 3 or 4 and then decreased, but consistently very low expression levels were maintained in MJY (Fig. 1-5). In contrast, expression levels of *DvCHS2* were slightly lower in MJY, but the expression pattern of *DvCHS2* in MJOr and MJY was the same (Fig. 1-5). This result supported the results of RT-PCR analyses and suggested that *DvCHS1*, but not *DvCHS2*, is regulated by DvIVS.

Characterization of DvIVS

The full-length *DvIVS* cDNA was 2483 bp containing a 649-amino acid open reading frame (ORF). The *DvIVS* ORF retained the bHLH domain at 472–530 amino acids (Fig. 1-6A). BLASTP search (http://blast.ncbi.nlm.nih.gov/Blast.cgi) revealed that the deduced amino acid sequence was 48% identical to InIVS (*Ipomoea nil*), 50% identical to An1 (*P. hybrida*), and 48% identical to AtTT8 (*Arabidopsis thaliana*). To compare genetic distance among the bHLH proteins associated with anthocyanin synthesis in higher plants, a phylogenetic tree was constructed. The phylogenetic tree showed that *DvIVS* belonged to the *An1* subgroup (Fig. 1-6B).

Analysis of the DvIVS genomic region

The *DvIVS* genomic region coding for full length mRNA (AB601010) of MJOr

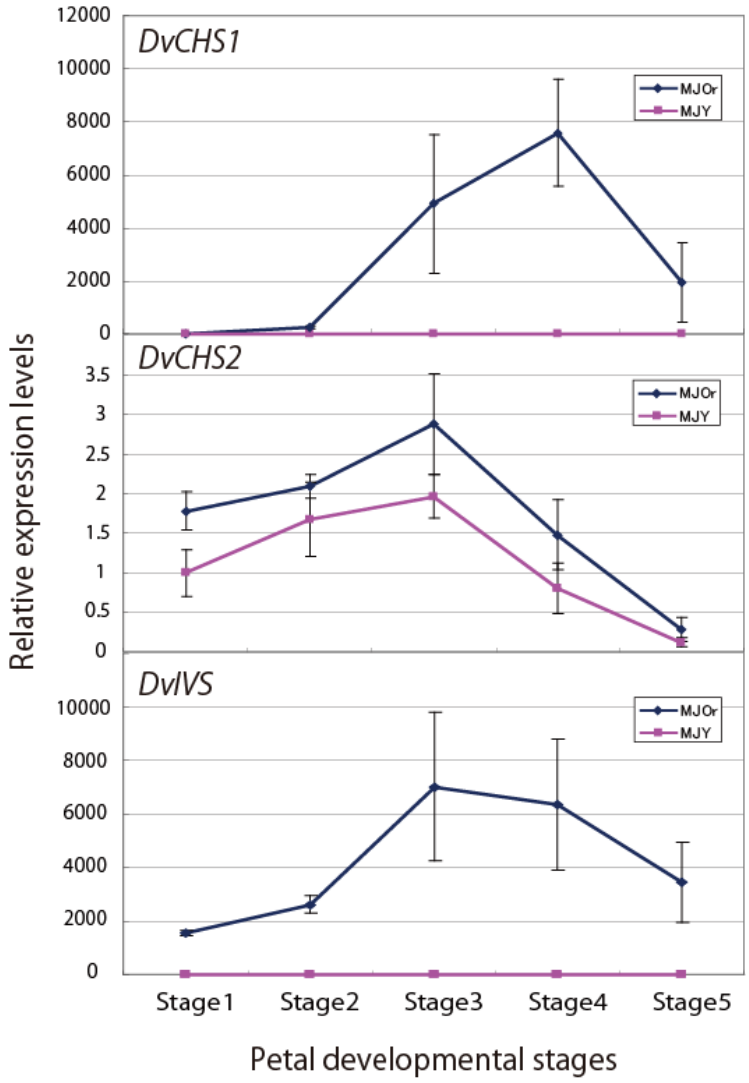

Fig. 1-5. Temporal relative expression levels of *DvCHS1*, *DvCHS2*, and *DvIVS* in MJOr compared to those in MJY at each petal developmental stage. The vertical bars indicate the ±SE (n = 3). The constitutively expressed gene for actin in *D. variabilis* was used as an internal control.

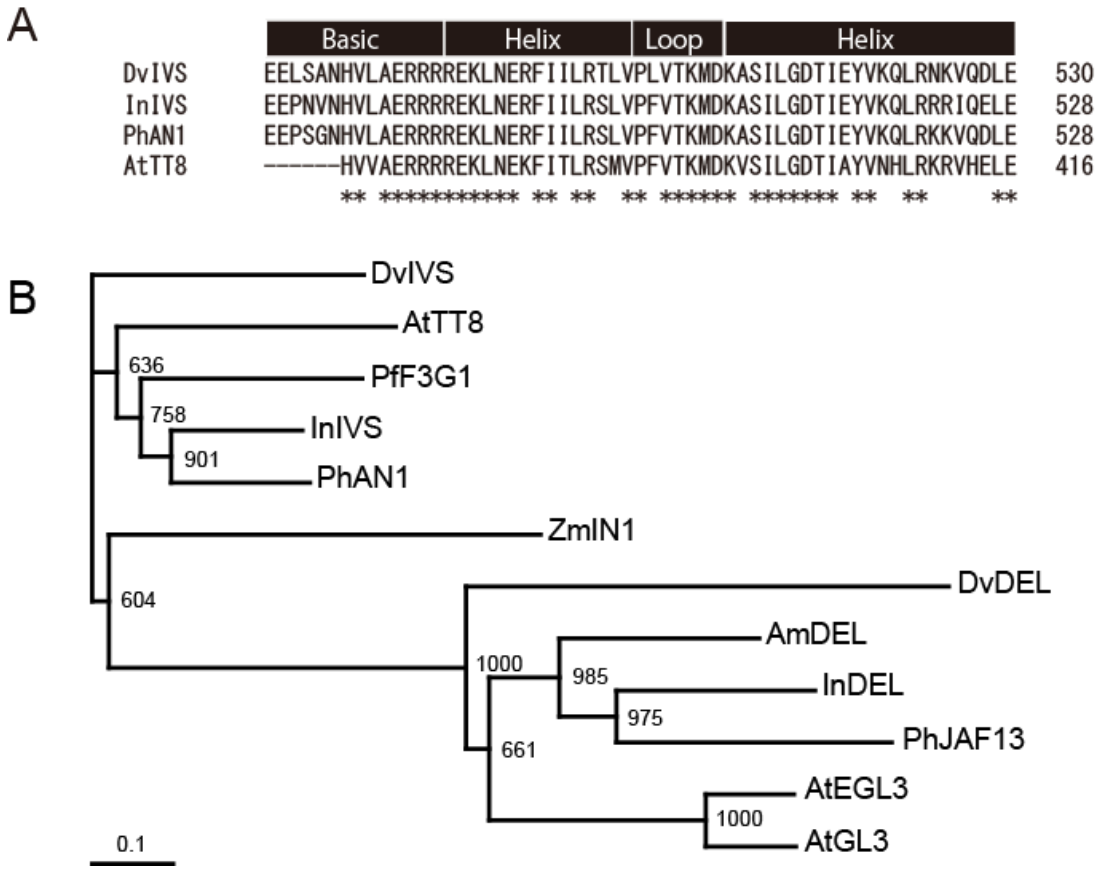

Fig. 1-6. Phylogenetic analysis of DvIVS. A, amino acid comparison of the bHLH domain of *DvIVS*, *InIVS*, *PhAN1*, and *AtTT8*. Numbers (*) indicate amino acids that are fully conserved in each of the proteins. B, phylogenetic tree for bHLH transcription factors associated with anthocyanin synthesis pathways. The entire amino acid sequences were aligned using ClustalW, and the tree was constructed by the neighbor-joining method. Bootstrap values of 1000 retrials are indicated on each branch, and scale shows 0.1 amino acid substitutions per site. The abbreviations shown in front of each protein indicate plant species: Dv, *Dahlia variabilis*; Am, *Antirrhinum majus*; At, *Arabidopsis thaliana*; In, *Ipomoea nil*; Pf, *Perilla frutescens*; Ph, *Petunia hybrida*; Zm, *Zea mays*. Accession number of each protein: DvIVS (BAJ33515), DvDEL (BAJ33516), AmDEL (AAA32663), AtEGL3 (NP_176552), AtGL3 (NP_680372), AtTT8 (CAC14865), InDEL (BAE94393), InIVS (BAE94394), PfF3G1 (BAC56998), PhAN1 (AAG25927), PhJAF13 (AAC39455), and ZmIN1 (AAB03841).

was 8477 bp and contained 9 exons and 8 introns (Fig. 1-7A). Genomic PCR was performed to examine whether a transposable element was inserted in the *DvIVS* gene of MJY. An approximately 8.2-kb amplified product was obtained from MJOr, and an approximately 13.6-kb amplified product was obtained from MJY (data not shown). The 5385-bp insertion sequence (AB601009) was found in the fourth intron, 903-bp downstream of the fourth exon, of the *DvIVS* gene of MJY. To characterize the structure of the *DvIVS* gene of MJW, genomic PCR was performed using the primer set IVS Full-F and IVS-G2869R. Not only the genomic fragment (8.2 kb) that should include the insertion sequence but also shorter fragment (2.8 kb) without the insertion sequence were detected in MJW (Fig. 1-7A).

The inserted element of MJY carried a terminal inverted repeat (TIR) starting with 5'-CACTA-3' (Table 1-8), which is a characteristic of a CACTA superfamily transposable element. The insertion generated a 3-bp (TGG) target site duplication (TSD), similar to TSD generated by other CACTA-type transposable elements (Inagaki et al., 1994; Zabala and Vodkin, 2008; Xu et al., 2010). It also contained ORF for antisense orientation (Fig. 1-7A) (nucleotides 1735 –3555), encoded a 606-amino acid polypeptide, and shared high identity with other CACTA superfamily transposable elements [41% identical to TNP2 in *A. majus Tam1* (Nacken et al., 1991), 33% identical to TNP2 in *Glycine max Tgm9* (Xu et al., 2010), and 32% identical to *En-1* in *Z. mays* (Pereira et al., 1986)]. To test whether the insertion sequence has ability to excise from *DvIVS* gene, approximately 620-bp fragments containing the insertion site in MJW were amplified and cloned into plasmid vectors. Twenty-three clones with small rearrangements presumed to be footprint sequences of the insertion sequence were obtained (Table 1-9, Fig. 1-7B). From these results, the insertion sequence was regarded as an active transposable element and named *Transposable element of D. variabilis 1* (*Tdv1*). This 628-bp fragments completely identical to *DvIVS* genome was obtained from MJOr but not from MJY. Instead, two different gene fragments which were shorter than the *DvIVS* fragments and showed 97% identity to the *DvIVS* gene were obtained from MJY (Table 1-9). It suggested

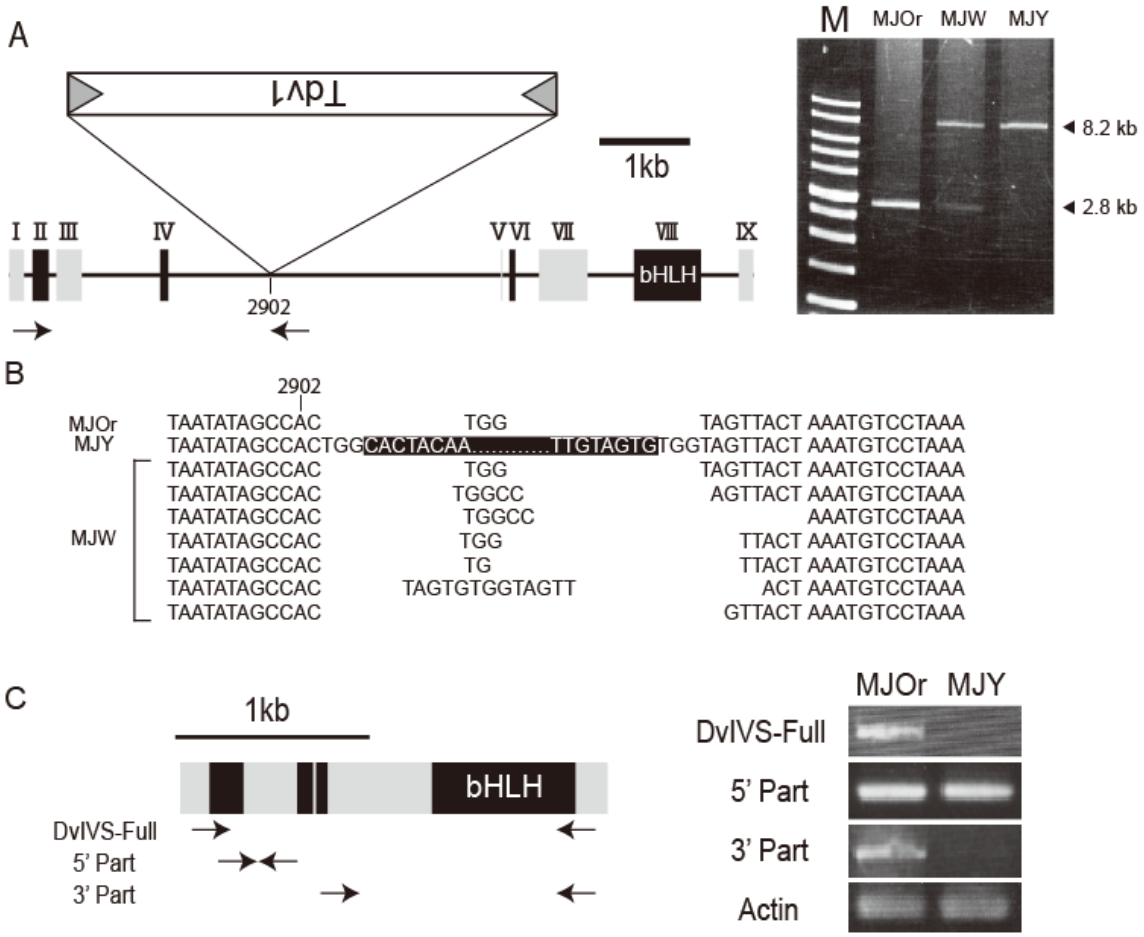

Fig. 1-7. Structure of the *DvIVS* gene. A, structure of the *DvIVS* gene and genomic PCR. Rectangles with roman figures indicate exons. The bHLH domain is located in the eighth exon. *Tdv1* is inserted in the fourth intron in the antisense direction of the MJY genome. Arrows indicate the primer set used for genomic PCR. M indicates a 1-kb marker; B, footprints of *Tdv1*. Uppermost sequence is assumed to be the standard sequence. Sequences in the black box indicate the *Tdv1* sequence. With respect to MJW, *Tdv1*-inserted sequences were not analyzed; C, truncated transcripts of *DvIVS* in MJOr and MJY. Gray rectangular indicates odd number exons and black rectangular indicates even number exons. Arrows indicate primer sets used for RT-PCR.

Table 1-8. Comparison of TIRs with the reported transposable elements of the CACTA superfamily

Name	TIR sequences	Length (bp)	Species	Reference
Tdv1	CACTACAA	8	*Dahlia variabilis*	In this study
En1	CACTACAAGAAAA	13	*Zea mays*	Pereira *et al.* (1986)
Tam1	CACTACAACAAAA	13	*Antirrhinum majus*	Nacken *et al.* (1991)
Cac1	CACTACAA	8	*Arabidopsis thaliana*	Miura *et al.* (2001)
Tpn1	CACTACAAGAAAAATGCACATAGCAAC	27	*Pharbitis nil* (*Ipomoea nil*)	Inagaki *et al.* (1994)
Tgm1	CACTATTAGAAAA	13	*Glycine max*	Vodkin *et al.* (1983)
Cs1	CACTATGTGAAAAAAGCTTA	20	*Sorghum bicolor*	Chopra *et al.* (1999)
Pis1	CACTACGCCAAA	12	*Pisum sativum*	Shirsat (1988)
Psl	CACTACAAAAAA	12	*Petunia hybrida*	Snowden and Napoli (1998)
Tdc1	CACTACAAGAAAACGCGAGA	20	*Daucus carota*	Ozeki *et al.* (1997)
Tnr3	CACTAGAAGGGAT	13	*Oryza sativa*	Motohashi *et al.* (1996)

This table is based on Tian (2006).

Table 1-9. Number of fragments amplified with IVS-G2241F and IVS-G2869R

Type	Length (bp)	Identity to *DvIVS* genome (%)	MJOr	MJY	MJW
1	628	100	10	0	23*
2	625	97	6	16	24
3	615	97	1	3	16

*Footprint sequences were unconsidered in Type 1 of MJW.

that the dahlia lines using here have at least three types of *DvIVS* genes.

To test whether the all three *DvIVS* genes are expressed in the flowers, *DvIVS* cDNA fragments from MJOr were sequenced. All 20 clones of *DvIVS* cDNA were identical to the *DvIVS* gene (data not shown). The result suggested that the anthocyanin pigmentation in the petals depend on the *DvIVS* gene and that the two other *DvIVS* genes are not expressed in the petals.

To characterize the *DvIVS* transcripts in MJY, RT-PCR was performed using three primer sets. Successful amplification was performed only by the primer set amplifying the region upstream of *Tdv1* insertion sites in both MJOr and MJY, however, other primer sets did not successfully amplify the regions in MJY (Fig. 1-7C). It suggested that *Tdv1* insertion into the fourth intron of *DvIVS* resulted in truncated *DvIVS* mRNA in MJY. On analyzing *DvIVS* mRNA expression in MJY by 3' RACE, truncated *DvIVS* mRNA containing the fourth exon and a short part of the fourth intron (nucleotides 125–250 downstream of the fourth exon/fourth intron junction) was detected (data not shown). Thus, *Tdv1* insertion into the *DvIVS* gene of MJY resulted in generation of short-sized *DvIVS* transcripts lacking the bHLH domain, thereby leading to an inability of transcriptional regulation of anthocyanin synthesis genes.

Sequence comparison of DvCHS1*,* DvCHI*,* DvF3H *and* DvDFR

Transcript sequences of *DvCHS1*, *DvCHI*, *DvF3H*, and *DvDFR* were isolated from MJOr and MJY petals and compared based on SNPs (Tables 1-10, 1-11, 1-12 and 1-13). Based on sequence analysis of transcripts, 17 and 15 sequences of *DvCHI* (Table 1-11), 9 and 12 sequences of *DvF3H* (Table 1-12), and 9 and 8 sequences of *DvDFR* (Table 1-13) were observed in MJOr and MJY, respectively. Because drastic differences were not observed in the number of sequences expressed in both lines, whole copies were assumed to be suppressed in MJY. However, 12 different sequences of *DvCHS1* were detected in MJOr, while only 1 sequence was detected in MJY (Table 1-10). At least, three major transcripts (*DvCHS1* Type 1, 2 and 4) were detected in MJOr, while only one

Table 1-10. SNPs of *DvCHS1* cDNA in MJOr and MJY

Line	Deduced AA type	Number of clones	Base number																																		
			27	45	47	197	203	**287**	377	446	491	602	611	614	623	641	644	**657**	719	761	**764**	773	809	942	953	**1024**	1025	1154	**1178**	1184	1237	1345	1348
MJOr	1	3	C	C	G	G	T	C	A	A	T	G	T	T	G	A	C	A	C	T	G	C	T	T	T	A	A	G	G	G	T	T	C
		1	C	C	G	G	T	C	A	A	T	G	T	T	G	A	C	A	C	T	G	C	T	T	T	A	A	G	G	G	T	A	C
	2	15	G	A	A	A	C	A	C	G	T	G	C	T	G	G	C	A	A	C	T	C	G	C	C	A	G	G	C	G	T	A	T
		1	G	A	A	A	C	A	C	G	T	G	C	T	G	G	C	A	A	C	T	C	G	C	C	A	G	G	C	G	T	A	C
		1	G	A	A	A	C	A	C	G	T	G	C	T	G	G	C	A	A	C	T	C	G	C	C	A	G	C	G	A	C	A	C
		1	C	C	G	A	C	A	C	G	T	G	C	T	G	G	C	A	A	C	T	C	G	C	C	A	G	G	C	G	T	A	T
		1	C	C	A	A	C	A	C	G	T	G	C	T	G	G	C	A	A	C	T	C	G	C	C	A	G	G	C	G	C	A	C
		1	G	C	G	A	C	A	C	G	C	G	C	T	G	G	C	A	A	C	T	C	G	C	C	A	G	G	C	G	T	A	T
	3	1	C	C	G	A	C	A	C	G	C	C	A	C	C	G	T	G	C	C	G	T	G	C	C	A	G	C	C	G	T	A	T
	4	12	C	C	G	A	C	A	C	G	C	C	A	C	C	G	T	G	C	C	G	T	G	C	C	G	G	C	G	A	C	A	C
		1	C	C	G	A	C	A	C	G	C	C	A	C	C	G	T	G	C	C	G	T	G	C	C	G	G	C	G	A	C	T	C
		1	G	A	A	A	C	A	C	G	C	C	A	C	C	G	T	G	C	C	G	T	G	C	C	G	G	C	G	A	C	A	C
MJY	4	11	C	C	G	A	C	A	C	G	C	C	A	C	C	G	T	G	C	C	G	T	G	C	C	G	G	C	G	A	C	A	C

The same number of deduced AA type indicates the same deduced amino acid sequence.

Open reading flame is from 51 to 1220 base.

SNPs of 287, 657, 764 and 1024 cause the amino acid substitution.

SNPs observed only in one clone are omitted.

Table 1-11. SNPs of *DvCHI* cDNA in MJOr and MJY

Line	Deduced AA type	Number of clones	Base number												
			12	62	78	114	197	225	266	300	396	464	486	655	713
MJOr	1	11	T	C	A	C	C	C	G	G	T	T	G	T	T
		1	T	C	A	C	C	C	G	G	T	T	G	C	T
		9	G	C	A	C	C	C	G	G	T	T	G	T	T
		1	G	C	C	C	C	C	G	G	T	T	G	T	T
	2	2	T	C	C	A	C	G	C	A	A	C	A	C	T
		1	G	C	C	A	C	G	C	A	A	C	A	C	T
		1	G	C	C	A	C	G	C	A	A	C	A	T	T
	3	3	G	C	C	C	G	G	C	G	A	C	A	T	A
		2	T	C	C	C	G	G	C	G	A	C	A	T	A
		1	G	C	C	C	G	G	C	G	A	C	A	T	T
		1	T	C	C	C	G	G	C	G	A	C	A	T	T
	4	1	T	T	C	C	C	C	G	G	T	T	G	T	T
		1	G	T	C	C	C	C	G	G	T	T	G	T	T
	5	2	T	T	C	C	C	C	G	G	A	C	A	C	T
		1	G	T	C	C	C	C	G	G	A	C	A	C	T
	6	1	G	T	C	C	G	G	C	G	A	C	A	T	A
MJY	1	12	T	C	A	C	C	C	G	G	T	T	G	T	T
		1	T	C	A	C	C	C	G	G	T	T	G	T	A
		1	T	C	C	C	C	C	G	G	T	T	G	T	T
		4	G	C	A	C	C	C	G	G	T	T	G	T	T
		1	G	C	C	C	C	C	G	G	T	T	G	T	T
		1	T	C	A	C	C	C	G	G	T	T	G	C	T
	2	6	T	C	C	A	C	G	C	A	A	C	A	C	T
		1	G	C	C	A	C	G	C	A	A	C	A	C	T
	3	2	T	C	C	C	G	G	C	G	A	C	A	T	A
		1	G	C	C	C	G	G	C	G	A	C	A	T	A
		1	T	C	A	C	G	G	C	G	A	C	A	T	A
	4	1	G	T	C	C	C	C	G	G	T	T	G	T	T
	5	2	G	T	C	C	C	C	G	G	A	C	A	C	T
	7	1	G	C	A	C	C	C	G	G	A	C	A	C	T
		2	T	C	C	C	C	C	G	G	A	C	A	C	T

The same number of deduced AA type indicates the same deduced amino acid sequence.

Open reading flame is from 1 to 675 base.

SNPs of 62, 197, 225, 266 and 464 cause the amino acid substitution.

SNPs observed only in one clone are omitted.

Table 1-12. SNPs of *DvF3H* cDNA in MJOr and MJY

Line	Deduced AA type	Number of clones	Base number																				
			36	**118**	**228**	**259**	**270**	**282**	314	380	**467**	617	635	**705**	728	797	890	905	**1018**	1073	1102	1133
MJOr	1	26	G	T	C	A	T	T	G	C	G	A	A	G	G	C	G	A	C	T	G	T
		1	G	T	C	A	T	T	G	C	G	G	A	G	G	C	A	A	C	C	T	T
		1	G	T	C	A	T	T	G	C	G	A	A	G	G	C	G	A	C	T	G	-
	2	2	A	A	C	T	C	C	C	T	G	G	G	A	A	T	A	A	C	C	G	T
		4	A	A	C	T	C	C	C	T	G	G	G	A	A	T	A	A	C	C	T	T
	3	2	G	A	T	T	C	T	C	C	C	G	A	G	G	C	G	G	C	T	G	T
		1	G	A	T	T	C	T	C	T	C	A	A	G	G	C	G	G	C	T	G	-
	4	1	G	T	C	A	T	T	G	C	G	A	A	G	G	C	G	A	T	T	G	T
	5	1	G	T	C	T	C	C	C	T	G	G	A	G	G	C	G	A	C	C	T	T
MJY	1	20	G	T	C	A	T	T	G	C	G	A	A	G	G	C	G	A	C	T	G	T
		2	G	T	C	A	T	T	G	C	G	A	A	G	G	C	G	A	C	T	T	T
	2	5	A	A	C	T	C	C	C	T	G	G	G	A	A	T	A	A	C	C	G	T
		1	A	A	C	T	C	C	C	T	G	G	G	A	A	T	A	A	C	T	G	T
	3	1	G	A	T	T	C	T	C	C	C	G	A	G	G	C	G	G	C	T	G	T
		1	G	A	T	T	C	T	C	C	C	G	A	G	G	C	G	G	C	T	T	T
	6	1	G	T	C	A	T	T	G	C	C	G	A	G	G	C	G	G	C	T	G	T
	7	1	G	A	C	A	T	C	C	C	G	A	A	G	G	C	G	A	C	T	G	T
	8	1	G	A	T	T	C	C	C	C	G	A	A	G	G	C	G	A	C	T	G	T
	9	1	G	A	C	T	C	C	C	T	G	G	G	A	A	T	A	A	C	C	G	T
	10	1	A	A	C	T	C	C	C	T	G	A	A	G	G	C	G	A	C	T	G	T
	11	1	A	A	C	T	C	C	C	T	G	G	G	A	A	T	A	A	T	T	G	T

The same number of deduced AA type indicates the same deduced amino acid sequence.

Open reading flame is from -10 to 1076 base.

SNPs of 36, 118, 228, 259, 270, 282, 467, 705 and 1018 cause the amino acid substitution.

SNPs observed only in one clone are omitted.

Table 1-13. SNPs of *DvDFR* cDNA in MJOr and MJY

Line	Deduced AA type	Number of clones	Base number																			
			43	219	**241**	258	285	**353**	486	**490**	**589**	**601**	**628**	738	834	922	**940**	942	**986**	1131	1134
MJOr	1	13	A	T	A	A	T	C	G	G	A	G	T	A	G	C	G	C	C	G	T
	2	7	A	T	T	G	A	C	G	G	A	G	T	A	G	C	G	C	C	G	T
	3	2	C	T	A	G	A	T	G	G	G	A	T	A	G	C	G	C	T	G	T
	4	5	A	T	A	A	T	C	G	G	A	G	T	A	G	C	G	C	T	G	T
		2	A	T	A	G	A	C	G	G	A	G	T	A	G	C	G	C	T	G	T
	5	3	A	T	A	G	A	T	A	A	A	G	G	G	A	T	A	T	T	C	–
	6	1	A	T	A	G	A	T	G	G	G	A	T	A	G	C	G	C	C	G	T
	7	1	A	T	A	A	T	C	G	G	G	A	T	A	G	C	G	C	C	G	T
	8	1	C	T	A	G	A	T	A	A	A	G	G	G	A	T	A	T	T	C	–
MJY	1	9	A	T	A	A	T	C	G	G	A	G	T	A	G	C	G	C	C	G	T
		1	A	A	A	A	T	C	G	G	A	G	T	A	G	C	G	C	C	G	T
	2	5	A	T	T	G	A	C	G	G	A	G	T	A	G	C	G	C	C	G	T
	3	8	C	T	A	G	A	T	G	G	G	A	T	A	G	C	G	C	T	G	T
		1	C	C	A	G	A	T	G	G	G	A	T	A	G	C	G	C	T	G	T
	4	4	A	T	A	G	A	C	G	G	A	G	T	A	G	C	G	C	T	G	T
	9	1	C	T	T	G	A	C	G	G	A	G	T	A	G	C	G	C	C	G	T
	10	1	C	T	A	G	A	C	G	G	A	G	T	A	G	C	G	C	C	G	T

The same number of deduced AA type indicates the same deduced amino acid sequence.

Open reading flame is from 18 to 1028 base.

SNPs of 43, 241, 353, 490, 589, 601, 628, 940 and 986 cause the amino acid substitution.

SNPs observed only in one clone are omitted.

Table 1-14. SNPs in the exon reagion of *DvCHS1* genome in MJOr, MJY and MJW

Line	Deduced AA type	Number of clones	Base number																																				
			27	45	47	197	203	287	377	446	491	602	611	614	623	641	644	657	719	761	764	773	809	942	953	1024	1025	1154	1178	1184	1237	1345	1348
MJOr	1	6	C	C	G	G	T	C	A	A	T	G	T	T	G	A	C	A	C	T	G	C	T	T	T	A	A	G	G	G	T	T	C
	2	1	C	C	G	A	C	A	C	G	T	G	C	T	G	G	C	A	A	C	T	C	T	T	T	A	A	G	G	G	T	T	C
		9	–	–	–	A	C	A	C	G	T	G	C	T	G	G	C	A	A	C	T	C	G	C	C	A	G	G	C	G	T	A	T
	4	9	C	C	G	A	C	A	C	G	C	C	A	C	C	G	T	G	C	C	G	T	G	C	C	G	G	C	G	A	C	A	C
MJY	1	5	C	C	G	G	T	C	A	A	T	G	T	T	G	A	C	A	C	T	G	C	T	T	T	A	A	G	G	G	T	T	C
		1	C	C	G	A	C	C	A	A	T	G	T	T	G	A	C	A	C	T	G	C	T	T	T	A	A	G	G	G	T	T	C
		1	G	A	A	G	T	C	A	A	T	G	T	T	G	A	C	A	A	C	T	C	G	T	T	A	A	G	G	G	T	T	C
	2	1	–	–	–	A	C	A	C	G	T	G	C	T	G	G	C	A	A	C	T	C	G	C	C	A	G	G	C	G	T	A	T
	4	9	C	C	G	A	C	A	C	G	C	C	A	C	C	G	T	G	C	C	G	T	G	C	C	G	G	C	G	A	C	A	C
MJW	1	7	C	C	G	G	T	C	A	A	T	G	T	T	G	A	C	A	C	T	G	C	T	T	T	A	A	G	G	G	T	T	C
	2	3	–	–	–	A	C	A	C	G	T	G	C	T	G	G	C	A	A	C	T	C	G	C	C	A	G	G	C	G	T	A	T
	4	6	C	C	G	A	C	A	C	G	C	C	A	C	C	G	T	G	C	C	G	T	G	C	C	G	G	C	G	A	C	A	C

The same number of deduced AA type indicates the same deduced amino acid sequence.

Open reading flame is from 51 to 1220 base.

We couldn't determine the sequence from 1 to 54.

SNPs observed only in one clone are omitted.

Table 1-15 SNPs in the intron reagion of *DvCHS1* genome in MJOr, MJY and MJW

Line	Deduced AA type	Number of clones	Base number																																
			17-21	121	123	171	221	222	243	260	284	285	298	341	343	396	411	412	429	481	484	512-626	641	658	700	730	731	732	740	741	771	780	781
MJOr	1	5	—	T	–	C	G	C	T	–	G	G	T	T	T	T	A	A	A	A	T	—	G	T	T	T	A	C	–	–	T	A	A
	2	9	○	A	T	C	G	T	T	A	C	A	C	T	G	T	A	A	G	G	A	—	G	C	A	A	G	T	T	–	C	C	C
	4	8	○	A	A	T	A	C	G	–	G	G	T	A	T	A	G	C	A	A	A	○	A	C	A	T	G	T	T	T	C	A	A
		1	○	A	T	C	G	T	T	A	C	A	C	T	G	—	—	—	—	A	A	○	A	C	A	T	G	T	T	–	C	A	A
		1	○	A	A	T	A	C	G	–	G	G	T	A	T	A	G	C	A	A	A	○	A	C	A	T	G	T	T	–	C	A	A
MJY	1	6	—	T	–	C	G	C	T	–	G	G	T	T	T	T	A	A	A	A	T	—	G	T	T	T	A	C	–	–	T	A	A
	2	1	○	A	T	C	G	T	T	A	C	A	C	T	G	T	A	A	G	G	A	—	G	C	A	A	G	T	T	–	C	C	C
	4	9	○	A	A	T	A	C	G	–	G	G	T	A	T	A	G	C	A	A	A	○	A	C	A	T	G	T	T	–	C	A	A
		1	○	A	T	C	G	T	T	A	G	G	T	T	T	T	A	A	A	A	T	—	G	T	T	T	A	C	–	–	T	A	A
MJW	1	7	—	T	–	C	G	C	T	–	G	G	T	T	T	T	A	A	A	A	T	—	G	T	T	T	A	C	–	–	T	A	A
	2	3	○	A	T	C	G	T	T	A	C	A	C	T	G	T	A	A	G	G	A	—	G	C	A	A	G	T	T	–	C	C	C
	4	6	○	A	A	T	A	C	G	–	G	G	T	A	T	A	G	C	A	A	A	○	A	C	A	T	G	T	T	T	C	A	A

The number of deduced AA type indicate deduced amino acid sequence which exon region codes.
SNPs observed in only one clone are omitted.
Circle indicates existence of insertion sequence.

transcript (*DvCHS1* Type 4) was detected in MJY (Table 1-10). For *DvCHS1* genomic fragments, not only MJOr and MJW, but also MJY has *DvCHS1* genes that have coding sequences identical to these three major transcripts (Tables 1-14, 1-15).

Discussion

DvIVS is a bHLH transcription factor associated with anthocyanin synthesis in dahlia

R2R3-MYB, bHLH, and WDR are well known transcription regulators of anthocyanin synthesis pathway enzymes (Koes et al., 2005; Hichri et al., 2011). Until date, many studies have been conducted to determine flavonoid synthesis pathway transcription factors. In petunia, *An1* and *JAF13*, *An2*, and *An11* have been isolated as bHLH, R2R3-MYB, and WDR transcription factors, respectively, (Quattrocchio et al., 1993; De Vetten et al., 1997; Quattrocchio et al., 1998; Spelt et al., 2000; Spelt et al., 2002). Similarly, bHLH, R2R3-MYB, and WDR transcription factors control anthocyanin synthesis in the three *Ipomoea* species (Park et al., 2004; Morita et al., 2006; Park et al., 2007).

bHLH proteins are well conserved in both animals and plants and constitute a superfamily of transcription factors. *Arabidopsis* has at least 147 bHLH genes, and these are divided into 21 subfamilies (Toledo-Ortiz et al., 2003). The bHLH genes associated with regulation of anthocyanin synthesis were first found in *Z. mays* (Ludwig et al., 1989), and have subsequently been found in many other species. Recent studies showed that *AtTT8* (Nesi et al., 2000), *AtGL3* (Payne et al., 2000), and *AtEGl3* (Zhang et al., 2003) regulate anthocyanin and proanthocyanidin synthesis in *A. thaliana*. These bHLH genes regulating anthocyanin synthesis are usually divided into two subgroups on the basis of their phylogenetic tree (Spelt et al., 2000): one subgroup includes *AtTT8*, *An1*, and *InIVS* and the other includes *AtGL3*, *AtEGL3*, *PhJAF13*, and *InDEL*. Usually, the bHLH domain in the former subgroup is not separated by an intron, while that in the latter group is separated by an intron. For example, the bHLH domain of *An1* (Spelt et al., 2000), *IpIVS*

(Park et al., 2007), *AtTT8* (Nesi et al., 2000), and *GtbHLH1* in *Gentiana triflora* (Nakatsuka et al., 2008) are encoded within a single exon, while that of *JAF13* and *ZmIn1* are encoded within two exons.

DvIVS shows high identity with *An1* (50%), *InIVS* (48%), and *AtTT8* (48%) in deduced amino acid sequences and is classified into the same subgroup with these bHLH in the phylogenetic tree (Fig. 1-6B). *DvIVS* has a bHLH domain encoded within a single exon (Fig. 1-7A), suggesting that the structure of the *DvIVS* gene is similar to that of the *An1* gene. These data suggest that *DvIVS* is an orthologue of *AtTT8*, *An1*, and *InIVS*. The cDNA fragment derived from the 5′ end of *DvIVS* mRNA containing the first to third exons was detected in MJY; however, the cDNA fragment from the 3′ end of *DvIVS* mRNA was not detected (Fig. 1-7C). This truncated mRNA did not contain a bHLH domain in the eighth exon, suggesting that the bHLH domain of DvIVS is important for anthocyanin synthesis in dahlia.

RT-PCR analysis (Fig. 1-3) suggests that six anthocyanin biosynthetic and transport associated genes (*DvCHS1*, *DvF3H*, *DvDFR*, *DvANS*, *Dv3MT* and *DvGST*) are under regulation of *DvIVS*. Anthocyanins accumulating in petals of dahlia are mainly pelargonidin 3-(6”-malonylglucoside-5-glucoside) and cyanidin 3-(6”-malonylglucoside)-5-glucoside (Takeda et al., 1986). Therefore, almost downstream from F3H of anthocyanin biosynthesis pathway might be regulated by DvIVS. On the other hand, both MJOr and MJY can accumulate flavones and butein. Thus, regulation scheme of anthocyanin and flavone/butein synthesis is separate in dahlia and genes without under regulation of DvIVS might be associated with synthesis of flavones and butein. In short, MJOr, where DvIVS functions and followed by activation of *DvCHS1*, *DvF3H*, *DvDFR*, *DvANS, Dv3MT* and *DvGST*, results in synthesis of anthocyanins. On the other hand, in MJY, due to *Tdv1* insertion, only partial *DvIVS* mRNA is expressed and transcriptional regulation cannot function. Although *DvCHS1*, *DvF3H*, *DvDFR*, *DvANS*, *Dv3MT* and *DvGST* are not activated, activated genes including *DvCHS2*, *DvCHS3*, *DvCHS4* and *DvCHI* might contribute to biosynthesis of flavone and butein. Therefore, MJOr produces

orange petals on account of the accumulation of anthocyanin and butein, while MJY produces yellow petals on account of the accumulation of butein only. This is coincided with the genetic inheritance model of A (pale anthocyanin), B (deep anthocyanin), I (flavone), and Y (yellow), anthocyanin and butein are separately inherited (Lawrence, 1931a; Lawrence and Scott-Honcrieff, 1935; Bate-Smith et al., 1955; Broertjes and Ballego, 1967; Singh et al., 1970).

Flower color variegation is caused by Tdv1

Flower color variegation is often caused by recurrent excision of transposable elements in a pigment biosynthetic gene. For example, *Tpn1*, a CACTA superfamily transposable element in *DFR* in *I. nil* (Inagaki et al., 1994); *Tip100*, a *h*AT superfamily transposable element in *CHS-D* in *I. purpurea* (Habu et al., 1998); and *Tgm9*, a CACTA superfamily transposable element in *DFR2* in *G. max* (Xu et al., 2010) resulted in variegated flower phenotypes. Therefore, an association of transposable elements with floret color was expected in 'Michael J'. It was hypothesized that MJOr was a complete revertant mutant line and MJY was a loss-of-function mutant line, where the transposable element could not transpose from a gene associated with anthocyanin synthesis.

A 5.4-kb insertion sequence, named *Tdv1*, was found in the fourth intron of the *DvIVS* gene in MJY. *Tdv1* shares a number of CACTA superfamily characteristic features. CACTA superfamily transposable elements are DNA transposons directly transposed from DNA to DNA (Feschotte et al., 2002), and almost all CACTA transposable elements harbor "CACTA" in the outermost region of TIR (Tian, 2006). *Tdv1* also has a CACTA superfamily characteristic TIR (CACTACAA) (Table 1-8) and a 3-bp (TGG) TSD was observed in the MJY genome (Fig. 1-7B). The 606-amino acid ORF in *Tdv1* shared high identity with other CACTA superfamily transposable elements [41% identical to TNP2 in *A. majus Tam1* (Nacken et al., 1991), 33% identical to TNP2 in *G. max Tgm9* (Xu et al., 2010), and 32% identical to *En-1* in *Z. mays* (Pereira et al., 1986)]. Further analysis of this translated amino acid sequence by NCBI's CDD (Marchler-Bauer et al., 2011)

showed high identity with Transposase_21 (pfam02992). The footprint sequences formed by excision of the transposable element were also found in the MJW genome (Fig. 1-7B), indicating that *Tdv1* is an active CACTA superfamily transposable element. Because PCR fragments with footprint sequences of *Tdv1* were not amplified in MJY (Fig. 1-7), transposition of *Tdv1* are completely suppressed in MJY. This inactivation of *Tdv1* in MJY might be due to genetic mutation in *Tdv1* or epigenetic silencing such as DNA methylation, PTGS of transposable elements by RNAi and chromatin modifications, which are known as silencing mechanisms that inactivate transposable elements (Miura et al., 2001; Slotkin and Martienssen, 2007).

Redundant copies regulated by DvIVS

Dahlia is believed to be an autoallooctoploid (Lawrence, 1929; Lawrence, 1931b; Lawrence and Scott-Honcrieff, 1935; Gatt et al., 1998), thus it is expected multiple alleles exist in one gene. Sequence of *DvCHS1* (Table 1-10), *DvCHI* (Table 1-11), *DvF3H* (Table 1-12), and *DvDFR* (Table 1-13) transcripts expressed in MJOr and MJY petals were determined and compared based on SNPs. Sequences of *DvCHI*, *DvF3H*, and *DvDFR* cDNA were almost the same in MJOr and MJY. However, a drastic difference was detected in the expression sequence of *DvCHS1*. At least three different major transcripts were detected in MJOr, but only one of those transcripts was detected in MJY. Genomic region of *DvCHS1* from MJOr, MJW, and MJY were the same, three common sequences were detected (Table 1-14, Table 1-15). Thus, mRNA differences were derived not from differences in genome DNA, but presumably from differences in *DvIVS* transcriptional regulation. Although, compared to MJOr, the expression level of *DvCHS1* was much lower in MJY (Fig. 1-5), one type of *DvCHS1* mRNA expressed in MJY was also expressed in MJOr, suggesting that *DvCHS1* expression is not completely regulated by DvIVS. *DvCHS1* was divided into two groups: the regulation of the first is totally dependent on DvIVS, while the other can also be activated independent of DvIVS. The common sequence belongs to the latter group and the others belong to the former group.

This imperfect regulation might be derived from genetic redundancy, nevertheless, further study is needed in this regard.

1.2 A basic helix-loop-helix transcription factor *DvIVS* determines flower color intensity in cyanic *Dahlia* cultivars

Introduction

In the previous section, it is demonstrated that a bHLH transcription factor DvIVS regulates anthocyanin synthesis via regulation of *DvCHS1*, *DvF3H*, *DvDFR*, *DvANS*, *Dv3MT* and *DvGST*. There are cultivars having different flower color intensity such as deep purple, purple, pink and ivory white cultivars in dahlia. Generally, higher amounts of pigments deepen color intensity (Grotewold, 2006; Tanaka et al., 2008). Inversely, lower pigment amounts in pigmented organs lead to paler coloring in carnation (*Dianthus caryophyllus*), eustoma (*Eustoma grandiflorum*), delphinium (*Delphinium*), and pelargonium (*Pelargonium* × *domesticum*) (Mato et al., 2001; Uddin et al., 2004; Hashimoto et al., 2000; Fujioka et al., 1991). In some cases, other factors such as cell shape and vacuolar pH strongly influence the flower color intensity (Mol et al., 1998). Thus, a new question was arose that how *DvIVS* was involved in the regulation of flower color intensity. Accordingly, a hypothesis was developed and tested that expression level of *DvIVS* determines the amount of anthocyanin and thereby flower color intensity. Because it is also likely that there are multiple *DvIVS* alleles in dahlia owing to its high polyploidy, the involvement of a specific *DvIVS* genotype in the regulation of flower color intensity was also investigated.

Materials and methods

Plant materials

Fifteen cultivars according to flower color were chosen for the experiment: purple cultivars: ‘Super Girl’, ‘Yukino’, ‘Cupid’, ‘Evelyn Rumbold’ and ‘Atom’; pink

cultivars: ‘Magokoro’, ‘Jyunn-ai’ and ‘Saffron’; ivory white cultivars: ‘Gitt’s Attention’, ‘Zannsetsu’, ‘Hakuba’ and ‘Hakuyo’ ; and red cultivars: ‘Agitato’, ‘Nekkyu’ and ‘Red Velvet’ (Fig. 2-1A-O). Some cultivars were purchased from Akita International Dahlia Park (Akita, Japan). All cultivars were grown in the experimental farm of Kyoto University (Kyoto, Japan) and their petals were used for this study. For inverse PCR analysis, genomic DNA from a red-white bicolor cultivar ‘Yuino’ was used. For analysis of *DvIVS* promoter types, total 55 cultivars or seedling lines were examined.

Color analysis

Color components of the CIE *L*a*b** co-ordinate were measured with the purpose of describing petal color differences of statistical significance. Color analyses were carried out following the Commission Internationale de l'Eclairage system. *L** indicates lightness (black: 0 to white: 100). Positive a* values indicate redness and negative *a** values indicate greenness. Positive *b** values indicate yellowness and negative *b** values blueness. Chroma (*c**), purity or saturation of the color, was calculated as follows; $C^* = (a^{*2} + b^{*2})^{1/2}$. The *L**, *a**, and *b** were measured with a hand held spectrophotometer (NR-3000, Nippon Denshoku Industries, Tokyo, Japan). Three areas of the adaxial surface were subjected to color measurement. A mean score of the three replicate petals from three different flowers was calculated.

HPLC analysis

To determine the composition of flavonoids and anthocyanidins, HPLC analysis was performed. In summary, petals were homogenized with acetic acid: methanol: water (1: 4: 5 v/v) solution for pigment extraction. The extracts were dried and re-dissolved in 2 mL of 20% hydrochloric acid. This solution was heated to evaporate the solvent, and 500 μL of 20% hydrochloric acid was added to measure crude aglycones. HPLC analysis was performed using an LC10A system (Shimadzu) with a C18 column (Nihon Waters K.K., Tokyo, Japan) maintained at 40°C and a photodiode array detector. The detection

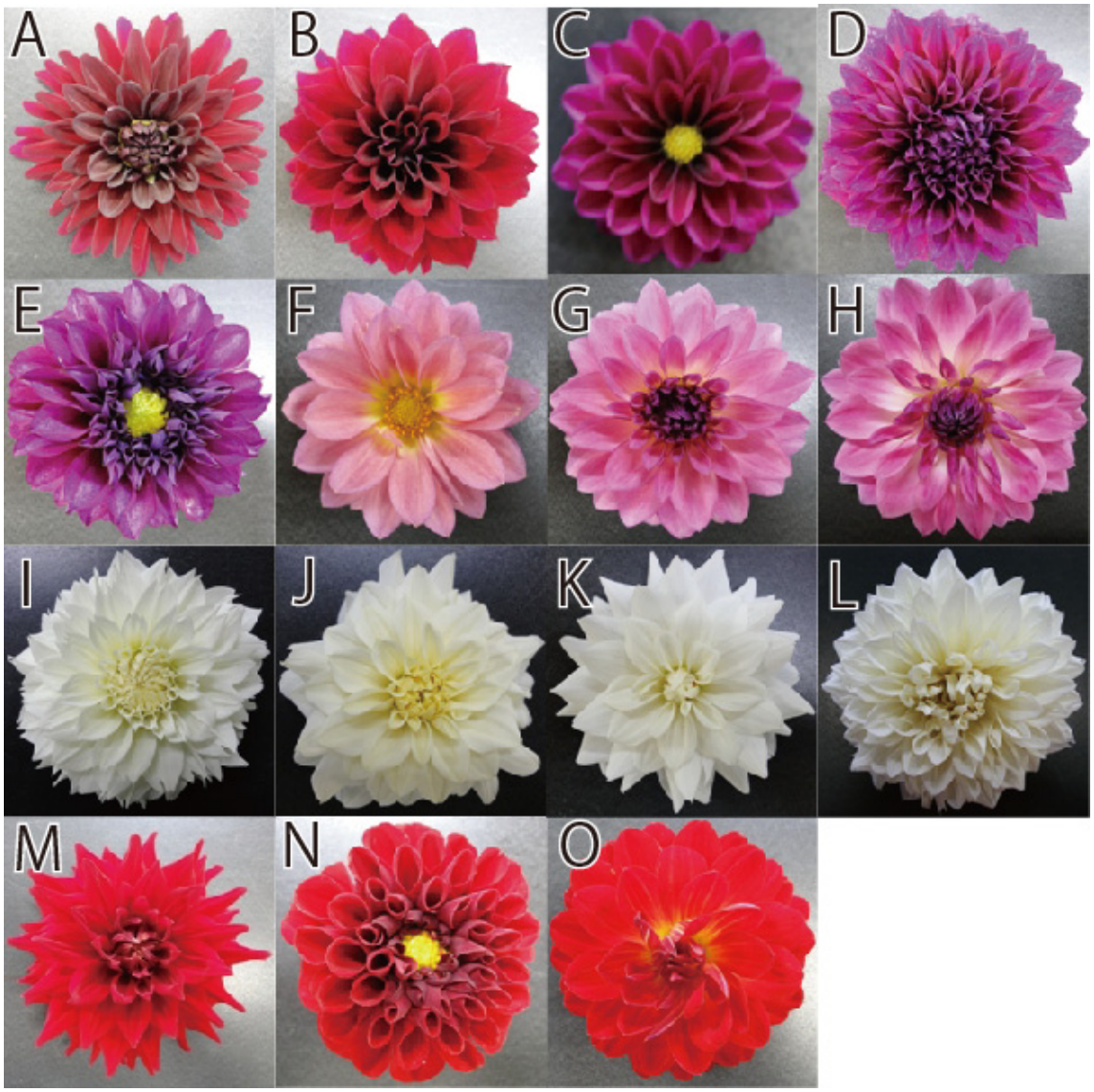

Fig. 2-1. Dahlia cultivars used in this experiment. The order of photos is the same as Table 2-6. A, ‘Super Girl’; B, ‘Yukino’; C, ‘Cupid’; D, ‘Evelyn Rumbold’; E, ‘Atom’; F, ‘Magokoro’; G, ‘Jyunn-ai’; H, ‘Saffron’; I, ‘Gitt’s Attention’; J, ‘Zannsetsu’; K, ‘Hakuba’; L, ‘Hakuyo’; M, ‘Agitato’; N, ‘Nekkyu’ and O, ‘Red Velvet’.

wavelength was 350 nm for flavone and chalcone aglycones and 530 nm for anthocyanin aglycones.

Anthocyanin measurement

For anthocyanin quantification, 100 – 200 mg of fresh petals were homogenized in liquid nitrogen and 1 mL of extraction buffer (acetic acid: methanol: water = 1: 4: 5 v/v) was added. The extracted samples were centrifuged for 2 min at 20,600 × g and the supernatant was collected. The supernatant was diluted 10 or 100 fold with the extraction buffer and the absorption at 520 nm was measured using a double beam spectrophotometer (U-2000A, Hitachi, Tokyo, Japan). The anthocyanin amount per 100 mg of fresh petals was recorded. A standard curve was prepared using cyanidin chloride (Polyphenols, Norway). The assay was performed with three petals from three independent inflorescences.

Other characteristics of petals

The pH of the petals was measured using previously described methods (Quattrocchio et al., 2006). Petals (200 mg) were ground in 6 mL of distilled water. The pH was directly measured with a pH meter within 1 min. A mean of the three values was used for further data analysis.

To determine whether pigments were accumulating only in epidermal cells, fresh sections of ray florets were observed using a VHX-100 digital microscope (KEYENCE, Osaka, Japan). Epidermal cell structures were examined in resin sections prepared as follows. Petals were fixed in an FAA (ethanol: water: formalin: acetic acid, 12: 6: 1: 1 v/v) solution and cut into 5 mm squares. Samples were dehydrated in a graded ethanol series, and subsequently exchanged for Technovit 7100 resin (Heraeus Kulzer, Wehrheim, Germany) by immersing the samples in liquid resin for more than 3 h. Samples were solidified in the resin according to the manufacturer's protocol. The embedded samples were cut into 5 μm sections using a motorized rotary microtome (RM2155, Leica, Wetzlar,

Germany). Sections were stained with a 0.05% toluidine blue solution for 30 min and washed with water for 5 min. The dyed sections were observed and photographed with a VHX-100 digital microscope (KEYENCE).

Real-time RT-PCR

Total RNA was extracted with Sepasol®-RNA I Super G (Nacalai Tesque, Kyoto, Japan), purified with High-Salt Solution for Precipitation (Takara), and reverse transcribed with ReverTra Ace (Toyobo), and 2 μL of 50-fold diluted RT product was used as template for real-time RT-PCR. Real-time RT-PCR was performed with SYBR® Premix Ex Taq™ II (Takara) according to the manufacturer's instructions using a 7900HT Fast Real-Time PCR System (Applied Biosystems). The primers used are shown in Table 2-1. The PCR program was set at 95°C for 10 s, followed by 40 cycles of 95°C for 10 s, 60°C for 30 s, and subsequent dissociation steps. Three technical replications for two biological replications were performed and *actin* was used for an internal standard.

Correlation analysis

Correlations between *L** and anthocyanin amount, *L** and vertical-horizontal ratio of epidermal cell shape, *L** and petal pH, anthocyanin content and anthocyanin synthesis pathway genes, and anthocyanin synthesis genes and *DvIVS* expressions were calculated. All correlation analysis was performed using Microsoft Excel.

Isolation of DvIVS promoter region

The promoter region of *DvIVS* was isolated by inverse PCR. Genomic DNA of 'Yuino' petals was isolated using a modified cetyltrimethylammonium bromide method (Murray and Thompson, 1980) and purified with MagExtractor™-Plant Genome- (Toyobo). One microgram of genomic DNA was digested with *Hin*d III (Toyobo) and enzymes were removed with phenol/chloroform/ isoamyl alcohol (25: 24: 1) (Nacalai Tesque). After ethanol precipitation, 200 ng of digested DNA, 350 U of T4 DNA ligase

Table 2-1. Primers used for real-time RT-PCR

Genes	Forward primers	Reverse primers
DvCHS1	CATGTGCTAAGCGAATACGG	CCTCTCCGGTGGTATTGAAC
DvCHS2	TGTCCCAACTACCATGCCGATTTC	TTACACATTAAAATGACACAGTGA
DvCHI	AGAAGCTGGGAATGCAGTGT	GAGATCTGAGAGCCTTGATGC
DvF3H	TTGGAGGGAGATTGTGACCT	GGCCCATTAACTCCTTGCTA
DvDFR	CAACTTCCGGTCTATGACGAG	TTTCGGCCAATGTTTTTGAC
DvANS	GCTCCAACTCTTCTACAACG	GAAATCCTGACCTTCTCCTT
DvIVS	CATAACCCAAGTAAAGAAAGCCATT	CATCCATTTTTAAATTGTTTGTGGT
DvMYB1	GTTCACTACTTTAGCAAACG	GACTTTGATATCAACCGGAT
DvMYB2	TTTGCTCTCCATAGATCAAC	GCCGTGAGTTCTAATATAAG
DvR3MYB	ATCAACCATTGACGATATCAACAAT	GATTTGTTAAAAAGACTAATGATAA
DvDEL	ATCTAAGTTAAAGAGTTGTACAGC	TGAAACTTGGAAAATTGGACTCAA
DvWDR1	AGGCGTTGTGGAAACTCAAT	TTATCGCGAAGGTCGAAAAC
DvActin	TGCTTATGTTGGTGATGAAG	CCCTGTTAGCCTTAGGATTT

(Takara), and 10 × buffer were mixed and water was added to 20 μL. The mixture was incubated at 16°C overnight and PCR was performed with LA Taq (Takara) using 1 μL of ligation product as a template in a 10 μL volume. The PCR program was set at 94°C for 1 min, followed by 35 cycles of 98°C for 10 s, 55°C for 10 s, and 68°C for 15 min. Primers used in this PCR were IVS-113R and IVS-G1163F (Table 2-2) designed for our reported sequence (AB601010). PCR products were cloned into pTAC-1 vectors using Dyna-Express TA PCR Cloning Kit (BioDynamics Laboratory, Tokyo, Japan) and all sequencing was performed using a BigDye ® Terminator v 3.1 Cycle Sequencing Kit and a 3100 Genetic Analyzer (Applied Biosystems).

Genotyping of DvIVS promoter and cDNA sequences

For genotyping of *DvIVS* promoter region, primers were designed according to isolated promoter region sequence as shown in Table 2-3 and PCR was performed with Blend Taq polymerase (Toyobo) through the following steps and subsequently sequenced: initial denaturation at 94°C for 2 min, 30 cycles of denaturation at 94°C for 30 s, annealing at 55°C for 30 s, and extension at 72°C for 1 min, and a final extension at 72°C for 4 min.

Table 2-2. Primers used for inverse PCR and transcript sequencing

	Primers	Objects
IVS-113R	TATTCGAATTTCACGTCAAATATTG	Inverse PCR
IVS-G1163F	TCCCAGCTCACGGTTCAGTTTTAAA	Inverse PCR
IVS-Full-F	TTTGACGTAATTTTGGACCTAATTT	Transcript sequencing
IVS-474F	CGGTGAGCAACAGGTGGCGGAGAA	Transcript sequencing
IVS-625F	GCATATGCAAAGCAGCAAGATCTAT	Transcript sequencing
IVS-725F	CGGTGATATGCATCCCTGTACTAAA	Transcript sequencing
IVS-826R	TGAAGAAAAGTTTCACATGTTGAAT	Transcript sequencing
IVS-1037F	GACGGACTTCATGAAAGAAACATA	Transcript sequencing
IVS-1082F	TGCCTCACAATAATAAAGATTCAAT	Transcript sequencing
IVS-1316F	CAGAAGAATTTGCACCGGAGTTTA	Transcript sequencing
IVS-1614R	GAGCTCTTCGTGCGACGTCGTTTT	Transcript sequencing
IVS-Full-R	CATCCATTTTTAAATTGTTTGTGGT	Transcript sequencing

Table 2-3. Primers used for analyzing the *DvIVS* promoter type

Primer	Promoter type	Forward primers	Reverse primers
IVS-Pro2F	1, 2, 4, ZAN	ATAATTTTCTTTTAAGTTACGGATT	
IVS-Pro3F	2, 3, 4, 5	TTTGAGTTACAGAATTGATTGTGCT	
IVS-Pro4F	Type 3	GCCGAATTGCGATTGGGGGGATT	
IVS Type1Pro-1F	Type 1	TTTCTTTTAAGTTACGGATTTTCGC	
IVS Type2Pro-1F	Type 2	GTGCTGCCAGTAACCCCACGACTTT	
Zannsetsu IVS 1F	ZAN	ATTGGTTTTTAAATTTAACGAGACA	
IVS-Type3-realtime R	Type 3		GCAAGGGACCTCATATTTATACA
IVS-Type2-realtime R	2, ZAN		GCAATTCGGTTCCCTTTTTTCCT
IVS-Pro-1R	All types		GAAGGGGGGTTGCGGTTGACTGGTT
IVS-113R	All types		TATTCGAATTTCACGTCAAATATTG

The *DvIVS* cDNAs in ‘Super Girl’, ‘Yukino’, ‘Cupid’, ‘Evelyn Rumbold’, ‘Atom’, ‘Magokoro’, ‘Jyunn-ai’ and ‘Saffron’ were amplified with Blend Taq polymerase (Toyobo) using IVS Full-F and IVS Full-R primers. The PCR products were cloned and sequenced as described above, using primers shown in Table 2-2 designed for our reported sequence (AB601010). Subsequently, primers were designed to detect the specific transcript (Table 2-4) and were amplified by RT-PCR with KOD FX polymerase (Toyobo) through the following steps: initial denaturation at 94°C for 2 min, 30 cycles of denaturation at 98°C for 10 s, annealing at 55°C for 30 s, and extension at 68°C for 2 min, and a final extension at 68°C for 5 min.

To amplify the combination of promoter and transcribed RNA types, PCR was performed using newly designed primers shown in Table 2-4 and Table 2-5 with Blend Taq polymerase (Toyobo) through the following steps: initial denaturation at 94°C for 2 min, 30 cycles of denaturation at 94°C for 30 s, annealing at 55°C for 30 s, and extension at 72°C for 2 min, and a final extension at 72°C for 10 min. Twelve primer combinations (3 promoter type × 4 mRNA types) were analyzed.

Table 2-4. Primers used for analyzing the *DvIVS* mRNA type

mRNA type	Forward primers	Reverse rimers
mRNA-1	GAAACAATAATGGCTGCCGCTGGTT	TCTTCTGCCTCATCATCATCATCGT
mRNA-2	GAAACAATAATGGCTGCCGCTGGTC	GCCTCATCACATCCTGCATCTTCAC
mRNA-3	GAAGAAACAATAATGGCTGCTGACG	ACCCTCATCATCATCATCATCATCA
mRNA-4	GAAACAATAATGGCTGCCGCTGACG	TGCATCTTCACCCTCATCATCATCT

Table 2-5. Primers used for analyzing the combination of promoter and mRNA type

	Forward primers	Reverse primers
Type 1 promoter	TTTCTTTTAAGTTACGGATTTTCGC	
Type 2 promoter	GTGCTGCCAGTAACCCCACGACTTT	
Type 3 promoter	GCCGAATTGCGATTGGGGGGATT	
DvIVS mRNA-1		CTTTCAATCCGTCATCGTTTACGGA
DvIVS mRNA-2		AACATCTCTTTCAATCCGTCATCA
DvIVS mRNA-3		ACATCTCTTTCAATCCGTCAGCAG
DvIVS mRNA-4		TCTCTTTCAATCCGTCAGCGGCAG

Results

Flavonoid compositions and color differences

As difference among cultivars with respect to the modification of anthocyanidins and flavones was not observed (data not shown), the hydrolyzed aglycones were analyzed. In ivory white cultivars, only flavones, apigenin, and luteolin were detected, whereas in pink and purple cultivars, cyanidin, and pelargonidin were detected in addition to flavones (Table 2-6). In red cultivars, flavones, anthocyanidins, and chalcones, isoliquiritigenin and butein were detected (Table 2-6). To simplify the experiments, only purple, pink, and ivory white cultivars were used for further the study.

Because deeper color generally shows lower L^* value, L^* value was used as an indicator of flower color intensity. When the color characteristics of 12 cultivars were plotted with c^* on the X axis and L^* on the Y axis, they could be classified into three groups corresponding to their appearances (Fig. 2-2). Ivory white cultivars had the highest L^* and the lowest c^* value. In contrast, purple cultivars had the lowest L^* and the highest c^* value. Pink cultivars had intermediate values for both the indices.

Anthocyanin contents and pH measurement

The anthocyanin contents of the 12 cultivars are shown in Fig. 2-3A. Purple cultivars contained the highest, with ‘Super Girl’ and ‘Yukino’ containing exceedingly high amounts of 0.7–1.0 mg anthocyanin per 100 mg petals. Other purple cultivars (‘Cupid’, ‘Evelyn Rumbold’ and ‘Atom’) contained 0.3–0.4 mg per 100 mg petals. Accordingly, the former was designated as deep purple cultivars and the latter as purple cultivars. Pink cultivars had lower anthocyanin amounts than purple cultivars, with < 0.1 mg. In ivory white cultivars, no anthocyanin was detected, which was consistent with the HPLC results (Table 2-6). An inverse relationship between L^* and anthocyanin content was observed among eight cyanic (deep purple, purple, and pink) cultivars (Fig. 2-3B), suggesting that anthocyanin content was the key factor determining flower color intensity

Table 2-6. Flavonoid compositions of petals used in this experiment

Cultivars	Petal colors	Chalcone		Aurone	Flavone		Anthocyanidin	
		Isoliquiritigenin	Butein	Sulfuretin	Apigenin	Luteolin	Cyanidin	Pelargonidin
'Super Girl'	Deep purple	-	-	-	+	+	+	+
'Yukino'	Deep purple	-	-	-	+	+	+	+
'Cupid'	Purple	-	tr	-	+	+	+	tr
'Evelyn Rumbold'	Purple	-	-	-	+	+	+	+
'Atom'	Purple	-	tr	-	+	+	+	tr
'Magokoro'	Pink	tr	tr	-	+	+	+	+
'Jyunn-ai'	Pink	-	-	-	+	+	+	+
'Saffron'	Pink	-	-	-	+	+	+	+
'Gitt's Attention'	Ivory white	tr	tr	tr	+	+	-	-
'Zannsetsu'	Ivory white	-	-	-	+	+	-	-
'Hakuba'	Ivory white	-	-	-	+	+	-	-
'Hakuyo'	Ivory white	-	-	-	+	+	-	-
'Agitato'	Red	tr	+	-	+	+	+	+
'Nekkyu'	Red	+	+	-	+	+	+	+
'Red Velvet'	Red	+	+	-	+	+	+	+

+: detected, tr: trace detected -: not detected

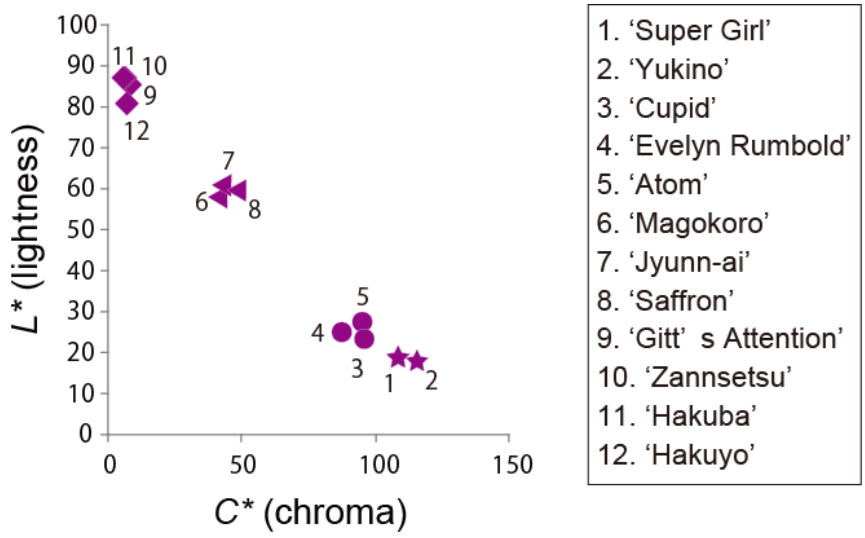

Fig. 2-2. Distribution of *L** (lightness) and *C** (Chroma) values of petals in twelve cultivars carrying flavones or anthocyanins and flavones. Squares, triangles, circles, and stars indicate ivory white, pink, purple, and deep purple cultivars, respectively.

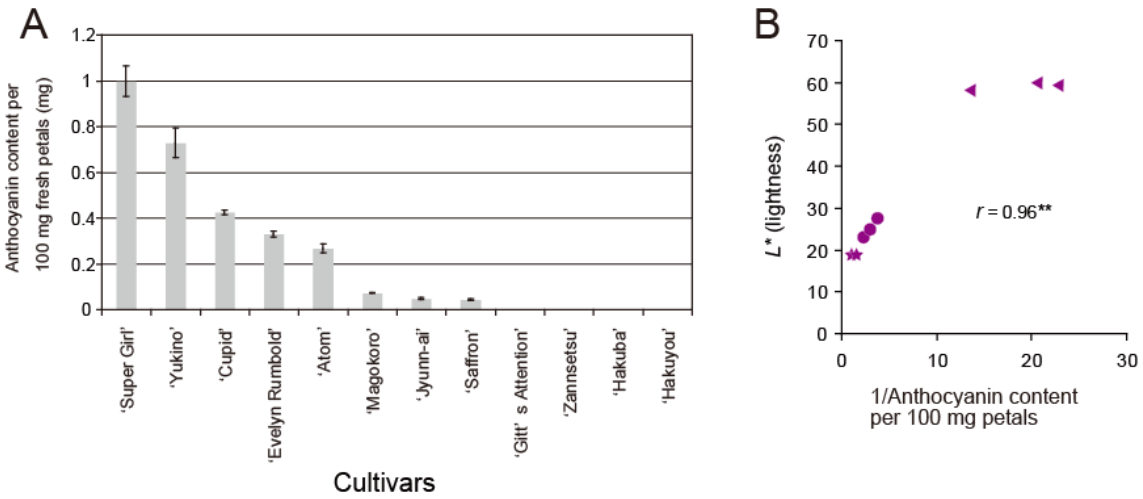

Fig. 2-3. Anthocyanin content analysis by spectrophotometer. A, anthocyanin contents of cultivars. Vertical bars indicate standard errors (n = 9); B, correlation between *L** (lightness) and the reciprocal of anthocyanin content. Squares, triangles, circles, and stars indicate ivory white, pink, purple, and deep purple cultivars, respectively.

(L^*) in these cultivars.

The petal pH of the cultivars examined was 4.9–5.8 (Table 2-7). No significant correlation was detected between L^* and petal pH (data not shown), suggesting that petal pH does not contribute to L^*.

Observation of petal sections

Observation of sections of fresh petals showed that anthocyanin accumulated only in epidermis (Fig. 2-4A-D). No characteristic morphology was observed in resin sections of the eight cultivars (Fig. 2-4E-H). To confirm the correlation between L^* and the vertical–horizontal ratio was analyzed, but no significant correlation was detected (r = −0.50; Fig. 2-4I).

Table 2-7. Measurement of color hue and cellular pH

	L^*	a^*	b^*	C^*	pH
'Super Girl'	19.0 ± 0.3	107.8 ± 1.8	12.6 ± 0.6	108.5 ± 1.8	5.4 ± 0.0
'Yukino'	18.9 ± 0.7	114.1 ± 2.2	14.1 ± 0.5	115.0 ± 2.2	5.2 ± 0.0
'Cupid'	23.3 ± 1.4	96.0 ± 1.9	-1.4 ± 2.8	96.2 ± 1.8	5.4 ± 0.0
'Evelyn Rumbold'	24.9 ± 1.1	87.0 ± 2.5	-5.1 ± 3.7	87.4 ± 2.3	5.5 ± 0.0
'Atom'	27.5 ± 0.6	94.4 ± 1.6	-13.0 ± 0.5	95.3 ± 1.5	5.4 ± 0.0
'Magokoro'	58.1 ± 2.2	43.0 ± 3.2	0.61 ± 1.7	43.1 ± 3.1	not measured
'Jyunn-ai'	60.1 ± 1.9	43.3 ± 2.3	-10.6 ± 0.9	44.5 ± 2.4	5.8 ± 0.1
'Saffron'	59.5 ± 2.3	47.8 ± 2.7	-11.5 ± 0.2	49.2 ± 2.6	5.4 ± 0.0
'Gitt's Attention'	85.4 ± 0.7	-3.6 ± 0.3	7.4 ± 0.3	8.3 ± 0.5	5.8 ± 0.1
'Zannsetsu'	87.2 ± 0.6	-2.5 ± 0.3	6.0 ± 0.2	6.5 ± 0.3	5.5 ± 0.0
'Hakuba'	86.9 ± 0.4	-2.0 ± 0.1	5.3 ± 0.5	5.6 ± 0.5	5.5 ± 0.0
'Hakuyo'	80.9 ± 1.0	-3.3 ± 0.1	5.8 ± 0.5	6.7 ± 0.4	5.7 ± 0.0
'Agitato'	26.6 ± 1.2	88.9 ± 2.7	27.5 ± 1.6	93.1 ± 2.2	5.5 ± 0.0
'Nekkyu'	26.8 ± 0.5	92.2 ± 0.9	26.3 ± 0.9	95.9 ± 0.7	4.9 ± 0.0
'Red Velvet'	39.9 ± 2.9	73.0 ± 5.9	38.5 ± 1.2	82.8 ± 4.6	5.3 ± 0.0

The data indicate the mean ± SE of n = 3 replicates.

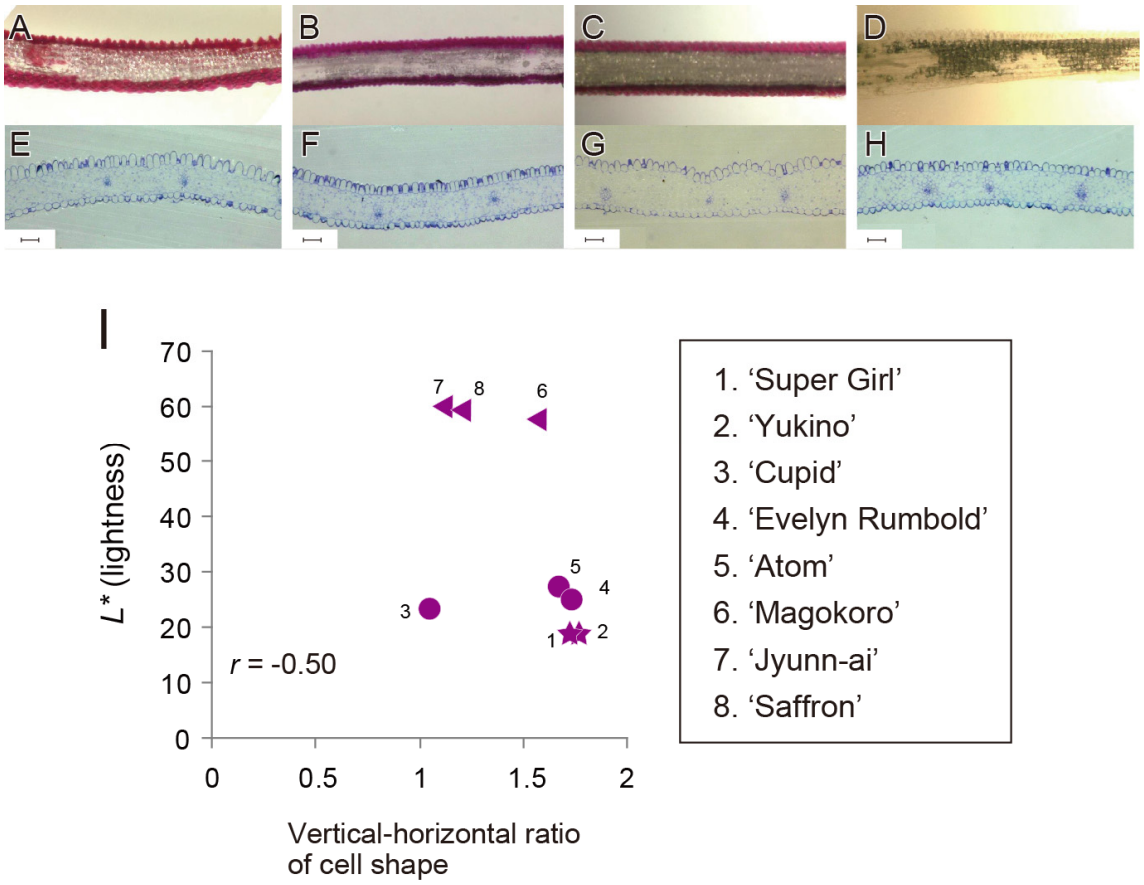

Fig. 2-4. The observation of petal sections. Representative fresh petal sections (A-D) and resin sections (E-H) of some cultivars are shown. A and E, 'Super Girl'; B and F, 'Evelyn Rumbold'; C and G, 'Jyunn-ai'; D and H, 'Gitt's Attention'. Bars in E-H panels indicate 100 μm. I, pearson correlation analysis between *L** and vertical–horizontal ratio of cell shape. Squares, triangles, circles, and stars indicate ivory white, pink, purple, and deep purple cultivars, respectively.

Real-time RT-PCR analysis

In a previous section, it is demonstrated that a bHLH transcription factor DvIVS regulates the expression of *DvCHS1*, *DvF3H*, *DvDFR,* and *DvANS*. In the real-time RT-PCR analysis of *DvCHS1*, *DvF3H*, *DvDFR,* and *DvANS*, comparatively high expression levels were measured in 'Super Girl' and 'Yukino' and little or no expression was detected in ivory white cultivars (Fig. 2-5). The same expression patterns were detected for *DvIVS* (Fig. 2-5). In contrast, high expressions were detected in ivory white cultivars for *DvCHS2* and *DvCHI* (Fig. 2-5). Other transcription factors, *DvMYB1*, *DvMYB2*, *DvR3MYB*, *DvDEL* and *DvWDR1* showed different expression patterns from *DvCHS1*, *DvF3H*, *DvDFR, DvANS* and *DvIVS* (Fig. 2-5).

Correlation analysis was performed to investigate the relationships among anthocyanin contents, anthocyanin synthesis structural gene expression, and *DvIVS* expression. The *r* values (correlation coefficients) between anthocyanin content and *DvCHS1*, *DvCHS2*, *DvCHI*, *DvF3H*, *DvDFR,* and *DvANS* expressions were 0.97, 0.09, 0.15, 0.87, 0.69, and 0.90, respectively (Fig. 2-6A-F). The *r* values between *DvIVS* and *DvCHS1*, *DvCHS2*, *DvCHI*, *DvF3H*, *DvDFR,* and *DvANS* expressions were 0.99, 0.10, 0.22, 0.96, 0.81, and 0.97, respectively (Fig. 2-7A-F). The *r* value between anthocyanin contents and *DvIVS* expression was 0.96 (Fig. 2-6G), showing that anthocyanin content and the expression of *DvIVS* were strongly and positively correlated. In contrast, the *r* values between anthocyanin content and *DvMYB1*, *DvMYB2*, *DvR3MYB*, *DvDEL*, and *DvWDR1* expressions were 0.01, 0.41, 0.41, 0.32, and 0.39, respectively (data not shown).

Length polymorphisms in DvIVS promoter region

Because the expression levels of a gene are usually affected by its promoter region, the promoter region of *DvIVS* was isolated. Fragments of 253 bp upstream of the *DvIVS* transcription start site were isolated by inverse PCR using 'Yuino', and this obtained promoter sequence was subsequently named Type 2. PCR analysis of cyanic cultivars showed there were three length polymorphisms. These three fragments were

sequenced and named Type 1–3.

Type 1 promoter was detected in the deep purple and purple cultivars (‘Super Girl’, ‘Yukino’, ‘Cupid’, ‘Evelyn Rumbold’ and ‘Atom’) by using IVS-2F and IVS-113R primers (Fig. 2-8A). Type 2 promoter was detected in ‘Cupid’, ‘Evelyn Rumbold’, ‘Atom’, ‘Jyunn-ai’, ‘Saffron’ and ‘Hakuyo’ by using IVS-3F and IVS-113R primers (Fig. 2-8A). Type 3 promoter was detected in ‘Cupid’, ‘Magokoro’, and ‘Saffron’ by using IVS-4F and IVS-113R primers (Fig. 2-8A). Thus deep purple cultivars carried only Type 1 promoters, purple cultivars carried Type 1 and Type 2 or all three promoters, pink cultivars carried Type 2 and/or Type 3 promoter(s), and ivory white cultivars except for ‘Hakuyo’ carried none of the promoter types (Fig. 2-8A). Type 2 promoter had a 125 bp insertion just behind the IVS-2F primer sequence, and Type 3 had another 103 bp insertion just behind IVS-3F primer sequence instead of 40 bp Type 2 specific fragment (Fig. 2-8B). In the putative TATA-box region, Type 1 had TTAAGTAG, while Type 2 and Type 3 had TTAAATAG (Fig. 2-8C).

Analysis of DvIVS transcripts and combination with promoter region

To analyze the relationship between polymorphisms of *DvIVS* promoter region and *DvIVS* mRNA expression levels, *DvIVS* cDNA from all cyanic cultivars were sequenced. Four different *DvIVS* cDNA sequences were isolated and named mRNA-1 to mRNA-4 (AB787557–AB787560) based on the differences at amino acid positions 235–295 of the putative protein (Fig. 2-9). All these mRNAs might encode complete putative proteins.

To determine the expressing mRNA types in cyanic cultivars, RT-PCR was performed using type-specific primers for each mRNA (Table 2-4). mRNA-1 was detected in the deep purple and purple cultivars (‘Super Girl’, ‘Yukino’, ‘Cupid’, ‘Evelyn Rumbold’ and ‘Atom’); mRNA-2 in ‘Yukino’, ‘Cupid’ and ‘Jyunn-ai’; mRNA-3 in ‘Magokoro’ and ‘Saffron’; and mRNA-4 in ‘Evelyn Rumbold’ and ‘Saffron’ (Table 2-8).

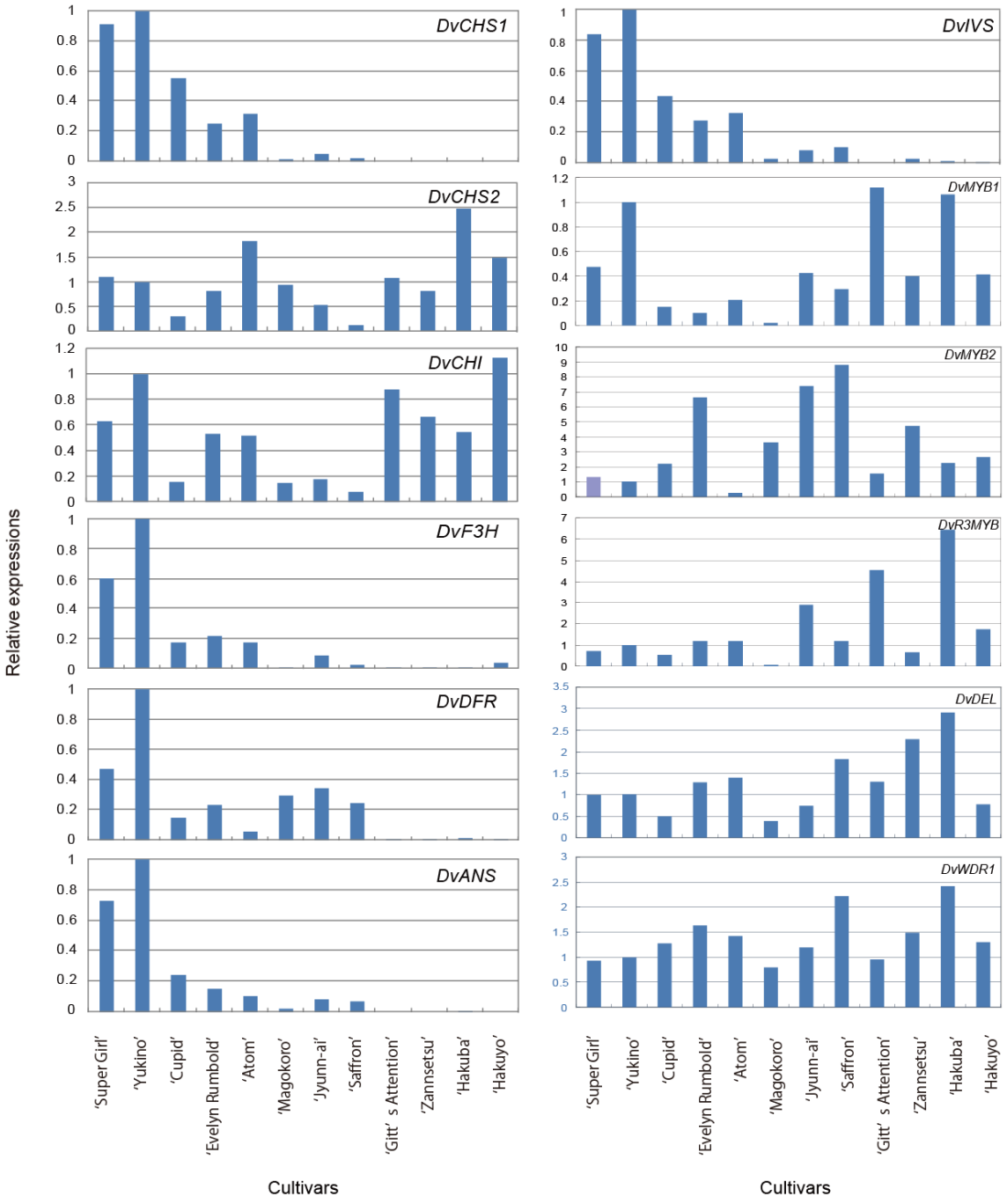

Fig. 2-5. Relative expression levels of *DvCHS1*, *DvCHS2*, *DvCHI*, *DvF3H*, *DvDFR*, *DvANS*, *DvIVS*, *DvMYB1*, *DvMYB2*, *DvR3MYB*, *DvDEL*, and *DvWDR1*. The constitutively expressed gene for actin was used as an internal standard. All plots are based on a value of unity for 'Yukino'. The data are shown as an average of two biological replications.

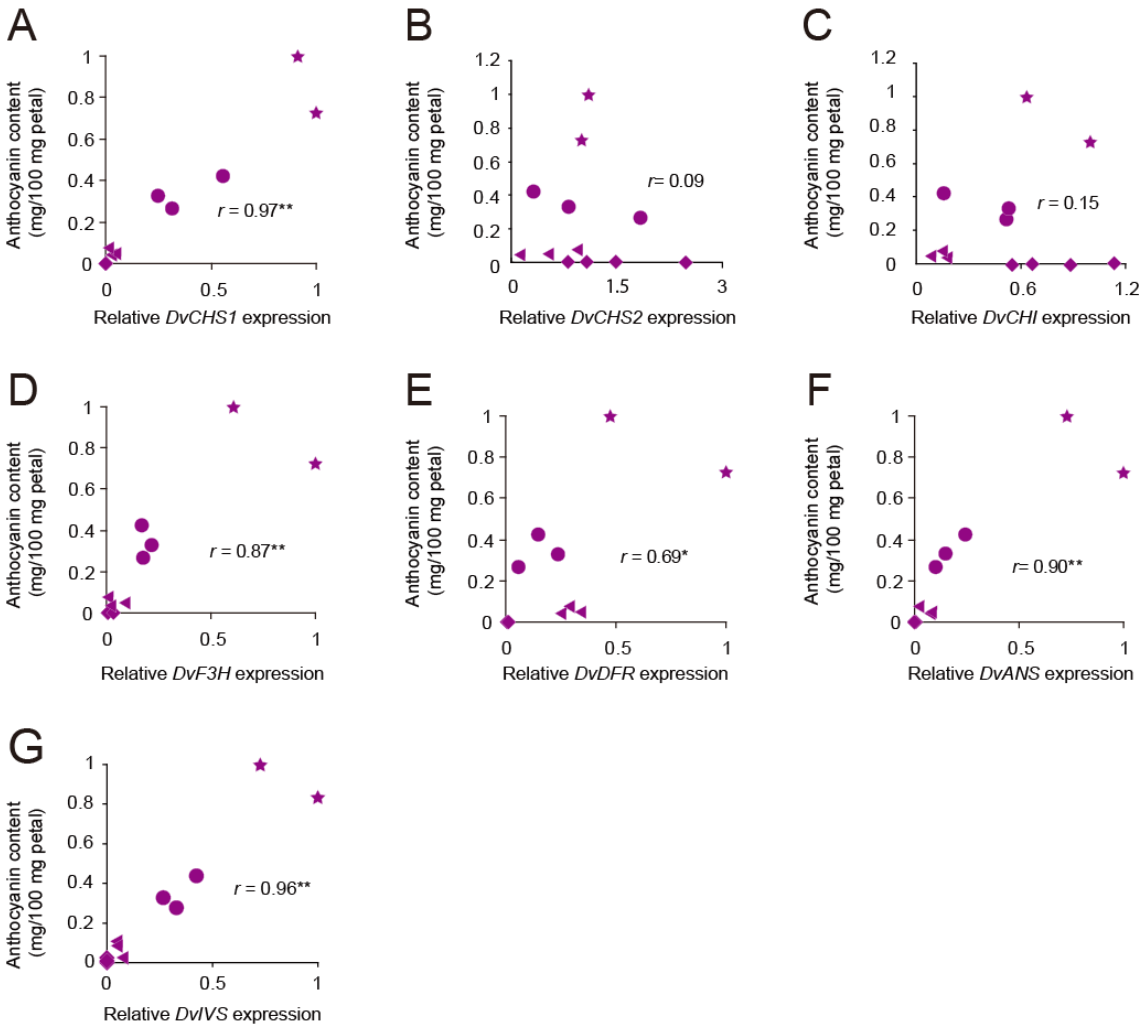

Fig. 2-6. Pearson correlation analysis between anthocyanin contents and expression of genes involved in anthocyanin synthesis (A, *DvCHS1*; B, *DvCHS2*; C, *DvCHI*; D, *DvF3H*; E, *DvDFR*; F, *DvANS* and G, *DvIVS*). Each relative gene expression is shown in Fig. 2-5. Squares, triangles, circles, and stars indicate ivory white, pink, purple, and deep purple cultivars, respectively.

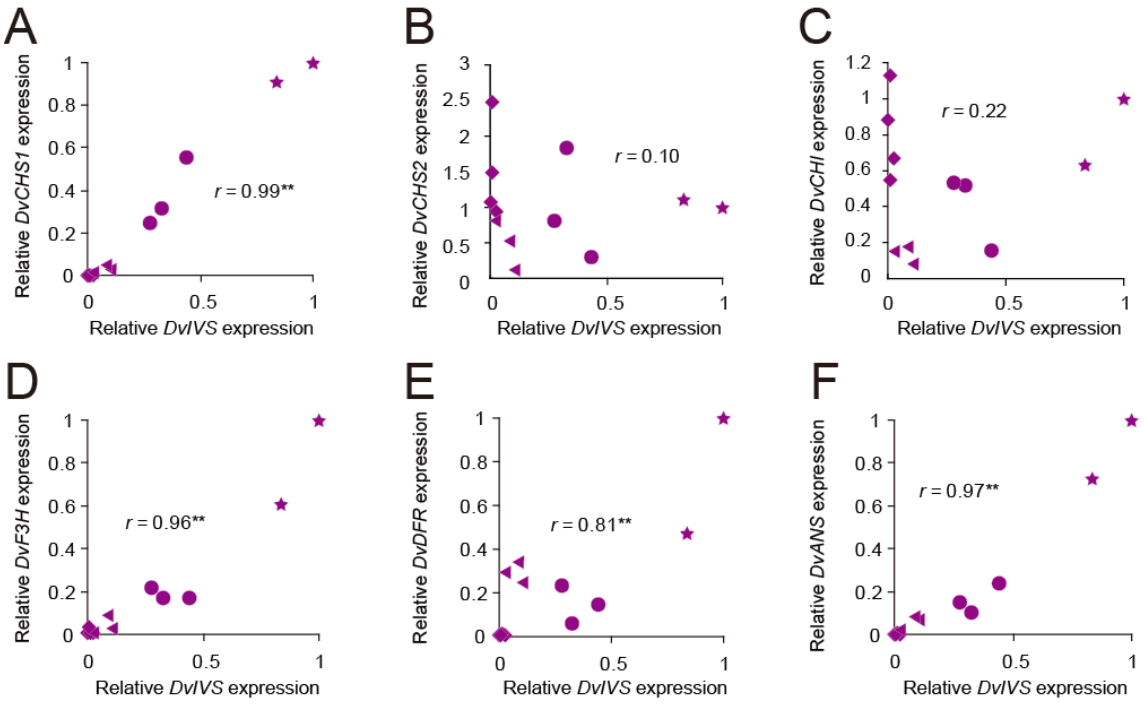

Fig. 2-7. Pearson correlation analysis between *DvIVS* and anthocyanin synthesis structural gene (A, *DvCHS1*; B, *DvCHS2*; C, *DvCHI*; D, *DvF3H*; E, *DvDFR* and F, *DvANS*) expression in Fig. 5. Squares, triangles, circles, and stars indicate ivory white, pink, purple, and deep purple cultivars, respectively.

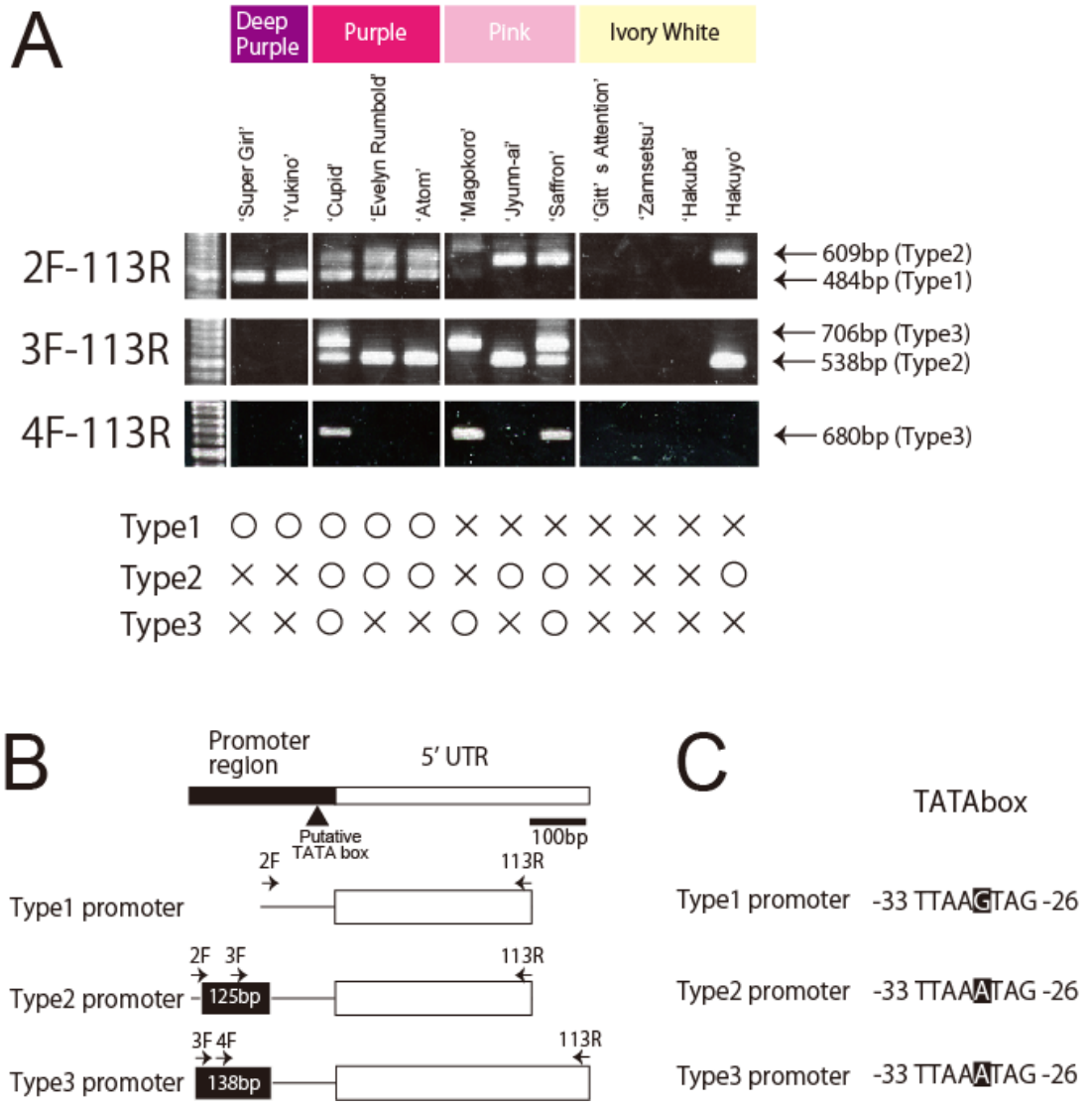

Fig. 2-8. Polymorphisms in the *DvIVS* promoter region. A, PCR polymorphisms in promoter region by IVS-113R and IVS-Pro2F, IVS-Pro3F, or IVS-Pro4F primers (Table 2-3); B, summary figure based on sequence of *DvIVS* promoter region. Type 1 is according to the sequence of 'Super Girl', 'Yukino', 'Cupid', 'Evelyn Rumbold' and 'Atom.' Type 2 is according to the sequence of 'Jyunn-ai', 'Saffron' and 'Hakuyo', and Type 3 is according to 'Magokoro'; C, the single-nucleotide polymorphism in the putative TATA-box region of *DvIVS*. All sequenced cultivars retained a polymorphism.

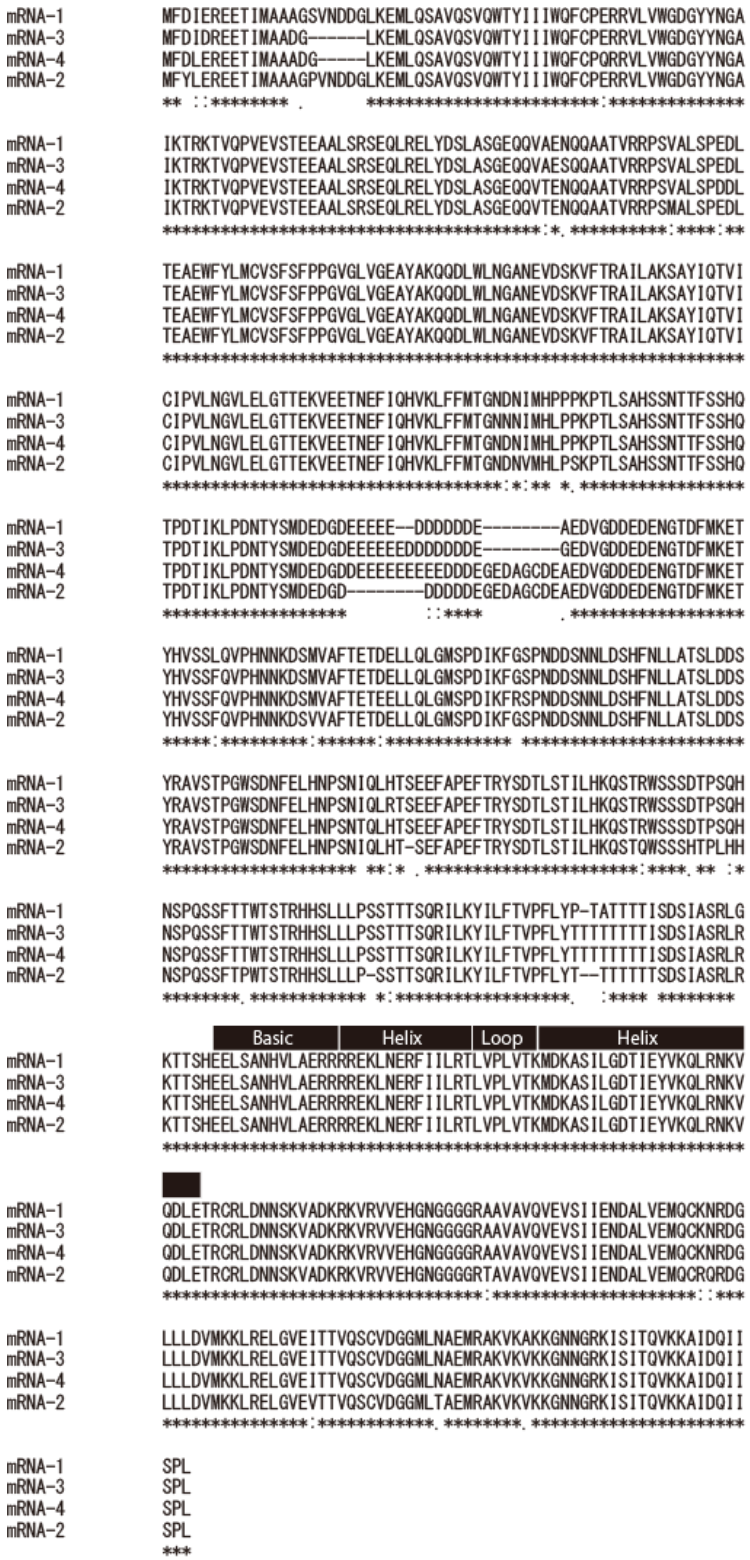

Fig. 2-9. Alignment of deduced amino acid sequences encoded by *DvIVS* mRNA-1 to mRNA-4. The basic helix-loop-helix domain is shown below the black boxes.

Table 2-8 Putative promoter-mRNA combination inferred from PCR analyses

Cultivars		Deep purple		Purple			Pink			Ivory white			
		Super Girl	Yukino	Cupid	Evelyn Rumbold	Atom	Magokoro	Jyunn-ai	Saffron	Gitt's Attention	Zannsetsu	Hakuba	Hakuyo
Promoter type	1	○	○	○	○	○	–	–	–	–	–	–	–
	2	–	–	○	○	○	–	○	○	–	–	–	○
	3	–	–	○	–	–	○	–	○	–	–	–	–
mRNA type	1	○	○	○	○	○	–	–	–	–	–	–	–
	2	–	○	○	–	–	–	○	–	–	–	–	–
	3	–	–	–	–	–	○	–	○	–	–	–	–
	4	–	–	–	○	–	–	–	○	–	–	–	–
Promoter-mRNA combination		p1-m1	p1-m1	p1-m1 p2-m2	p1-m1 p2-m4	p1-m1 p2-×	p3-m3	p2-m2	p2-m4 p3-m3				p2-×
Putative			p?-m2	p3-m?									

Further, to confirm that Type 1 promoter actually encodes a functional protein, promoter–mRNA combinations were investigated using specific primers (Table 2-5). Consequently, the combinations of Type 1 promoter–mRNA-1, Type 2 promoter–mRNA-2, Type 3 promoter–mRNA-3, and Type 2 promoter–mRNA-4 were inferred (Table 2-8). Type 1 promoter–mRNA-1 combination was detected in the deep purple and purple cultivars ('Super Girl', 'Yukino', 'Cupid', 'Evelyn Rumbold' and 'Atom'); Type 2 promoter–mRNA-2 in 'Cupid' and 'Jyunn-ai' ; Type 3 promoter–mRNA-3 in 'Magokoro' and 'Saffron'; and Type 2 promoter–mRNA-4 in 'Evelyn Rumbold' and 'Saffron' (Table 2-8). The coding region associated with 'Atom' and 'Hakuyo' Type 2 was not identified, but no full-length *DvIVS* transcript for this promoter was detected, it was suggested this promoter might be non-functional. Although, the promoter region associated with 'Yukino' mRNA-2 and the coding region associated with 'Cupid' Type 3 promoter, were neither identified, all deeply colored (deep purple and purple) cultivars retained Type 1 promoter–mRNA-1 combination, suggesting this allele is important for high anthocyanin accumulation.

DvIVS *promoter types in other cultivars or seedling lines*

For further analysis, *DvIVS* promoter region of total 55 cultivars or seedling lines were analyzed. Six sequences were identified and named Type 1, Type 2, Type 3, Type 4, Type 5 and Type ZAN (Table 2-9, Fig. 2-10). Type 2, Type 3, Type 4, Type 5 and Type ZAN has some insertion sequence(s) with respect to Type 1. Type ZAN was at first discovered from 'Zannsetsu' and named after it. This promoter type has an insert sequence including 8-bp CAGGGCCG terminal inverted repeat and 8-bp AATTTCTC target site duplication. Thus, it was suggested that this insertion sequence was a fragment of transposable element. Twenty-two of 55 tested cultivars or seedling lines carried Type 1 promoter, and all 22 Type 1-carrying cultivars or seedlings showed deep coloring (purple, red or black).

Table 2-9. *DvIVS* promoter genotypes in various dahlia cultivars

Cultivar	Flower color	Anthocyanin	*DvIVS* promoter type					
			Type1	Type2	Type3	Type4	Type5	TypeZAN
Agitato	Red	High	-	-	-	○	-	-
Bishops Children	Red	High	-	-	○	-	-	-
Michael J Orange	Red	High	○	-	-	-	-	-
Nekkyu	Red	High	○	○	-	-	-	-
Nessho	Red	High	○	-	-	○	-	-
Orihime Seedling1	Red	High	○	-	-	-	-	-
Pechka	Red	High	-	○	-	-	-	-
Red Seed	Red	High	○	-	-	-	-	-
Red Velvet	Red	High	-	-	-	○	-	-
Rigoletto Mix	Red	High	○	-	-	-	-	-
Hana-no-Utage	Red-white bicolor	High	○	-	-	-	-	-
Matsuribayashi	Red-white bicolor	High	○	-	-	-	-	-
OrWi2	Red-white bicolor	High	○	-	-	-	-	-
Santa Claus	Red-white bicolor	High	○	-	-	○	-	-
Yuino	Red-white bicolor	High	-	○	-	-	-	-
Black Cat	Black	High	○	-	-	-	-	-
Fidalgo Blacky	Black	High	○	○	-	-	-	-
Kokucho	Black	High	○	-	-	-	-	-
Ms Noir	Black	High	○	-	-	○	-	-
Super Girl	Deep purple	High	○	-	-	-	-	-
Yukino	Deep purple	High	○	-	-	-	-	-
Princess Diana	Parple variegation in white	High	○	-	-	-	-	-
Atom	Purple	High	○	○	-	-	-	-
Cupid	Purple	High	○	○	○	-	-	-
Douwa	Purple	High	-	○	-	-	-	-
Evelyn Rumbold	Purple	High	○	○	-	-	-	-
Kaiosei	Purple	High	-	-	○	-	-	-
Maihime	Purple	High	○	-	-	-	○	-
Taisho-romann	Purple	High	-	-	○	○	-	-
Kazusa-shiranami	Black-white bicolor	High	-	○	-	-	-	-
Chowa	Purple-white bicolor	High	○	-	-	-	-	-
Rosemary	Purple-white bicolor	High	-	○	-	-	-	-
Jyunn-ai	Pink	Low	-	○	-	-	-	-
Koigokoro	Pink	Low	-	-	-	-	-	-
Magokoro	Pink	Low	-	-	○	-	-	-
Moon Waltz	Pink	Low	-	-	-	-	-	-
Saffron	Pink	Low	-	○	○	-	-	-
Twilight after Night	Ivory white	Low	-	-	○	-	○	-
Senjyu-biyori	Orange	Low	-	-	-	-	-	-
Hamabe-no-Uta	Yellow	-	-	-	-	-	-	-
Humming	Yellow	-	-	○	-	-	-	-
Lemon Seed	Yellow	-	-	○	-	-	-	○
OriW1	Yellow-white bicolor	-	-	-	-	-	-	-
W4	Yellow-white bicolor	-	-	-	-	-	-	-
Gitt's Attention	Ivory white	-	-	-	-	-	-	-
Hakuba	Ivory white	-	-	-	-	-	-	-
Hakuho	Ivory white	-	-	○	-	-	-	-
Hakuyo	Ivory white	-	-	○	-	-	-	-
Jyuhyo	Ivory white	-	-	-	-	-	-	-
Kamakura	Ivory white	-	-	○	-	-	-	-
Malcoms White	Ivory white	-	-	-	-	-	-	-
Smile White	Ivory white	-	-	○	-	-	-	-
Vada	Ivory white	-	-	-	-	-	-	-
Yukimukae	Ivory white	-	-	○	-	-	-	-
Zannsetsu	Ivory white	-	-	-	-	-	-	○

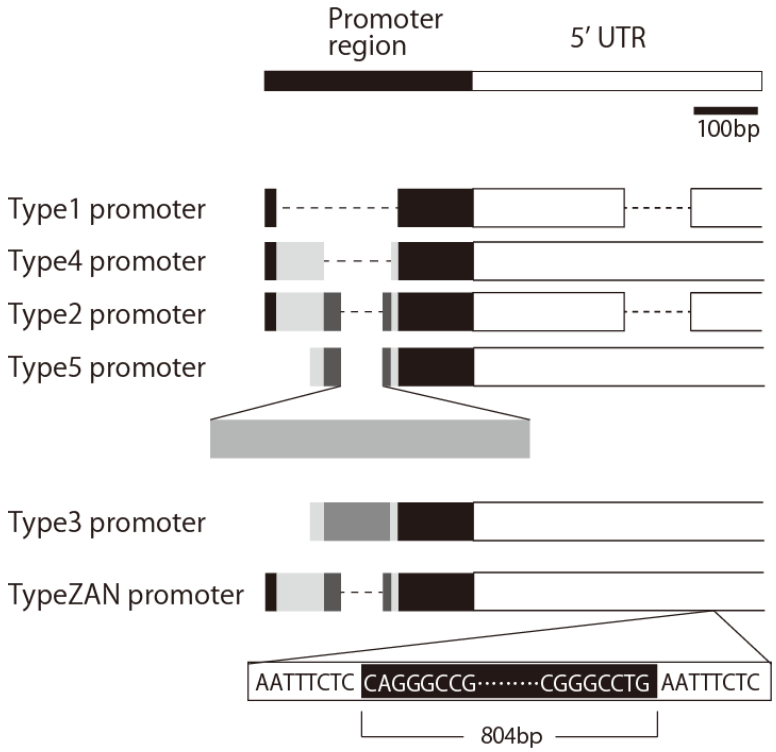

Fig. 2-10. *DvIVS* promoter types discovered from total 55 cultivars or seeding. Type ZAN has the transposon-like insertion in the 5' UTR.

Discussion

Anthocyanin contents determine flower color intensities in cyanic dahlia cultivars

In this study, the factors determining the flower color intensity of cyanic dahlia cultivars were analyzed. Usually flower color is determined by pigment composition and amount. Fifteen cultivars were classified into three groups by flavonoid composition: cultivars with flavones, cultivars with flavones and anthocyanins, and cultivars with flavones, anthocyanins, and butein (Table 2-6). All commercial red cultivars belonged to the last group, indicating that the purple anthocyanin pigments and the yellow pigment butein confer red flower color, and were excluded from further analysis. The remaining twelve cultivars containing anthocyanins and/or flavones were used for further studies.

Although no difference was observed in flavonoid composition among deep purple, purple, and pink cultivars, their L^* values, an indicator of flower color intensity, were different (Fig. 2-2, Table 2-7). Anthocyanin contents and L^* values of the twelve cultivars showed an inverse relationship (Fig. 2-3B), suggesting that the anthocyanin contents determined flower color intensities.

All cultivars accumulated pigments in petal epidermal cells (Fig. 2-4A-D). In the snapdragon (*A. majus*) *mixta* mutant, cell shape is associated with flower intensity (Noda et al., 1994). From a comparative observation of epidermal cell shape, no relationship was detected between flower color intensity and cell shape (Fig. 2-4I), indicating that cell shape is not involved in flower color intensity in cyanic dahlias. In Japanese morning glory (*I. nil*), an increase in vacuolar pH is correlated with bluish flower display (Yoshida et al., 1995). In our study, no significant correlation between L^* value and petal pH was detected (data not shown) suggesting that petal pH contributes little to flower color intensity. From these results, it was concluded that the quantity of total anthocyanins was the principal factor determining flower color intensity in cyanic dahlia cultivars.

Quantitative levels of DvIVS transcripts correlate flower color intensity by regulating

anthocyanin contents

In general, anthocyanin synthesis is regulated by bHLH, MYB, and WDR transcription factors (Koes et al., 2005; Hichri et al., 2011). Overexpression of one of these transcription factors induced high accumulation of anthocyanin in the flower (Laitinen et al., 2008; Pattanaik et al., 2010; Bai et al., 2011). In petunia, common morning glory and tobacco, bHLH transcription factors have been shown to be one of the key factors for floral anthocyanin biosynthesis (Spelt et al., 2000; Park et al., 2007; Bai et al., 2011). In dahlia, demonstrated in the previous section, a bHLH transcription factor *DvIVS* regulates anthocyanin synthesis. Thus, it was assumed that the expression levels of *DvIVS* determined flower color intensity in dahlia.

In the present study, expressions of *DvCHS1*, *DvF3H*, *DvDFR,* and *DvANS* were strongly co-ordinated with both anthocyanin content and the expression of *DvIVS* (Fig. 2-6A–F, 2-7A–F). A positive correlation between expression levels of *DvIVS* and anthocyanin content was detected (Fig. 2-6G). Similarly, in tepals of Asiatic hybrid lilies, a positive correlation between anthocyanin content and *LhMYB12* was found (Yamagishi et al., 2012). In addition, expression levels of *DvMYB1*, *DvMYB2*, *DvR3MYB*, *DvDEL*, and *DvWDR1* which are highly homologous to anthocyanin-regulating transcription factors, didn't show any significant correlation with anthocyanin synthesis gene expression or anthocyanin content (data not shown). These results suggest that *DvIVS* determines the anthocyanin content via regulation of structural genes, thereby regulating intensity of flower color.

The genotype of the DvIVS promoter region corresponds to the expression levels of DvIVS

Twelve cultivars were classified into four groups: deep purple cultivars with high anthocyanin content ('Super Girl' and 'Yukino'), purple cultivars with moderate anthocyanin content ('Cupid', 'Evelyn Rumbold' and 'Atom'), pink cultivars with low anthocyanin content ('Magokoro', 'Jyunn-ai' and 'Saffron'), and ivory white cultivars without anthocyanin ('Gitt's Attention', 'Zannsetsu', 'Hakuba' and 'Hakuyo') (Fig. 2-

3A). The observation of higher expression levels of *DvIVS* in deep purple and purple cultivars carrying Type 1 promoter than in the other cultivars suggested that the genotype of promoter region of *DvIVS* is an important factor in flower color intensity. There was only one allele with Type 1 promoter (mRNA-1) and Type 3 promoter (mRNA-3), whereas there were at least three alleles with Type 2 promoter (mRNA-2, mRNA-4, and an unidentified nonfunctional allele). However, all *DvIVS* transcripts except for the unidentified one encoded a predicted full-length protein and retained the same bHLH domain (Fig. 2-9). This finding suggests that high accumulation of anthocyanin resulted from the total quantity of *DvIVS* transcripts rather than from protein activity encoded by mRNA-1 and that the difference in expression levels of *DvIVS* was due to the difference in the promoter activity. If this inference is true, Type 1 promoter has a stronger activity than Type 2 or Type 3 promoters. Two hypotheses may account for the difference in promoter activity. First, a single nucleotide polymorphism was found in the putative TATA box of the promoter, which is believed to be important for the transcriptional activity. Type 1 promoter had TTAAGTAG, whereas Type 2 and Type 3 promoters had TTAAATAG upstream of the transcription initiation site (Fig. 2-8C). This G to A mutation is the probable cause of low expression. Second, the promoter region itself accounts for the differential expressions. The genomic structure of Type 2 and Type 3 promoter had insertions with respect to Type 1 promoter (Fig. 2-8B). The upstream region near the transcription initiation site is very important for its expression, thus the insertion lowers the expression of *DvIVS*.

There appeared to be at least two different non-functional alleles. The first allele was detected in ‘Hakuyo,’ which had a Type 2 promoter. ‘Hakuyo’ did not express full length transcripts, but expressed the 5′ untranslated region of *DvIVS* (data not shown). This observation indicated that some genomic rearrangement(s) in the coding region led this allele to non-functional. The second was an unidentified allele which other ivory white cultivars would have. Although it cannot be excluded the possibility that alleles act as a negative regulator such as AtMYBL2 (Dubos et al., 2008; Matsui et al., 2008) and

CPC (Zhu et al., 2009), a part of coding region of *DvIVS* were detected from these ivory white cultivars' genome (data not shown), suggesting some genomic rearrangement(s), perhaps in the promoter region, might lead this allele to non-functional. Thereby, further study of the genomic structure of ivory white cultivars will be required to clear the non-functional *DvIVS* alleles.

A functional allele is important for berry color in grape species (*Vitis* × *labruscana* and *V. vinifera*); that is, berry skin color is determined by the number of functional haplotype in MYB A genes (Kobayashi et al., 2002; Kobayashi et al., 2005; Kobayashi, 2009; Azuma et al., 2011). Although the promoter region of mRNA-2 in 'Yukino' was not able to identify, the observation that deep purple cultivars carried only the stronger *DvIVS* promoter, whereas purple cultivars carried a weaker promoter in addition to the stronger promoter, indicated that the functional combination of the *DvIVS* promoter region determines flower color intensity in dahlia. At least, Type 1 promoter may contribute to deep coloring, given that 22 of 55 tested cultivars or seedling lines carried Type 1 promoter and all 22 cultivars showed deep coloring (purple, red or black) (Table 2-9).

Genetic background for flower color of dahlia

Dahlias have one of the largest numbers of cultivars of any cultivated species. Not only flower shape and size, but color variation is very large, with combinations of these factors distinguishing thousands of cultivars. This rich variation may be due to its highly polyploidy genetic background. Gene redundancy is one of the advantages of polyploid species (Comai, 2005); however, from a breeding perspective it may interfere with the rapid development of new cultivars with desirable traits.

In the 1920s and 30s, Lawrence and his colleague proposed four elements of dahlia flower color inheritance; A: pale anthocyanin, B: deep anthocyanin, I: ivory flavone, and Y: yellow flavone (butein) (Lawrence, 1929; Lawrence and Scott-Honcrieff, 1935). In their reports, B (deep anthocyanin) was dominant to A (pale anthocyanin).

Applying these factors to cultivars used in this experiment, pink cultivars might carry only A and purple cultivars might carry B. Thus, it is expected that the weakly functioning *DvIVS* and might correspond to factor A and the strongly functioning *DvIVS* might correspond to B, and that I might correspond to the non-functional *DvIVS* allele carried by ivory white cultivars. Yellow and red cultivars usually contain buteins as a yellow pigment, and cultivars without buteins contain neither butein nor its precursor, isoliquiritigenin. It has shown that anthocyanin synthesis and butein synthesis are mutually independent in dahlia, thus the Y element might correspond to the chalcone reductase gene or its transcription regulation factor.

In this study, it is suggested that more than six *DvIVS* alleles are present in dahlia. Further analysis is required, but in view of the observation that all cultivars carrying Type 1 promoter are deeply colored cultivars, it is suggested that this Type 1 promoter–mRNA-1 allele is the allele responsible for deeply colored cultivars. The finding that the anthocyanin contents or flower color intensities in cyanic cultivars are determined by variation in only one gene, *DvIVS,* is an unexpected result. It is due to high polyploidy in dahlia that the *DvIVS* Type 1 promoter may have been unintentionally selected for breeding as a color regulation factor.

In conclusion, it is suggested that the genotype of *DvIVS* acts as a key factor determining flower color intensity in dahlia by controlling anthocyanin content via the regulation of anthocyanin pathway genes. In many floricultural species, a change in flower color is caused by mutation in specific structural genes. However, due to the presence of gene redundancy in highly polyploid plants such as dahlia, a mutation in one specific structural gene rarely affects its phenotype. Thus, allelic variations in transcription factors, for example a bHLH transcription factor *DvIVS* in the case of dahlia, mainly contributed to diverse phenotypes and were selected in the breeding history.

1.3 Simultaneous post-transcriptional gene silencing of multiple chalcone synthase genes resulting in pure white area formation in bicolor flowering *Dahlia*

Introduction

In dahlias, there are many bicolor flowering cultivars having petals with basal colored part and a white tip. To date, how flowers express white color was analyzed and white flower color could be classified into two groups: ivory white and pure white. Ivory white color is derived from accumulation of white to pale yellow pigments, while pure white is derived from the lack of pigments (Spribille and Forkmann, 1982; Markham and Ofman, 1993; Saito et al., 1994, Onozaki et al., 1999; Saito et al., 2006). In the white areas of petals in bicolor cultivars, no flavonoid derivatives were detected, indicating that their white areas are pure white. In this section, the mechanism underlying for the formation of bicolor pattering was analyzed by comparing with ivory white cultivars.

Material and methods

Plant materials

Three bicolor flowering dahlia cultivars ‘Yuino’ (Fig. 3-1A), ‘Matsuribayashi’ (Fig. 3-1B), and ‘Kazusa-shiranami’ (Fig. 3-1C), two commercial white-flowered cultivars ‘Hakuyo’ (Fig. 3-1D) and ‘Malcoms White’ (Fig. 3-1E), and two white-flowered strains OriW1 (Fig. 3-1F) and OriW2 (Fig. 3-1G) were used. OriW1 and OriW2, seedlings selected from the open crossing of ‘Orihime’ (Fig. 3-1H), were propagated by cuttings. They produce relatively stable, pure white flowers; however, they spontaneously produce flowers with white-colored and yellow- or red-colored petals, respectively (Fig. 3-1I, J). These colored petals were also used for the experiments. The rooted cuttings of all cultivars were transplanted to the Experimental Farm of Kyoto University (Kyoto,

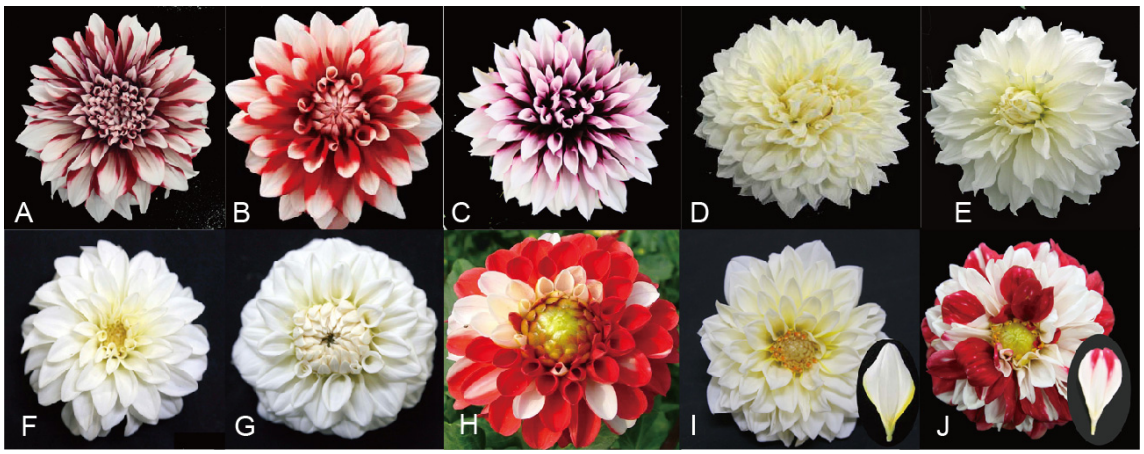

Fig. 3-1. Flowers of bicolor flowering cultivars, ivory white cultivars, pure white seedling cultivars, and their seed parents. Bicolor flowering cultivars: A, ‘Yuino’; B, ‘Matsuribayashi’; C, ‘Kazusa-shiranami’. Ivory white cultivars: D, ‘Hakuyo’; E, ‘Malcoms White’. Pure white varieties and their spontaneously produced colored flowers: F, OriW1 pure white inflorescence; G, OriW2 pure white inflorescence; their seed parent H, ‘Orihime’; I, OriW1 inflorescence with spontaneously produced yellow petals; J, OriW2 inflorescence with spontaneously produced red petals. OriW1 and OriW2 were selected from several seedlings of ‘Orihime’ as the seed parent, the flowers of which appeared pure white. ‘Orihime’ is a labile cultivar which rarely produces red and white petals in an inflorescence. OriW1 and OriW2 spontaneously produce inflorescences with partly or entirely yellow petals and red petals, respectively.

Japan) and the just-opened petals were collected during the flowering seasons.

Pigment analysis

HPLC (LC10A system, Shimadzu) was used to separate hydrolyzed pigments. Pigments were extracted from 1.0 g of fresh petals using 10% methanol-acetic acid solution (methanol: acetic acid = 9:1 v/v) for 24 h at 4ºC. For bicolor cultivars, harvested petals were separated into the colored and white areas using a razor blade. The 2M hydrochloric acid-extracted solutions of each cultivar were boiled for 2 h and used as crude aglycones. HPLC was conducted on an HPLC system with a C18 column (Nihon Waters K.K.), and peaks were detected with a photodiode array detector. The detection wavelength was 350 nm for flavones, 380 nm for chalcones and aurones, and 530 nm for anthocyanidins. Eluent A was 1.5% phosphate dissolved in water and eluent B was 1.5% phosphate, 20% acetic acid, and 25% acetonitrile dissolved in water. The analysis period for each sample was 45 min and comprised 0 min with 20%, 40 min with 85%, and 20% with eluent B at a flow rate of 1 mL min^{-1} at 40ºC.

As for standards, commercially available naringenin (Wako), apigenin (Wako), and luteolin (Wako) and thin layer chromatography (TLC) and HPLC-separated and -purified hydrolyzed cyanidin and pelargonidin from rose petals were used. To obtain hydrolyzed standards of butein, isoliquiritigenin, sulfuretin, and aurone, extracts from the orange petals of the dahlia strain HywR7R (a photograph not shown) were separated by paper chromatography and each band was eluted with methanol. Each elute was further dried and dissolved in a small amount of methanol. The color, Rf value, and maximum wavelength of the eluted compounds were measured (U-2000A, Hitachi) and the compounds were determined by comparing the data with those of authentic butein (kindly supplied by Dr. Norio Saito) and previously reported data (Nordström and Swain 1956). TLC was performed on cellulose-coated plastic sheets (Merck Chemicals Japan, Tokyo, Japan) using two mobile phases: BAW (*n*-butanol:acetic acid:water = 4:1:2 v/v/v) and 30% acetic acid (Harborne, 1984).

Feeding experiments

To confirm the stop position of the anthocyanin biosynthesis pathway, naringenin (product of CHI) or taxifolin (product of F3H) was fed to 'Hakuyo' petals or white areas of the petals of 'Yuino', OriW1, and OriW2. A sample of 500 mg of naringenin (Wako) or taxifolin (Wako) was dissolved in a small amount of ethanol and made up to 1 ml. Just-opened petals cut vertically to the midrib in the middle portion were each immersed in the solution and incubated at 20ºC overnight under dark conditions. The color changes of the immersed petals were determined by their appearances, and the pigments of the reddish petals were extracted and analyzed by HPLC according to the method described above.

Total RNA extraction

Total RNA was extracted from just-opened petals using QuickGene RNA Cultured Cell Kit S (Fujifilm) or Sepasol®-RNA I Super G (Nacalai Tesque) according to the manufacturer's instructions with some modifications. For bicolor cultivars, the whole colored or white area of petals, separated using a razor blade, was used for the extraction. A 0.5-g sample of fresh petals powdered in liquid nitrogen was suspended in the lysis buffer of the cultured cell kit containing 0.3 U α-amylase (Sigma-Aldrich Japan, Osaka, Japan) and incubated for 3 min at room temperature to allow the degradation of the large amount of polysaccharides in the sample. After the amylase treatment, the solution was introduced into the equipped column, and 20 U of DNase (Wako) was added. RNA concentrations were standardized to 100 ng per μL using a spectrophotometer (Nano drop 1000; Thermo Fisher Scientific, Waltham, MA, USA).

Sequencing of CHS *genes expressed in 'Yuino' petals*

Total RNA extracted from bicolor 'Yuino' petals were reverse transcribed by ReverTra Ace (Toyobo) using an oligo-$(dT)_{20}$ primer. Reverse transcripts were amplified

with Blend Taq polymerase (Toyobo) through the following steps: initial denaturation at 94ºC for 2 min, 30 cycles of denaturation at 94ºC for 30 s, annealing at 55ºC for 30 s, and extension at 72ºC for 2 min, and a final extension at 72ºC for 10 min. PCR products were cloned into pTAC-1 vectors using DynaExpress TA PCR Cloning Kit (BioDynamics Laboratory) and 20 plasmids of each gene were sequenced. All sequence analyses were performed using a BigDye Terminator v 3.1 Cycle Sequencing Kit and a 3100 Genetic Analyzer (Applied Biosystems). Primers used for PCR are shown in Table 1-1 and Table 3-1.

Semi-quantitative RT-PCR

Reverse transcription was performed with ReverTra Ace (Toyobo), and 1 μL of the RT product was used for PCR. PCR was performed with Blend Taq polymerase (Toyobo) in volume of 10 μL. The PCR reaction was as follows: 94ºC for 2 min, 30 cycles of 94ºC for 30 s, 55ºC for 30 s, 72ºC for 90 s, and finally 72ºC for 10 min. *DvActin* was used as an internal standard for the semi-quantitative RT-PCR. Primers used for semi-quantitative RT-PCR are shown in Table 3-1.

To quantify the two different *CHS* separately, primers were designed for the cDNA sequences that differed between *DvCHS1* and *DvCHS2*. We revealed two alleles each, *DvCHS1-1* and *DvCHS1-2* for *DvCHS1,* and *DvCHS2-1* and *DvCHS2-2* for *DvCHS2,* for each *CHS* which were expressed in 'Yuino' petals. Consequently, the primers for quantification of *DvCHS1* were designed from the homologous sequences of *DvCHS1-1* and *DvCHS1-2*, and primers for *DvCHS2* were designed from the homologous sequences between *DvCHS2-1* and *DvCHS2-2*.

Real-time RT-PCR

Real-time RT-PCR was performed with SYBR Premix Ex TaqII (Takara) according to the manufacturer's instructions and analyzed using a 7900HT Fast Real-Time PCR System (Applied Biosystems). The real-time RT-PCR reaction was conducted

Table 3-1. Primers used for semi-quantitative RT-PCR

Primer		Sequence (5'-3')
DvCHS1	Full-F	AATCCCGGTTTCAAGTGATTA
	Full-R	ATGCAATGTAAGTGACAACATA
DvCHS2	Full-F	TCTTATTACTGCTCGCAATATCTT
	Full-R	AGTTAGGGCGAAATCGGCATGGTA
FNS	F	CTGCGGGATTTCATATCCG
	R	GCAAGGCATTGGTTTTGGACT
FLS	F	CCTTCTGCCATTAACTATCAC
	R	GGTGGATTGTCTTGAGTTATG
DvCHI	Full-F	ATGGCTGGTCTK*GAGGTCGAA
	Full-R	GGGCTGAGCTTATTTATTAC
DvF3H	Full-F	CATCTTTGAAATGGGACGAGACTTC
	Full-R	GATTACTCAAAACACTTCATTATTT
DvDFR	Full-F	ATCGGCTCCTGGTTAGTTAT
	Full-R	CCATTAATAATATGAACTTTATTAA
DvANS	Full-F	TACCTTCCATCCATCATGGTCACTT
	Full-R	GTTCTTAGAATGACCCAAACAACAA
Dv3GT	Full-F	AAGCAATAAGAAAAATGGCGACTA
	Full-R	AAGGCTACCACGATGCAACCAACT
DvActin	F80	TGCTTATGTTGGTGATGAAG
	R276	CCCTGTTAGCCTTAGGATTT
DvMYB1	Full-F	CACAAACATTTTCAATAGAAAATTG
	Full-R	TAAGAAAGTTATACTCCGTTACATC
DvMYB2	Full-F	ACAAAAAAGATATCAAAAAGAACAA
	Full-R	AAATCCAAATGAGAATTCATTTCAT
DvR3MYB	Full-F	TTCTCAAGAATTGTATTGAGAAATT
	Full-R	GATTTGTTAAAAAGACTAATGATAA
DvDEL	Full-F	ATCTCCTCCAATTCATCAAGATTTT
	Full-R	CCTTTTCTACAGATCAATCAAACAT
DvIVS	Full-F	TTTGACGTAATTTTGGACCTAATTT
	Full-R	CATCCATTTTTAAATTGTTTGTGGT
DvWDR1	Full-F	TTTCTACTTTTCCAATAATATCACA
	Full-R	AGATTCTGTAAAACTTAATATGACT
DvWDR2	Full-F	GATACAGATTATCCCCAATTCCAAA
	Full-R	GTATTCCCAAACCTATATAGGCTAA

*K in *DvCHI* Full-F primer indicates T and G.

as follows: 95ºC for 30s followed by 40 cycles of 95ºC for 5 s and 60ºC for 15 s; the single target product proliferation was checked using dissociation curves. For the relative quantification of premature mRNA, CHS1-R1142 or CHS2-Full-R primer (Table 3-2) was used instead of a oligo-$(dT)_{20}$ primer to synthesize first-strand cDNA. The primer set for premature *DvCHS1* mRNA was designed from a number of genomic sequences of abundantly expressed *DvCHS1* alleles, as previously determined, and the primer set for premature *DvCHS2* mRNA was designed from identical regions of two different genome sequences of *DvCHS2* alleles. The intron lengths were 708bp and 822bp for *DvCHS1* and 96bp and 106bp for *DvCHS2*. *DvActin* was used as an internal standard.

Determination and mapping of small interfering RNA of CHS

Small interfering RNA (siRNA) was detected following the method of Hamilton and Baulcombe (1999) with some modifications. Crude total RNA containing siRNA was extracted from 0.5 g of just-opened petals with 1 ml Trizol reagent (Invitrogen). A 20-μg RNA sample was separated on 30% acrylamide gel in 0.5 × TBE buffer and subsequently electroblotted to a Hybond N+ membrane (GE Healthcare) in 0.5% TBE buffer. Digoxigenin-labeled RNA probe was synthesized using T7 RNA polymerase (F. Hoffmann-La Roche AG, Basel, Switzerland) by *in vitro* transcription of 3′ digested pTAC-1 vector carrying the full length of *DvCHS1* in the antisense orientation. For random digestion of the 1,500 bp dig-labeled RNA probe into sections approximately 150 bp long, 15 μg synthesized RNA probe was mixed with an equal volume of carbonic acid buffer (120 mM Na_2CO_3 and 80 mM $NaHCO_3$; pH 10.2) and incubated at 60ºC for 54 min. The reaction was stopped by adding 10% acetic acid to the solution to a final concentration of 0.5%. After EtOH precipitation, the probe was dissolved in ultrapure water, hybridized to the membrane at 42ºC overnight, and the membrane was washed with high- and low- stringency buffers at 42ºC and 25ºC, respectively. Detection was conducted with CDP Star (GE Healthcare) and the fluorescence image was obtained using a LAS-3000 Mini (Fujifilm).

Table 3-2. Primers used to detect mature and premature mRNAs

Primer			Purpose	Sequence (5'-3')
DvCHS1	mature mRNA	Oligo $dT_{(20)}$	RT	$T_{(20)}$
		F1037	qRT-PCR	CATGTGCTAAGCGAATACGG
		R1142	qRT-PCR	CCTCTCCGGTGGTATTGAAC
	premature mRNA	R1142	RT	CCTCTCCGGTGGTATTGAAC
		exon real-time F	qRT-PCR	GTGTGCTCCAAAGCGAGTATC
		intron real-time R	qRT-PCR	TGGAAGGTAAAGTTTTCCCAAA
DvCHS2	mature mRNA	Oligo $dT_{(20)}$	RT	$T_{(20)}$
		F669	qRT-PCR	GTTTCGTGGACCGACGG
		R762	qRT-PCR	CGCTCAGTTGTCAAGTCC
	premature mRNA	Full-R	RT	AGTTAGGGCGAAATCGGCATGGTA
		exon 2-F	qRT-PCR	TCATCGAATATTTAAAATTAGGGTTTT
		intron 2-R	qRT-PCR	CGGAGCCATGTACTCACAGA
DvActin	mature mRNA	Oligo $dT_{(20)}$	RT	$T_{(20)}$
		F80	qRT-PCR	TGCTTATGTTGGTGATGAAG
		R276	qRT-PCR	CCCTGTTAGCCTTAGGATTT

For deep sequencing analysis of small RNAs accumulating in the petals of 'Yuino', small RNAs were extracted from 1.0 g of pure white part or red part of a petals using a MirVana miRNA Isolation Kit (Applied Biosystems) according to the manufacturer's instructions. Small RNAs were sequenced using an Illumina Genome Analyzer or Illumina Hiseq (Illumina, San Diego, CA, USA). Small RNAs of 18-32 nt were mapped onto the transcript sequences of *DvCHS1-1*, *DvCHS1-2*, *DvCHS2-1*, *DvCHS2-2*, *DvCHS3-1*, *DvCHS3-2* and *DvCHS4* using Bowtie software without any mismatch.

Results

Pigment determinations

Flavones, such as apigenin and luteolin derivatives, were detected in the petals of the ivory white-flowered cultivars 'Hakuyo' and 'Malcoms White' (Fig. 3-1D, E), whereas anthocyanidin, chalcone and aurone derivatives remained undetected (Table 3-3). The colored areas of bicolor flowering cultivars 'Yuino', 'Matsuribayashi', and 'Kazusa-shiranami' (Fig. 3-1A–C) contained anthocyanidins. Among these, the chalcone derivatives and flavone derivatives were detected in 'Yuino' and 'Matsuribayashi'.

Table 3-3. Flavonoid compositions of petals used in the experiments

Cultivars	Chalcone derivatives		Aurone derivative	Flavanone derivatives	Flavone derivatives		Anthocyanidin derivatives	
	Butein	Isoliquiritigenin	Sulfuretin	Naringenin	Apigenin	Luteolin	Cyanidin	Pelargonidin
'Hakuyo'	-	-	-	-	+	+	-	-
'Malcoms white'	-	-	-	tr	+	+	-	-
'Yuino' white area	-	-	-	-	-	-	tr[z]	tr[z]
'Yuino' red area	+	tr	tr	-	+	+	+	+
'Matsuribayashi' white area	-	-	-	-	-	-	tr[z]	tr[z]
'Matsuribayashi' red area	+	tr	tr	-	+	+	+	+
'Kazusa-shiranami' white area	-	-	-	-	tr[z]	tr[z]	tr[z]	tr[z]
'Kazusa-shiranami' black area	-	-	-	-	-	-	+	+
OriW1 white petal	-	-	-	-	-	-	-	-
OriW1 yellow petal	+	tr	+	-	+	+	-	-
OriW2 white petal	-	-	-	-	-	-	-	-
OriW2 red petal	+	tr	tr	-	+	+	+	+

+: detected tr: trace detected -: not detected.

[z] Tr is considered to be due to contamination from the cut margin.

However, no flavonoid derivatives were detected in the white areas of these three bicolor flowering cultivars (Table 3-3). In the white areas of OriW1 and OriW2, no flavonoid compound was detected (Table 3-3). However, flavonoid derivatives were detected in the spontaneously produced colored petals in the inflorescences of these two strains (Fig.3-1I, J); chalcone, aurone, and flavone derivatives were detected in the yellow petals of OriW1 and anthocyanidin, chalcone, aurone and flavone derivatives in the red petals of OriW2 (Table 3-3). These results showed that the white area of bicolor flowering cultivars, OriW1 and OriW2 are pure white, whereas white petals of ivory white cultivars are not.

Feeding experiments

To predict the stop step of flavonoid biosynthesis in the pure white areas, chemical feeding experiments were performed using naringenin and taxifolin, which are synthesized by CHI and F3H, respectively. Since chalcone (4,2′,4′,6′-tetrahydroxychalcone) synthesized by CHS spontaneously converts to naringenin in solutions without CHI, we used naringenin instead of chalcone (4,2′,4′,6′-tetrahydroxychalcone). If the anthocyanin synthesis pathway below CHS is active, petals turn to red by synthesized anthocyanins. As expected, the pure white areas of 'Yuino' and OriW2 turned red by the feeding treatment (Fig. 3-2B, D). HPLC showed the red pigments to be cyanidin and pelargonidin derivatives (data not shown). However, anthocyanin production in the fed portion was not observed after naringenin and taxifolin feeding treatments in 'Hakuyo' and OriW1 (Fig. 3-2A, C). Consequently, anthocyanin derivatives were produced only in the pure white areas where the *DvIVS* gene was expressed, and all of the cultivars that did not express the *DvIVS* gene could not produce anthocyanin derivatives. These results indicate that all of the structural genes, except for *CHS*, are normally expressed in the pure white areas of 'Yuino' and OriW2.

Semi-quantitative RT-PCR

The expression of the genes involved in flavonoid biosynthesis was analyzed,

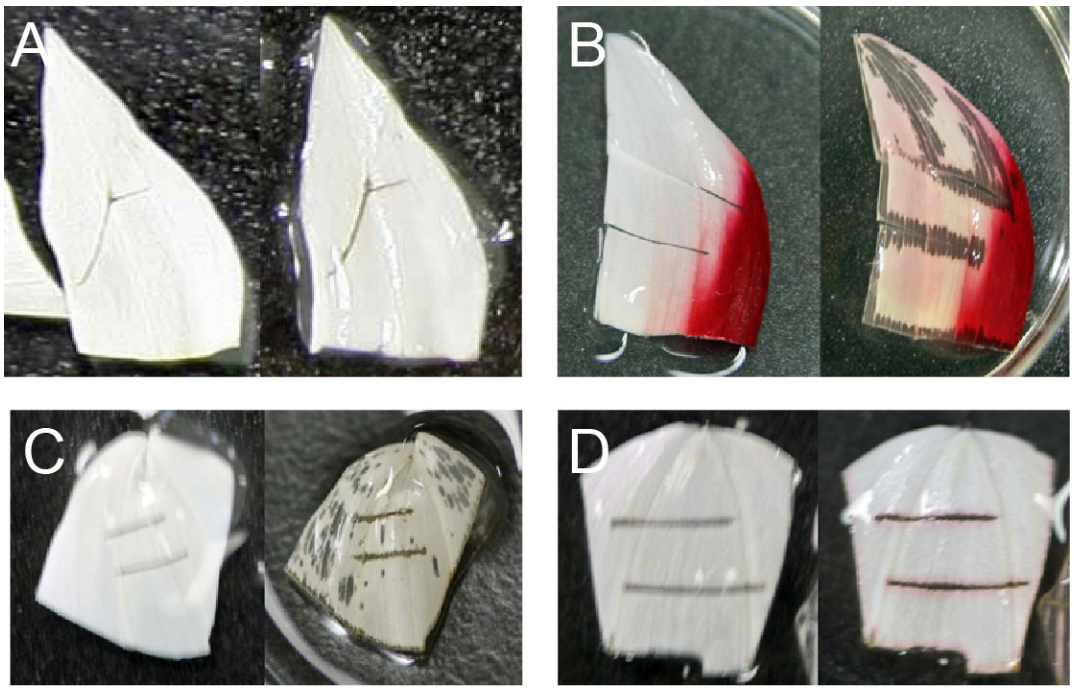

Fig. 3-2. Feeding experiments of anthocyanin precursors in white areas. Left, just after feeding treatment. Right, one day after treatment. A, 'Hakuyo'; B, 'Yuino'; C, OriW1 and D, OriW2. White areas of 'Yuino' and OriW2 turned to red in the fed areas, the other cultivars did not express red derivatives (right panels of A, B, C, and D). Red products were identified as anthocyanidin by HPLC. These photographs were those of taxifolin-(flavanonol) fed petals. The results of the naringenin feeding were same as those of taxifolin feeding.

including nine structural genes (*DvCHS1*, *DvCHS2*, *DvCHI*, *DvFNS*, *DvFLS*, *DvF3H*, *DvDFR*, *DvANS*, and *Dv3GT*) and seven regulatory genes (*DvMYB1*, *DvMYB2*, *DvR3MYB*, *DvIVS*, *DvDEL*, *DvWDR1*, and *DvWDR2*), by RT-PCR in 'Hakuyo', 'Malcoms White', 'Yuino', OriW1 and OriW2 (Fig. 3-3). In the commercial white cultivars, little or no expressions of *DvCHS1*, *DvF3H*, *DvDFR*, and *DvANS* were detected (Fig. 3-3). Of the seven regulatory genes, only *DvIVS* was not expressed (Fig. 3-3). *DvIVS* expression seemed to correspond with those of *DvCHS1*, *DvF3H*, *DvDFR*, and *DvANS* indicating that the expressions of these structural genes are activated by *DvIVS*.

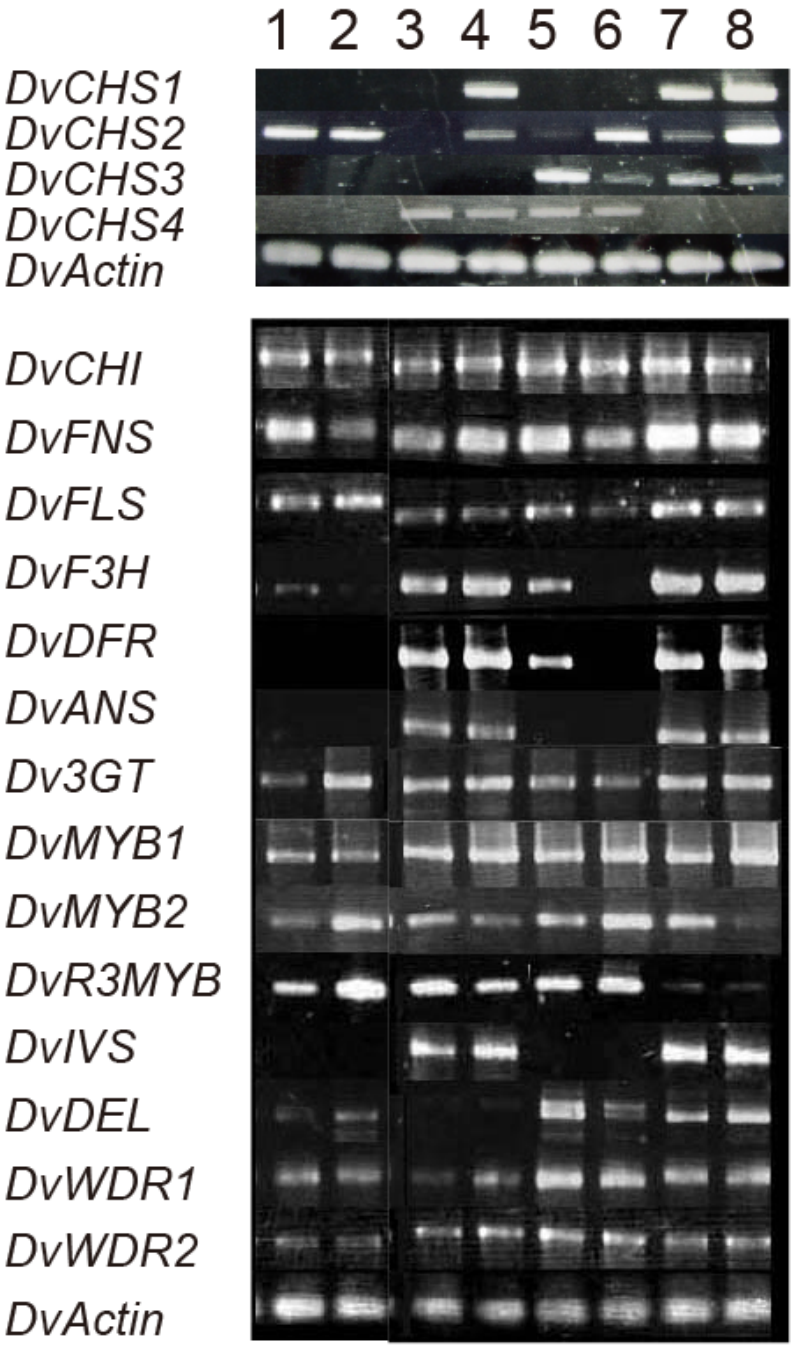

Fig. 3-3. Semi-quantitative analysis of RNA expression. Numbers above the lanes indicate each cultivar: 1, 'Hakuyo'; 2, 'Malcoms White'; 3, white area of 'Yuino'; 4, red area of 'Yuino'; 5, white area of OriW1; 6, yellow area of OriW1; 7, white area of OriW2 and 8, red area of OriW2.

Transcripts of other genes including *DvCHS2* were detected in these ivory white cultivars (Fig. 3-3). In both the colored and pure white areas of 'Yuino' and OriW2, transcripts of all the structural genes were detected. But the signals of the RT-PCR products of *DvCHS1* and *DvCHS2* in the pure white areas were weaker than those in the colored areas (Fig. 3-3). Although traces of *DvF3H* and *DvANS* in the pure white areas were observed in both the spontaneously produced yellow areas and the pure white areas of OriW1, suppressions of *DvCHS1*, *DvF3H*, *DvDFR*, *DvANS*, and *DvIVS* were also observed. In addition, lower expression levels of *DvCHS2* were observed in the pure white areas of OriW1 (Fig. 3-3).

The temporal expression of the *CHS* genes was further characterized. In the red areas of 'Yuino', transcripts of *DvCHS1* and *DvCHS2* were detected regardless of the petal developmental stage, except during the early stage. However, there appeared to be fewer transcripts in the pure white areas than in the red areas (Fig. 3-4).

Real-time RT-PCR of mature and premature DvCHS1 and DvCHS2 mRNAs

The relative expression levels of the *CHS* genes were compared among the cultivars by real-time RT-PCR. In 'Hakuyo' and 'Malcoms White', the *DvCHS1* mRNA was not detected but *DvCHS2* expression was detected by real-time RT-PCR (data not shown), which was consistent with the RT-PCR results (Fig. 3-3). In 'Yuino', the accumulation of the *DvCHS1* and *DvCHS2* mRNAs was lower in the pure white areas than in the colored areas by about 1/4 and 1/20, respectively (Fig. 3-5A, C). Similarly, the accumulation of the *DvCHS1* and *DvCHS2* mRNAs in the pure white areas of OriW2 was lower by about 1/4 and 1/7, respectively, than in the colored areas. In OriW1, the *DvCHS1* mRNA was not detected regardless of petal color, while the *DvCHS2* mRNA accumulated in the pure white areas was seven times lower than that in the spontaneously produced yellow areas (Fig. 3-5A, C).

In the pure white areas of 'Yuino' and OriW2, the accumulation of premature mRNA of *DvCHS1*, considered to reflect the transcription of the *DvCHS1* gene was almost the same as or rather higher than that in the colored areas (Fig. 3-5A, B). In OriW1,

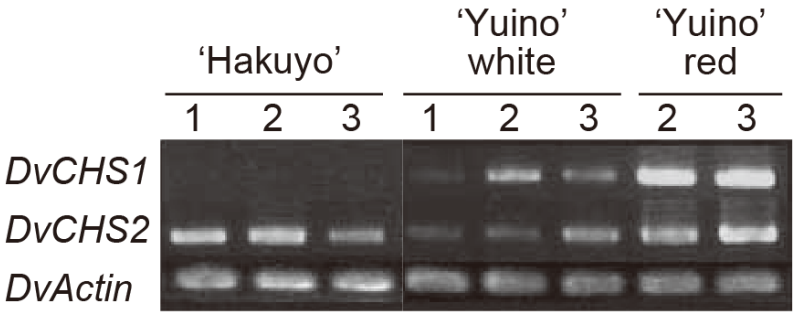

Fig. 3-4. Expression analysis of *DvCHS1* and *DvCHS2* during the stage of petal development. Petals of the commercial white cultivar 'Hakuyo' did not express *DvCHS1* at any developmental stage but expressed *DvCHS2* at all stages of development. Clear bands of *DvCHS1* and *DvCHS2* were observed in the red areas in 'Yuino'. However, in the white areas, the pale bands of both *CHS* genes were detected. The petals of 'Yuino' are not colored at stage 1, so the RNA extraction was conducted using whole petals of stage 1. Stage 1, 0.5 mm of unopened petal; stage 2, two-thirds sized petals of the fully open petals (at the stage of coloration) and stage 3, fully open petals.

premature *DvCHS1* mRNA was not detected regardless of petal color. The results were similar for *DvCHS2*; the accumulation of *DvCHS2* mRNA was lower in the pure white areas than in the colored areas, whereas the accumulation of the premature *DvCHS2* mRNA was not as low or rather higher in the pure white areas than in the colored areas (Fig. 3-5C, D).

Analysis of CHS small RNAs

To test whether the PTGS of the *CHS* genes is mediated by siRNA in the pure white areas of 'Yuino', OriW1, and OriW2, we characterized siRNA accumulation in these cultivars using RNA gel blot analysis. Using fragmented antisense *DvCHS1* as a probe, siRNA of approximately 24 nucleotides was detected in the pure white areas of 'Yuino', OriW1, and OriW2, whereas siRNA was not detected in 'Hakuyo' and 'Malcoms White' and in the colored areas of 'Yuino', OriW1, and OriW2 (Fig. 3-6).

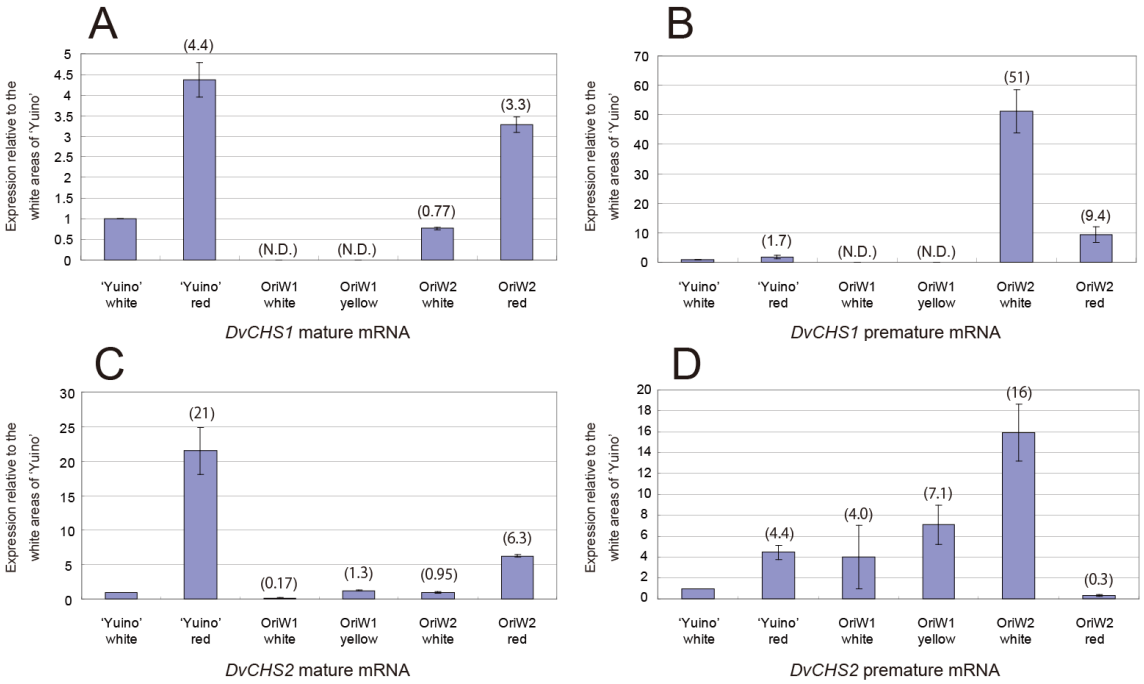

Fig. 3-5. Real-time RT-PCR for mature and premature *CHS* mRNA expression. A, mature *DvCHS1* mRNA; B, premature *DvCHS1* mRNA; C, mature *DvCHS2* mRNA and D, premature *DvCHS2* mRNA. Bars indicate the ± SE (n = 3). Each bar represents the expression levels relative to 'Yuino' and the figures on each bar represent the relative expression levels. In OriW1, mature and premature *DvCHS1* mRNA was not detected. *DvActin* was used as the internal standard and data were calculated as the expression relative to *DvActin* expression. Standard curves for each gene were prepared from the diluted series of cloned vectors, respectively.

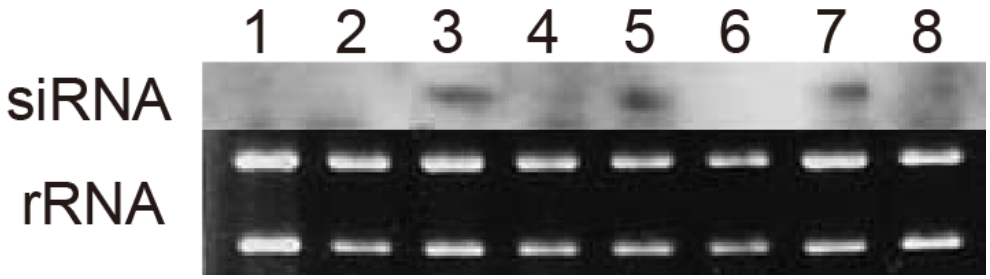

Fig. 3-6. RNA gel blot hybridization for *CHS* siRNA detection. 1, 'Hakuyo'; 2, 'Malcoms White'; 3, white area of 'Yuino'; 4, red area of 'Yuino'; 5, white area of OriW1; 6, yellow area of OriW1; 7, white area of OriW2 and 8, red area of OriW2.

To analyze further, the sequences of *DvCHS1*, *DvCHS2, DvCHS3* and *DvCHS4* transcripts expressed in 'Yuino' bicolor petals was determined. We found two sequences for *DvCHS1-3* and one for *DvCHS4*: *DvCHS1-1* and *DvCHS1-2* for *DvCHS1*, *DvCHS2-1* and *DvCHS2-2* for *DvCHS2, DvCHS3-1* and *DvCHS3-2* for *DvCHS3*. In the phylogenetic tree for coding sequences, *DvCHS1*, *DvCHS2* and *DvCHS4* are close to CHSs, while *DvCHS3* is close to other polyketide synthases (Fig. 3-7A). On the other hand, in the phylogenetic tree for putative amino acid sequence, *DvCHS1* and *DvCHS2* are close to CHSs, while *DvCHS3* and *DvCHS4* are close to other polyketide synthases (Fig. 3-7B). Comparing *DvCHS1-1* and *DvCHS2-1*, which share 69% identity with the nucleotide sequence in the open reading frame (ORF)(Table 3-4), the longest continuous identical sequence consisted of 17 nt (Fig. 3-8). Phylogenetic analysis of the nucleotide sequences in the ORFs of higher plants' *CHS,* including dahlia, petunia, and soybean, showed that *DvCHS1* and *DvCHS2* belong to a relatively distant subgroup than *PhCHSA* and *PhCHSJ* or *GmCHS3* and *GmCHS7* (Fig. 3-7A).

To ensure that the two phylogenetically different *CHS* genes are post-transcriptionally silenced by siRNAs, a deep sequencing analyses of the small RNAs accumulating in the red areas and pure white areas of 'Yuino' were performed. The total reads of 18–32 nt were 13,681,764 reads for a red petal, and 17,455,041 reads for the white part of a bicolor petal. When no mismatch was allowed, whereas small RNAs from a red petal was mapped only few (Fig. 3-9A), small RNAs from the white part of a bicolor petal were abundantly mapped on *DvCHS1-1*, *DvCHS1-2*, *DvCHS2-1*, and *DvCHS2-2* (Fig. 3-9B). Almost all small RNAs derived from sense and antisense strands were mapped on exon 2, as reported in other species (De Paoli et al., 2009; Kurauchi et al., 2009; Tuteja et al., 2009) (Fig. 3-9B). Two alleles of *DvCHS1* and *DvCHS2* genes could be identified by 19 single nucleotide polymorphisms (SNPs) and 39 SNPs, respectively, in their full length mRNAs (Table 3-5, Table 3-6). For *DvCHS1*, mapped abundance between *DvCHS1-1* and *DvCHS1-2* were nearly the same (Table 3-5), while for *DvCHS2*, *DvCHS2-1* was more abundantly mapped than *DvCHS2-2* (Table 3-6).

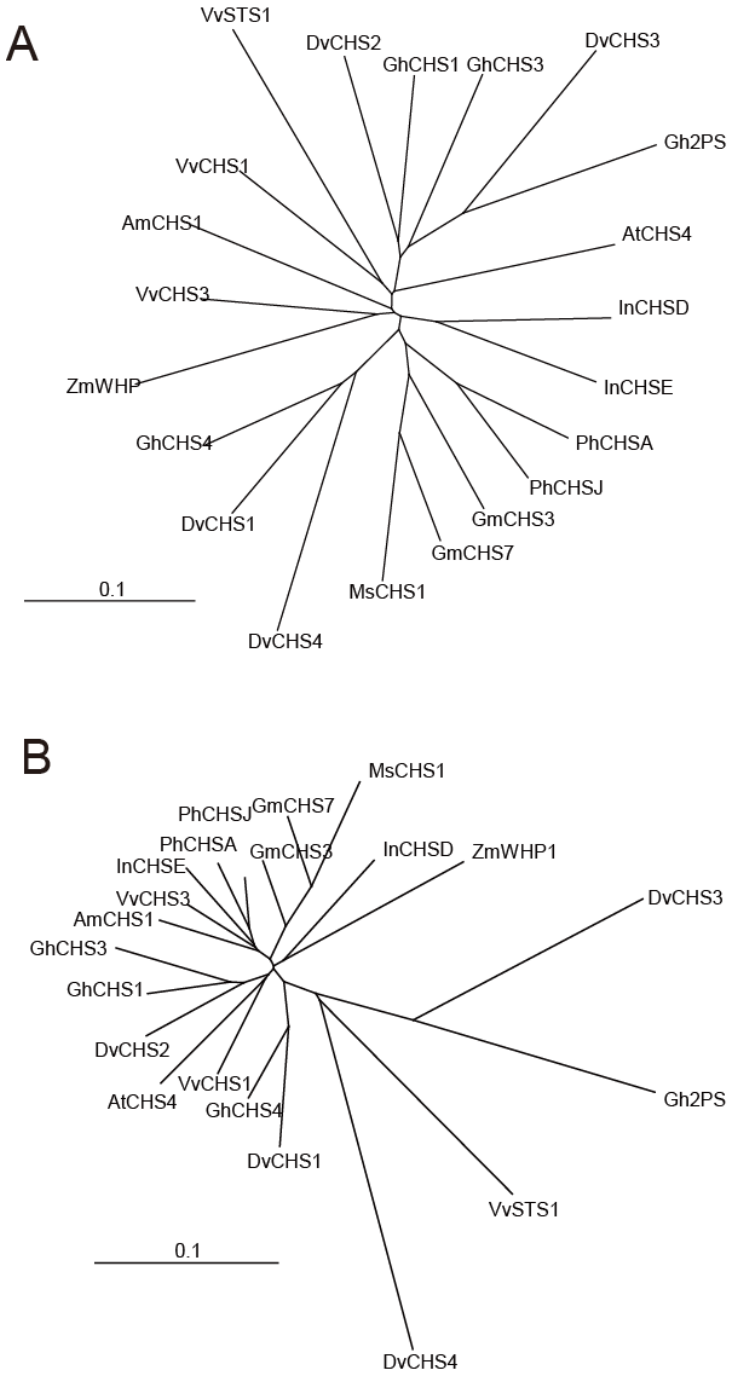

Fig. 3-7. Phylogenetic tree for CHS. A, the phylogenetic tree for coding region; B, phylogenetic tree for putative amino acid sequence. The abbreviation shown in front of each protein indicates plant species: Dv, *Dahlia variabilis*; Am, *Antirrhinum majus*; At, *Arabidopsis thaliana*; Gh, *Gerbera hybrida*; Gm, *Glycine max*; In, *Ipomoea nil*; Ms, *Medicago sativa*; Ph, *Petunia hybrida*; Vv, *Vitis vinifera*; Zm, *Zea mays*. The abbreviation for protein names: STS, Stilbene synthase; 2PS, 2-pyrone synthase.

Fig. 3-8. Comparison of the *DvCHS1-1* and *DvCHS2-1* genes. The alignment of the nucleotide sequences of two *CHS* ORFs is shown. Analysis was conducted using ClustalW. The letters in white on a black background indicate the continuum identity sequence of over 10 nucleotides.

Table 3-4. Percentage coding reagion and putative amino acid sequence identity of pair wise alignments of the CHS gene family in dahlia

	CHS1-1	CHS1-2	CHS2-1	CHS2-2	CHS3-1	CHS3-2	CHS4
CHS1-1	100(100)						
CHS1-2	98(98)	100(100)					
CHS2-1	69(82)	69(82)	100(100)				
CHS2-2	69(81)	69(82)	96(99)	100(100)			
CHS3-1	64(68)	64(69)	68(70)	68(69)	100(100)		
CHS3-2	64(67)	63(68)	67(69)	67(69)	95(94)	100(100)	
CHS4	73(73)	73(73)	63(67)	63(67)	62(61)	62(61)	100(100)

Numbers out of parentheses indicate the identity percentage of cording reagion sequence, and numbers in parentheses indicate the identity percentage of putative amino acid sequence.

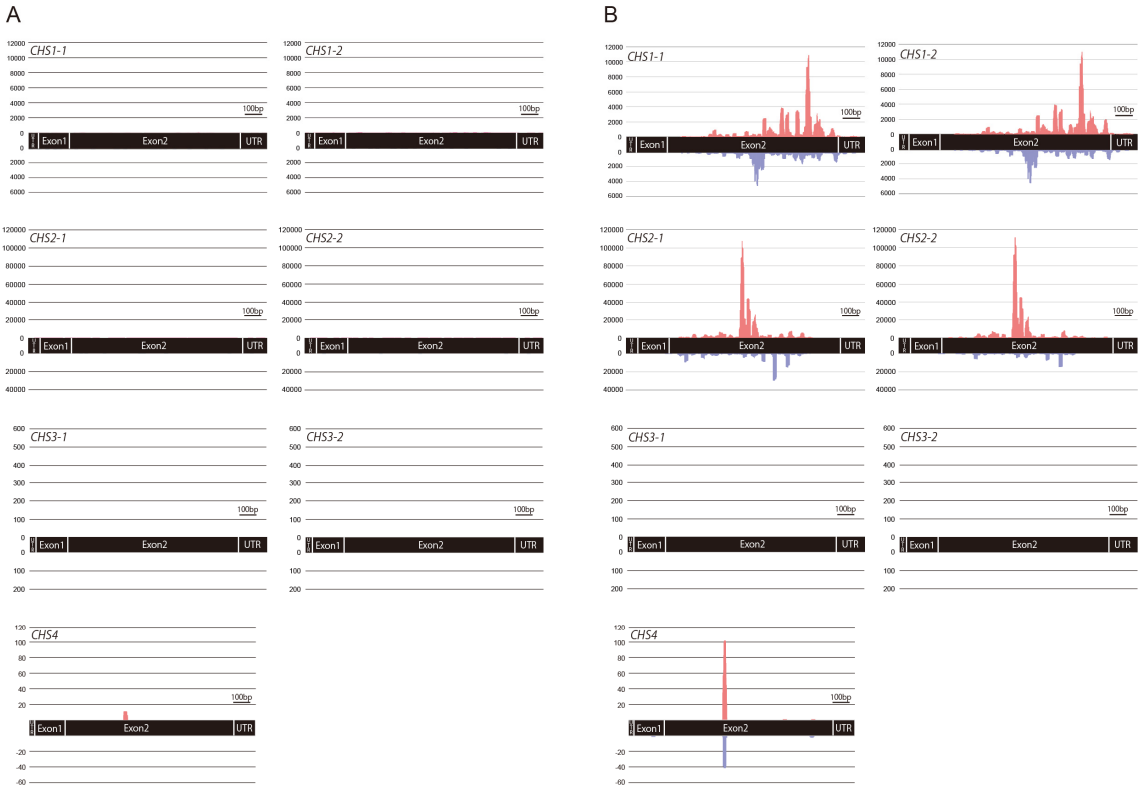

Fig. 3-9. Mapping of *CHS* small RNAs. A, a red petal; B, the white part of a bicolor petal. 18–32 nt small RNAs with 100% match to the *DvCHS1-1*, *DvCHS1-2*, *DvCHS2-1*, *DvCHS2-2*, *DvCHS3-1*, *DvCHS3-2* or *DvCHS4* genes were mapped on either the sense (pink: above the X-axis) or antisense (blue: below the X-axis) strand. The total reads of 18–32 nt were 13,681,764 reads for a red petal, and 17,455,041 reads for the white part of a bicolor petal.

Table 3-5. The number of mapped CHS small RNAs at SNPs between *DvCHS1-1* and *DvCHS1-2*.

DvCHS1-1	37G	-	124C	196G	202T	258C	418T	580A	601G	610C	613T	622G	656A	772C	955A	994G	1023A	1153G	1183G	1236T	1272C
DvCHS1-2	37A	40-46TCTAAAA	131T	203A	209C	265T	425G	587G	608C	617A	620C	629C	663G	779T	962G	1001A	1030G	1160C	1190A	1243C	1279T
1-1 sense	0	0	0	16	12	0	52	335	49	46	447	492	88	387	232	3321	680	30	1036	89	31
1-2 sense	0	0	7	8	8	15	38	314	24	130	232	319	58	386	141	1026	1394	59	1813	73	36
1-1 anti	0	0	0	0	0	0	88	71	32	44	46	127	393	898	92	136	701	62	69	38	43
1-2 anti	1	1	1	3	2	4	82	40	29	60	75	233	104	813	85	161	156	47	194	29	110

Table 3-6. The number of mapped CHS small RNAs at SNPs between *DvCHS2-1* and *DvCHS2-2*.

DvCHS2-1	151T	160G	298T	322G	325T	328C	331T	349T	406G	409T	412C	436A	484T	523T	526T	529C	598T	625G	628A	640T
DvCHS2-2	151C	160C	298C	322C	325C	328T	331C	349C	406T	409G	412G	436G	484C	523A	526G	529T	598C	625A	628C	640C
2-1 sense	8	13	200	1164	1269	1260	862	622	4523	3416	3361	154	1826	1190	1161	2295	1040	2568	2509	401
2-2 sense	1	0	327	43	59	62	53	54	144	113	98	34	2179	175	165	2793	316	3228	3219	183
2-1 anti	0	6	157	3426	2273	2186	2073	9746	1630	308	258	626	387	2310	2704	2739	860	673	717	869
2-2 anti	0	2	126	178	120	108	138	512	136	113	111	1534	226	517	276	268	218	214	120	219

DvCHS2-1	658T	736G	770A	811G	829G	868G	880T	889T	919G	952G	1003G	1024C	1042A	1052A	1075T	1141A	1148G	1222G	1237T
DvCHS2-2	658C	736T	770G	811A	829C	868T	880C	889C	919A	952A	1003A	1024T	1042G	1052C	1075C	1141G	1148T	1222T	1237C
2-1 sense	1611	2436	11792	1440	1535	463	776	662	4708	1448	598	1639	5761	1560	750	118	67	148	2
2-2 sense	639	873	7114	1	958	688	523	546	1303	383	178	893	2052	970	1653	246	244	1049	1
2-1 anti	850	319	2413	9165	676	30817	29346	193	656	15674	361	3441	927	625	178	50	46	15	38
2-2 anti	260	1663	1267	2	286	7696	6890	103	280	14668	669	1746	169	182	100	20	17	1	14

Discussion

The white areas of bicolor cultivars are pure white

Bicolor dahlia cultivars are attractive cultivars that produce inflorescences with petals characterized by a colored basal part and a white tip (Fig. 3-1). On exposure of petals to ammonia gas, the ivory white petals of commercial ivory white cultivars become yellow; however, the white areas of bicolor flowering dahlia cultivars remain white (data not shown), suggesting that the latter does not contain any flavonoids, namely pure white. The pure white phenotype in flower was caused by a mutation on *CHS* gene in *A. majus* (Spribille and Forkmann 1982), *I. nil* (Hoshino et al., 2009), and *Matthiola incana* (Hemleben et al., 2004). Feeding experiments suggested that downstream from F3H of anthocyanin biosynthetic pathway was functional (Fig. 3-2). Therefore it is suggested that the pure white area in bicolor cultivars is formed by loss of CHS function. This was completely different from ivory white cultivars that accumulate flavone derivatives in their petals.

DvCHS1 *and* DvCHS2 *are post-transcriptionally suppressed in the pure white area*

CHS is known to belong to multigene family, and dahlias have redundant *CHS* derived from their high polyploidy. Four different *CHS* genes, *DvCHS1*, *DvCHS2*, *DvCHS3* and *DvCHS4* are isolated in dahlia (see Chapter1, 1.1). All four *DvCHS* genes have the characteristic intron insertion site conserved in polyketide synthase (Zheng et al., 2001), while only *DvCHS1* and *DvCHS2* genes have almost conserved CHS active site residues (Ferrer et al., 1999; Ma et al., 2009). The phylogenetic tree of putative amino acid sequence (Fig. 3-7B) also suggested that DvCHS1 and DvCHS2 function as chalcone synthase, while DvCHS3 and DvCHS4 function as stilbene synthase rather than chalcone synthase.

The expressions of *DvCHS1* and *DvCHS2* were low in the pure white areas of ‘Yuino’ and OriW2, and that of *DvCHS2* was low in OriW1, compared to that in the

colored areas (Figs. 3-3, 3-5A, C). We could detect *DvCHS2* transcripts in the ivory white cultivars ‘Hakuyo’ and ‘Malcoms White’, at levels 3.8 and 4.2 times greater than those in the pure white areas of ‘Yuino’, respectively (data not shown). These results suggest that the pure white areas in ‘Yuino’, OriW1 and OriW2, develop due to the reduction in the level of *DvCHS1* and *DvCHS2* mRNAs. We also analyzed the transcription levels of premature *DvCHS1* and *DvCHS2* mRNA in the colored and pure white areas of ‘Yuino’, OriW1 and OriW2, because PTGS usually occurs only in mature mRNA and not in premature unspliced mRNA. Primers for mature mRNAs can also detect premature mRNAs. However, since the amounts of premature mRNAs were assumed to be much lower than those of mature mRNAs, we regarded the score to be similar to that of mature mRNAs. The results revealed that the quantity of premature *DvCHS1* mRNA was nearly the same in the pure white and colored areas of ‘Yuino’ and relatively higher in the pure white areas of OriW2 (Fig. 3-5C). In *DvCHS2*, the difference between the pure white and colored areas was lower for premature mRNA than for mature mRNA in ‘Yuino’ and OriW1, and the amount of premature mRNA in the pure white area was higher than that in the colored areas in OriW2 (Fig. 3-5D). Suppression of the transcript abundance (mature mRNAs) of *DvCHS1* and *DvCHS2* was greater than the decrease in the transcription levels (premature mRNAs) in the pure white areas. These results indicate that the transcription of both *DvCHS1* and *DvCHS2* occurs normally in the colored and pure white areas, while the suppression of mRNA occurs post-transcriptionally in the pure white areas. The decrease in premature mRNA levels observed in the pure white areas of ‘Yuino’ and OriW1 may be caused by epigenetic modifications, because endogenous siRNA induces not only target RNA cleavage but also epigenetic modifications, such as DNA methylation and histone modification (Ghildiyal and Zamore, 2009).

Simultaneous PTGS of DvCHS1 *and* DvCHS2 *are involved in pure white area formation*

In ‘Michael J’, 12 sequences of *DvCHS1* mRNA and two sequences of *DvCHS2* mRNA are expressed in petals (Table. 1-10), suggesting multiple alleles or loci must be

silenced for pure white phenotype. As an aggressive gene suppression process, PTGS, RNA interference and virus-induced gene silencing are known to suppress multigene family members and redundant genes simultaneously, for example, in polyploid species (Napoli et al., 1990; Van Der Krol et al., 1990; Lawrence and Pikaard, 2003; Fukusaki et al., 2004; De Paoli et al., 2009; Jiang et al., 2011). Thus, PTGS of *CHS* is expected to result in pure white areas of petals in dahlia.

The pure white areas of 'Yuino', OriW1 and OriW2, accumulated endogenous siRNA carrying *CHS* sequences (Fig. 3-6). siRNA was detected only in the pure white areas. Hence, siRNA-mediated PTGS of *CHS* is assumed to be the main cause of pure white phenotypic traits. However, RNA gel blot hybridization could not determine whether PTGS occurred in both *DvCHS1* and *DvCHS2*, since the *DvCHS1* antisense RNA used as a probe could hybridize to *DvCHS1* and *DvCHS2* siRNAs. Indeed, siRNA was detectable with the *DvCHS1* probe in OriW1, whose transcription of *DvCHS1* is inactive. This is believed to be the result of cross-hybridization of the *DvCHS1* probe to *DvCHS2* siRNA. In fact, it was ascertained that the *DvCHS1* probe was able to hybridize to *DvCHS2* RNA fragments transcribed *in vitro* under the same experimental conditions, and that the *DvCHS2* probe could also detect *DvCHS1* RNA fragments (data not shown).

From the deep sequencing analysis, small RNAs that accumulated in the pure white areas of 'Yuino' were mapped on *DvCHS1-1* and *DvCHS1-2* or *DvCHS2-1* and *DvCHS2-2* (Fig. 3-9B), while small RNAs that accumulated in the red areas of 'Yuino' were rarely mapped (Fig. 3-9A). Almost all small RNAs were mapped on exon 2 of *DvCHS1* and *DvCHS2* (Fig. 3-9B), as in soybean and petunia (De Paoli et al., 2009; Kurauchi et al., 2009; Tuteja et al., 2009; Morita et al., 2012), suggesting that the main cleavage site is located on exon 2. These results strongly indicate that the detected *CHS* siRNAs (Fig. 3-6) contained both *DvCHS1* and *DvCHS2*, and that all alleles of *DvCHS1* and *DvCHS2* were silenced in the pure white area of 'Yuino'. In the seed coats of yellow soybean (*G. max*), all nine *CHS* are simultaneously silenced by PTGS (Kurauchi et al., 2009; Tuteja et al., 2009). In star-type cultivars of petunia, PTGS of *CHS* producing pure

white flowers (Metzlaff et al., 1997; Koseki et al., 2005), and both *PhCHSA* and *PhCHSJ* are endogenously silenced (Morita et al., 2012). Transgenic petunia plants that exhibit cosuppression of *PhCHSA* also suppressed both *PhCHSA* and *PhCHSJ* (De Paoli et al. 2009). Because *CHS* genes have high sequence similarities, a specific sequence of siRNA is considered to induce simultaneous silencing of both *GmCHS*s or *PhCHSA* and *PhCHSJ*. However, in dahlia, the nucleotide sequence identity of ORFs between *DvCHS1* (*DvCHS1-1*; AB576660) and *DvCHS2* (*DvCHS2-1*; AB591825) is 69%, which is much lower than that of the *CHS* alleles analyzed in the petunia (85%; *PhCHSA* and *PhCHSJ*) and soybean (81%; *GmCHS4* and *GmCHS7*), and they are clearly located in different subgroups in the phylogenetic tree (Fig. 3-7). In addition, a continuous homologous sequence longer than 17 bp was not found between *DvCHS1-1* and *DvCHS2-1* (Fig. 3-8), and the untranslated regions between them differed greatly. Thus, it needs further analysis to elucidate the detail mechanisms underlying simultaneous silencing of *DvCHS1* and *DvCHS2*.

The mechanisms controlling pure white expression in dahlia

Taking findings together, I can explain the mechanism controlling pure white and ivory white flower expressions in dahlia. By both the anthocyanin synthesis and butein synthesis pathways, flavone synthase (presumably *DvFNS*) was expressed, and petals accumulated anthocyanins, chalcones, and flavones, as in the star-type cultivars (Fig. 3-10A). When the butein synthesis pathway is suppressed, the petals accumulate anthocyanins and flavones, as in the purple petals of ‘Kazusa-shiranami’. When *DvIVS* expression is suppressed, petals accumulate chalcones and flavones, as in the OriW1 yellow areas (Fig. 3-10B). When *DvIVS* expression and the butein synthesis pathway are suppressed, petals accumulate only flavones, as in the commercial white cultivars (Fig. 3-10C). When *DvCHS1* and *DvCHS2* are simultaneously suppressed, no flavonoid derivatives accumulate in the petals, producing pure white areas, such as the white areas of ‘Yuino’ and OriW2 (Fig. 3-10D). *DvCHS2* expression is only detected in the yellow

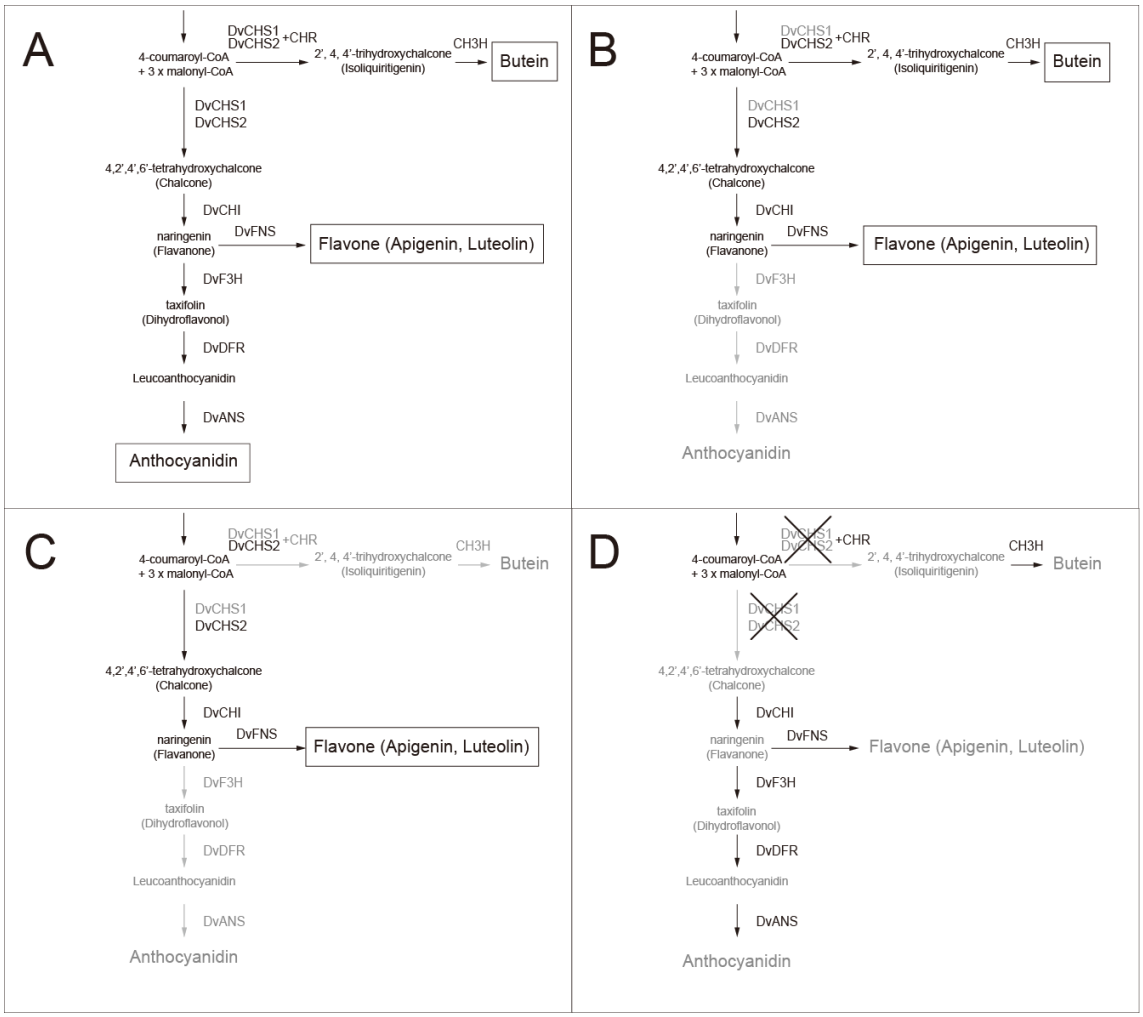

Fig. 3-10. Conclusive pathways for ivory white and pure white flower expressions. A, pathway for 'Yuino' and OriW2 colored areas; B, pathway for OriW1 colored area; C, pathway for the ivory white flower expression mechanism in commercial cultivars; D, pure white expression mechanisms in white areas of star-type cultivars and OriW2. ''X'' marks indicate the simultaneous post-transcriptional suppression of *DvCHS1* and *DvCHS2*. Abbreviations: 3GT, anthocyanidin 3-glucosyltransferase; ANS, anthocyanidin synthase; CH3H, chalcone 3-hydroxylase; CHI, chalcone isomerase; CHR, chalcone reductase; CHS, chalcone synthase; DFR, dihydroflavonol 4-reductase; F3H, flavanone 3-hydroxylase; FNS, flavone synthase.

areas of OriW1, due to a combination of *CHS* siRNA-mediated suppression and non-expression of *DvIVS*; only *DvCHS2* is degraded by siRNA because *DvCHS1* is not expressed. In feeding experiments, 'Yuino' and OriW2 produced anthocyanin when taxifolin or naringenin was fed to their pure white petals (Fig. 3-2, data not shown), suggesting that downstream of CHS are functional. This result supports my explanation. Moreover, differences in the expression of *DvCHI*, *DvF3H*, and *DvDFR* between the pure white and colored areas were not observed using real-time RT-PCR in the star-type cultivar 'Matsuribayashi' (data not shown). These results indicate that suppression of the *CHS* contributes to the pure white trait (Fig. 3-10D).

Pure white flowers of dahlia

Suppression of the structural and regulatory genes for anthocyanin biosynthesis induces white flower coloration in *A. majus* (Martin et al., 1985), *I. nil* (Morita et al., 2006; Hoshino et al., 2009), *D. caryophyllus* (Mato et al., 2000), and *Gentiana* (Nakatsuka et al., 2005). Termination of the anthocyanin biosynthesis pathway at its initial step leads to pure white flower coloration. Thus, it may also be possible to produce a pure white cultivar in dahlia, if all *CHS* are silenced. However, despite a huge numbers of cultivars being produced, there are no pure white cultivars. I suggest two possible reasons for this, 1) gene redundancy in dahlia and 2) the lack of vigor in pure white cultivars as described below.

In several cases, gene redundancy resulting from polyploidy may have a beneficial effect on the diversification of plants, but this makes it difficult to breed knock-out plants. If there are redundant genes, even if a mutation occurs in a single gene, other genes can compensate for the mutated gene function. Because garden dahlias are autoallooctoploids (Gatt et al., 1998), they may have redundant genes derived from different subfamilies. Therefore, in order to breed pure white dahlia cultivars, all *CHS* belonging to different subfamilies must be suppressed. Dahlias have at least two *CHS* subfamilies and several alleles for each gene, making it difficult to accumulate loss-of-

function mutations. This is one of the reasons for absence of any pure white cultivars in dahlia. One way to overcome gene redundancy is by inducing PTGS silencing to all the redundant genes. In the yellow bean cultivar of *G. max*, an inverted repeat of *CHS* in the genome causes endogenous PTGS (Senda et al., 2002). In addition, in a marginal picotee cultivar of petunia, the direct repeat of *PhCHSA* is assumed to be a trigger of *CHS* PTGS (Stam, 1997). Thus, genetic mechanisms that exist at PTGS of *CHS* should also exist in the star-type cultivars, OriW1 and OriW2. Although we did not elucidate such mechanisms in pure white plants, investigation of the mechanism that induces simultaneous silencing of low homology genes, such as *DvCHS1* and *DvCHS2*, will provide an interesting insight into the breeding of pure white dahlia cultivars, and also to the breeding of polyploidy plants with simultaneous PTGS in several genes with low homology.

Lack of vigor in pure white plants has been reported by Nordström and Swain (1958). They named the pure white plants that had no flavone in their petals as ‘Clare White’; these plants lacked vigor and had a low survival rate. ‘Clare White’ is inferred to have deficiencies in the biosynthesis of flavonoid derivatives. Because flavonoid derivatives have a wide range of biological functions associated with vigorous growth (Hichri et al., 2011), plants that could not synthesize flavonoids have been discarded even though the flowers were pure white in color. Although OriW1 and OriW2 produce pure white flowers, *DvCHS2* is expressed in the leaves, which accumulate flavone derivatives (data not shown). This result indicates that the two *CHS* are specifically suppressed in the flowers of OriW1 and OriW2. Thus, breeding of pure white flower cultivars in dahlia is quite difficult. However, star-type cultivars including OriW1 and OriW2 may be vital in breeding of pure white cultivars.

Chapter 2

Analysis of petal color lability in bicolor flowering *Dahlia*

Introduction

Bicolor dahlias are attractive cultivars that produce inflorescences with petals characterized by a colored basal part and a white tip (Fig. 4-1A). The tip is pure white with an absence of flavonoids (Chapter1, 1.3). The prominent common characteristic of bicolor dahlia cultivars is the lability or instability of petal colors; in addition to bicolor petals, they frequently produce single-colored petals without a white tip (Fig. 4-1B). This petal color lability is observed irrespective of the color of basal part. In some cases, an inflorescence has only single-colored petals, and in other cases, an inflorescence has both bicolor and single-colored petals. Loss of the white area in single-colored petals is independently observed by the increase or decrease of the white area, and it is clearly distinguished from the change of "picotee" pattern observed in a eustoma (Fukuta and Nakayama, 2008). Because this petal color lability prevents uniform production of cut or pot flowers of bicolor dahlias, and reduces the economic value of bicolor cultivars, it is important to prevent the occurrence of single-colored petals.

Although the causal factors of petal color lability in bicolor flowering dahlia are largely unknown, there are two common observations. First, single-colored petals are generally observed during summer. Second, the frequency of single-colored petal occurrence increases with repeat of propagation. The explanation of a red–white bicolor flowering dahlia 'Yuino' in a catalog published by the A. A. A. Garden System (Tokyo, Japan) stated that "recently, single-colored petals were often observed". Because farmers recognize the occurrence of single-colored petal as a mutation, plants that once had single-colored petals are thrown away (Mr. Fukuda, personal communication). These facts indicate that some feature(s) of petal color determinant factor(s) can vary among

vegetatively propagated siblings.

In this chapter, I characterized the occurrence pattern of single-colored petals in a red–white bicolor flowering cultivar ‘Yuino’ (Fig. 4-1C), which produced red petals with a higher frequency than other bicolor flowering cultivars in the preliminary experiment. Because it was expected that phenotypic lability was occurred not only in petal colors but also at whole plant level, I analyzed the relationship between petal colors and leaf flavonoid accumulation and discussed about the mechanisms controlling petal color lability.

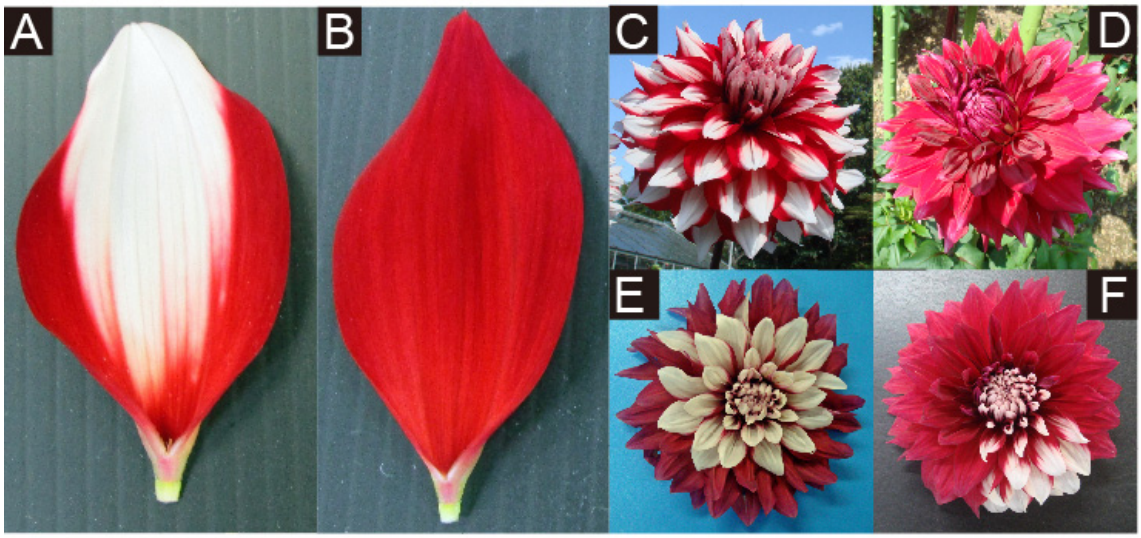

Fig. 4-1. A red–white bicolor flowering cultivar ‘Yuino’. A, predominant red–white bicolor petal; B, red single-colored petal; C, predominant bicolor inflorescence constituted only by bicolor petals; D, single red colored inflorescence constituted only by red petals; E, mixed inflorescence with red petal occurrence in the outer whorl; F, mixed inflorescence with sectorally occurring red petals. A and B were sampled from the same inflorescence.

Materials and methods

Plant materials and cultivation condition

A red–white bicolor flowering dahlia cultivar 'Yuino' (informal decorative, approximately 20 to 25 cm in diameter, bred by Yusaku Konishi in 1994 from 'Zorro' × 'Holland Festival') was used for the experiment. 'Yuino' plants were obtained from Nara Prefectural Agricultural Research and Development Center. The leaf primordia-free shoot apical meristem (SAM) domes of 'Yuino' plants were cultured during 2005 according to the method of Hosokawa et al. (2004), and maintained *in vitro* by subculture at intervals of one to three months on modified Murashige and Skoog (MS) medium (Murashige and Skoog, 1962). The *in vitro* plants were placed *ex vitro* for use as mother plants for cuttings in April 2008, February 2009, September 2009, December 2010, and February 2012, and clones of the mother plants were named the 08-line, 09-line, 10-line, 11-line, and 12-line, respectively. All mother plants were kept under a night break condition, and cut back to prevent flowering. All cuttings were inserted into a 24-hole plug tray filled with vermiculite, and, if necessary, were placed under a mist condition until sufficient rooting. Plants used for experiments in each year and the detailed date of cutting and transplanting to the field are shown in Table 4-1.

For the analysis of petal color lability during summer cultivation in 2009–2013, cuttings were taken from one or several lines shown in Table 4-1. In 2009, cuttings were obtained from shoots sprouted from tuberous roots of mother plants after 1-year cultivation of the 08-line. Rooted cuttings were planted 30–50 cm apart, and grown in the field of the experimental farm of Kyoto University (Kyoto, Japan). During 2009 and 2010, lateral shoots were removed until the first inflorescence bloomed, and then the plants were allowed to grow without removal of latelal shoots naturally, and nearly full bloomed inflorescences were collected for evaluation of petal color. During 2011, 2012, and 2013, all plants were left to develop naturally from the beginning, and nearly full bloomed inflorescences were collected.

Table 4-1. Plant materials and date of the experiment.

Year	Mother plants	Date when cuttings were obtained	Date of planting	Result
2009	08-Line	At the beginning of June	July 14 – 15th	Fig. 4-2A
2010	10-Line	April 27th – August 20th	June 1st – September 9th	Fig. 4-2B
2011	09-Line, 11-Line	April 22nd – July 11th	May 25th – August 27th	Fig. 4-2C
2012	09-Line, 10-Line, 11-Line, 12-Line	April 16th – June 20th	May 18th – July 14th	Fig. 4-2D
2013	09-Line	April 21st – May 1st	May 29th	Fig. 4-2E
2011	11-Line	September 28th and October 13th	October 27th and November 24th	Fig. 4-2F
2011	09-Line	September 28th, and stored at 30°C	October 26th	Fig. 4-3
2013	12-Line, R-line	June 7th	June 23rd	Fig. 4-4A
	12-Line, R-line	October 22nd	November 21st	Fig. 4-4B
	11-Line, 12-Line, R-Line	October 22nd	January 7th 2014	Fig. 4-4C
2014	12-1, 12-2, R-1, R-2	February 14th	April 28th	
	12-1, 12-2, R-1, R-2	March 10th	May 20th	
	09-1, 09-2, 12-1, 12-2, R-1, R-2	April 10th	June 4th	Fig. 4-8
	09-1, 09-2, 12-1, 12-2, R-1, R-2	May 12th	June 25th	
	09-1, 09-2, 12-1, 12-2, R-1, R-2	June 10th	July 15th	
	09-1, 09-2, 12-1, 12-2, R-1, R-2	June 26th	September 3rd	Fig. 4-6A, 4-7A, 4-8
2014	09-2, 12-2, R-3	November 20th – December 2nd	January 30th 2015	Fig. 4-6B, 4-7B

For the analysis of petal color lability during winter cultivation, cuttings of 11-line were obtained during September to October 2011, and transplanted in October 27th and November 24th 2011, respectively, to 24 cm pots filled with mixed soil, mainly composed of Metro-Mix 360 (Sun Gro Horticulture, Agawam, MA), and situated in the greenhouse (set minimum temperature at 5°C from November to April) of the experimental farm of Kyoto University (Kyoto, Japan). Light condition of greenhouse in winter was natural light condition without any supplemental lighting.

To analyze leaf flavonoid accumulation, cuttings were obtained from February to June 2014 from each two mother plants of the 09-line (09-1 and 09-2), 12-line (12-1 and 12-2), and R-line (R-1 and R-2), and transplanted to the field from April to September 2014, and cuttings were obtained during November 20th to December 2nd 2014 from 09-2, 12-2, and R-3, and transplanted to the 24 cm pots situated in the greenhouse. All plants were left to develop naturally from the beginning and nearly full bloomed inflorescences, and collected for the analysis.

Evaluation of petal color

The "red petal ratio" was used as an index for evaluation of petal color. This score was calculated as [(number of red petals)/(number of total petals)]. If all petals are red, the score would equal 1, whereas if all petals are bicolor, this score would equal 0. To avoid biases (for example, red petals are produced only in a plant having many inflorescences), the average score of all inflorescences of the plant was used for comparison among individuals, and the average score of individuals was used for comparison among populations.

The R-line

Cuttings of 09-line plants were obtained in September 28th 2011, and stored at 30°C in a growth chamber (NS360; Takayama, Kyoto, Japan) for a month with 16 h photoperiod under light intensity 190 $\mu mol \cdot m^{-2} \cdot s^{-1}$ using cool white fluorescent lights.

Subsequently, these plants were transplanted to a 24 cm pot filled with mixed soil mainly composed of Metro-Mix 360 situated in a greenhouse. Among 46 plants, one plant showing the highest average red petal ratio was selected, and named the R-line. Subsequently, to use as a mother plant, cuttings were obtained from the R-line.

To assess the characteristics of the R-line to produce red petals with high frequency, the R-line was maintained through vegetative propagation. Cuttings were obtained from the R-line and 12-line and planted in the field in June 2013. In addition, cuttings were obtained from these two lines in October 2013, planted in a 24 cm pot filled with mixed soil mainly composed of Metro-Mix 360 and situated in the greenhouse (set minimum temperature at 5°C). The average red petal ratio of inflorescences fully opened from September to November 2013 in the field and from February to June 2014 in the greenhouse, respectively, was compared between these two lines.

To determine the characteristics of the R-line that was maintained after experience of the *in vitro* condition, node sections were collected from the R-line, 11-line and 12-line in July 2013. These nodes were sterilized with 70% ethanol and then 10% antiformin (Wako), and placed in MS solid medium. After propagation *in vitro*, they were placed outdoors in October 2013, and planted in 24 cm pots filled with mixed soil and grown in a greenhouse in January 2014. Average red petal ratio of inflorescences fully opened from March to June 2014 was compared between these two lines.

Analysis of flavonoid accumulation in leaves

For the analysis of uppermost leaf flavonoid accumulation, the uppermost leaves were collected from field grown plants in 2014. When there were two uppermost leaves, both leaves were mixed and then extracted. For the analysis of whole plant leaf flavonoid accumulation, leaves in all nodes were collected as they developed. Leaves of field grown plants were collected during August 6th to November 21st 2014, and leaves of greenhouse grown plants were collected during January 7th to April 15th 2015. Since dahlia has opposite leaf arrangement, two leaves from each node were collected and separately

extracted. For the analysis of leaf flavonoid accumulation in each mother plant, a leaf attached on the middle of plant was collected during March 12th to March 27th after taking some cuttings.

HPLC was used to analyze flavonoid accumulation. A total of 50–200 mg of leaves were homogenized in liquid nitrogen, and 1 mL of extraction buffer (acetic acid:methanol:water=1:4:5 v/v) was added. The extracted samples were centrifuged for 10 min at 20,600 × g, and the supernatant was collected for HPLC analysis. HPLC analysis was performed according to Chapter1, 1.2. The absorption spectrum of each peak was measured by photodiode array detector appurtenant to HPLC.

To simplify the analysis of flavonoid accumulation, 50–200 mg of leaves were homogenized in liquid nitrogen, and 1 mL of extraction buffer was added. Extracted samples were centrifuged for 10 min at 20,600 × g, and the supernatant was collected. The absorption of this supernatant at 200–600 nm was measured using a double beam spectrophotometer (U-2000A; Hitachi), or a UV spectrophotometer (UV-1800; Shimadzu), and the score of ABS_{400}/ABS_{370} was calculated. When leaf extract with rich flavonoid confirmed by HPLC was measured by a spectrophotometer, the score of ABS_{400}/ABS_{370} exceeded 0.8 in a preliminary experiment. Thus, when the score of ABS_{400}/ABS_{370} exceeded 0.8, the leaf was considered to be a rich flavonoid accumulator.

Next generation sequencing (NGS) analysis

A leaf was separated along midrib by a razor and one half was used for a measurement of a spectrophotometer and the other half was used for RNA extraction. Determination of leaf flavonoid accumulation was performed by a spectrophotometer to measure the score of ABS_{400}/ABS_{370}. The score of ABS_{400}/ABS_{370} was 0.969 and 0.178 for a flavonoid rich leaf and a flavonoid poor leaf respectively, and then flavonoid accumulation was confirmed by HPLC. RNA was extracted using a MirVana miRNA Isolation Kit (Applied Biosystems) and small RNA enriched sample was used for small RNA analysis and RNA fraction that is depleted of small RNAs was used for RNA-seq

analysis.

RNA-seq analysis was performed using HiSeq2000 (Illumina). Total reads for flavonoid-rich leaf and flavonoid-poor leaf was 4,059,802 and 4,579,744. The differently expressed genes between these samples was evaluated using edgeR (Robinson et al., 2010) with border value of logFC as 3.

Small RNAs were sequenced using Hiseq (Illumina), and 18-30nt small RNAs were mapped onto *DvCHS* genes (*DvCHS1-1*, *DvCHS1-2*, *DvCHS2-1*, *DvCHS2-2*, *DvCHS3-1*, *DvCHS3-2*, *DvCHS4*) using Bowtie software without any mismatch. The number of mapped reads was 12,046,092 for flavonoid-rich leaf, and 11,465,948 for flavonoid-poor leaf.

Real-time RT-PCR analysis

A leaf was separated along midrib by a razor and one half was used for a measurement of a spectrophotometer and the other half was used for RNA extraction. RNAs were extracted from five flavonoid rich leaves (ABS_{400}/ABS_{370}: 0.922-1.005) and five flavonoid poor leaves (ABS_{400}/ABS_{370}: 0.114-0.344). RNA of total six leaves each including one sample used in NGS analysis were used for a real-time RT-PCR analysis. Real-Time PCR was performed using a LightCycler 480 System II (F. Hoffmann-La Roche AG). Ten times diluted RT product was used as templates. The primers used are shown in Table 4-2. The PCR program was set at 95°C for 30 s, followed by 45 cycles of 95°C for 5 s, 60°C for 30 s, and the subsequent dissociation steps. *DvActin* was used as an internal standard.

DNA gel blot analysis

Genomic DNA was extracted using MagExtractor Plant Genome (Toyobo) from six bicolor cultivars (‘Yuino’, ‘Matsuribayashi’,‘Kazusa-shiranami’, ‘Santa Claus’, ‘OriW1’ and ‘OriW2’) and four single-color cultivars (‘Kokucho’, ‘Ms. Noir’,’Yukino’ and ‘Michael J’). A 20-μg DNA sample was digested with a restriction enzyme (*Bam*HI

Table 4-2. Primers used for real-time RT-PCR

Genes	Forward primers	Reverse primers
DvCHS1	CATGTGCTAAGCGAATACGG	CCTCTCCGGTGGTATTGAAC
DvCHS2	TGTCCCAACTACCATGCCGATTTC	TTACACATTAAAATGACACAGTGA
DvCHS3	CACCGGTGAAGGTTTAGATTGGGGT	CATTATTACATCAACCGTTACTTAT
DvCHS4	TTGGTATGCCCTATTTTCATCATGC	AAATTACATGAACAAAACATGTTT
DvActin	TGCTTATGTTGGTGATGAAG	CCCTGTTAGCCTTAGGATTT

or *Hin*dIII) and separated on 0.8% agarose gel in 0.5 × TAE buffer and subsequently blotted to a Hybond N+ membrane (GE Healthcare) in 20 X SSC buffer. For the probe, PCR product was purified from agarose gel slices with illustra GFX PCR DNA and Gel band Purification Kit (GE Healthcare) and labeled with AlkPhos Direct Labelling and Detection System (GE Healthcare). The probe was hybridized to the membrane at 55ºC overnight. Detection was conducted with CDP Star (GE Healthcare) and the fluorescence image was obtained using a LAS-3000 Mini (Fujifilm).

Inverse PCR

Genomic DNA of 'Yuino' and 'Michel J' was digested with a restriction enzyme (*Bam*HI, *Hin*dIII or *Xba*I). A 300-ng digested DNA sample was self-ligated by T4 DNA ligase (Takara) in a 200-μL volume. Inverse PCR was performed with Blend Taq (Toyobo) or Takara EX Taq (Takara). Primers used for inverse PCR and sequencing were shown in Table 4-3.

Statistical analyses

Data of the uppermost leaf flavonoid accumulation and the petal colors were analyzed with the independent chi-square test using Microsoft Excel 2013.

Table 4-3. Primers used for identification of *DvCHS2* flanking region

Cultivar	Target region	Purpose		Sequence (5'-3')
Yuino	CHS2 5' flanking region	Inverse PCR-F	CHS2-3'Race-nested	GCTCGGTAAAGATGCGGCTGTCAAA
		Inverse PCR-R	CHS2 Right Walk-2	CCACGTCCTGACGGGCGTCCAAAGA
	CHS2 3' flanking region	Inverse PCR-F	CHS2 1146F	AAGGTTTGGATTGGGGTGTTCTGTT
		Inverse PCR-R	CHS2 924R	GGCGAAAACGCTTGCACCAACGCCT
		Inverse PCR-2nd-F, Sequencing	CHS2 3'Genome 6F	AATGTAATTGTCTATTTTGTTCTCT
		Inverse PCR-2nd-R	CHS2 762R	CGCTCAGTTGTCAAGTCC
		Sequencing	CHS2 3'Genome 1F	GTTGTGTTGTATGGTTCTGCTTTCT
		Sequencing	CHS2 3'Genome 2F	CCGGAGGTGCCACGCGGGGCCTTTT
		Sequencing	CHS2 3'Genome 3F	CGTGGCAATTAAACACGTTCACCT
		Sequencing	CHS2 3'Genome 4F	TCGCAAGATAATTCACGCGTGGCAA
		Sequencing	CHS2 3'Genome 5F	AGATCATAAGCGGGACG
		Sequencing	CHS2 3'Genome 7F	TCCGGCGTGAGAATCAGTATACAA
		Sequencing	CHS2 3'Genome 8F	TTGTTTTTGCGGGATGACGTCATGT
		Sequencing	CHS2 3'Genome 9F	TCACGCAAGTTCATCCGTTGGGGAT
		Sequencing	CHS2 3'Genome 1R	GGAGAAGAAAGAACAAGAAGAAAAC
		Sequencing	CHS2 3'Genome 2R	AACAGTTGACCCGACACATTCATAT
		Sequencing	CHS2 3'Genome 3R	GGAAACACAAAATGTGTCAAAAACT
		Sequencing	CHS2 3'Genome 4R	CCTCACGCGCACCATCCCCAACGG
Michael J	CHS2 3' flanking region	Inverse PCR-F	CHS2-1216F	TGTCCCAACTACCATGCCGATTTC
		Inverse PCR-R	CHS2 762R	CGCTCAGTTGTCAAGTCC
		Sequencing	CHS2-Inv-MJR-Bam-Clone1-1R	GAGGGATATAAGTTTGATAAACTT
		Sequencing	CHS2-Inv-MJR-Bam-Clone2-1R	TATATGCTGTATGACTATAGTAGA
		Sequencing	CHS2-Inv-MJR-Bam-Clone1-2R	TAACCAAGGGGGAGTGTTATAAA
		Sequencing	CHS2-Inv-MJR-Bam-Clone2-2R	AGATTGATTAACAATCGAAGTTA

Results

Petal color lability of a red–white bicolor flowering cultivar, 'Yuino'

The predominant petal color of 'Yuino' is a red–white bicolor (Fig. 4-1A), but it frequently produced red single-colored petals (Fig. 4-1B). 'Yuino' predominantly produced inflorescences with only bicolor petals (Fig. 4-1C), but often produced inflorescences with only red petals (Fig. 4-1D), or mixed inflorescences with both red petals and bicolor petals (Fig. 4-1E, F). In a mixed inflorescence, red petals were located in the outer whorls (Fig. 4-1E), or sectorally (Fig. 4-1F) in many cases. From the observation of > 10,000 inflorescences, bicolor petals were invariably located at the inner whorls, and red petals were located at the outer whorls of the inflorescence (Fig. 4-1E).

For analyzing the frequency of red petal production, the red petal ratio, (the number of red petals)/(the number of total petals), was used as an index of petal color change. Among total 4271 inflorescences in the field experiment from May to December in 2009, 2010, 2011, 2012, and 2013, 3,201 inflorescences (75.0%) showed the score of

red petal ratio 0, and 1,070 inflorescences (25.0%) showed the score of red petal ratio more than 0. Here, 194 of the 1,070 inflorescences (4.5%) showed the score of red petal ratio less than 0.8, and 876 inflorescences (20.5%) showed the score of red petal ratio at 0.8 or above (Fig. 4-2A–E). The mean score of red petal ratio varied from year to year, ranging from 0.02 in 2010 to 0.30 in 2013 (Fig. 4-2A–E). On the other hand, in the greenhouse experiment from October 2011 to July 2012, the mean score of red petal ratio was 0.01 (Fig. 4-2F), thus red petal occurrence was lower than that in the field experiment.

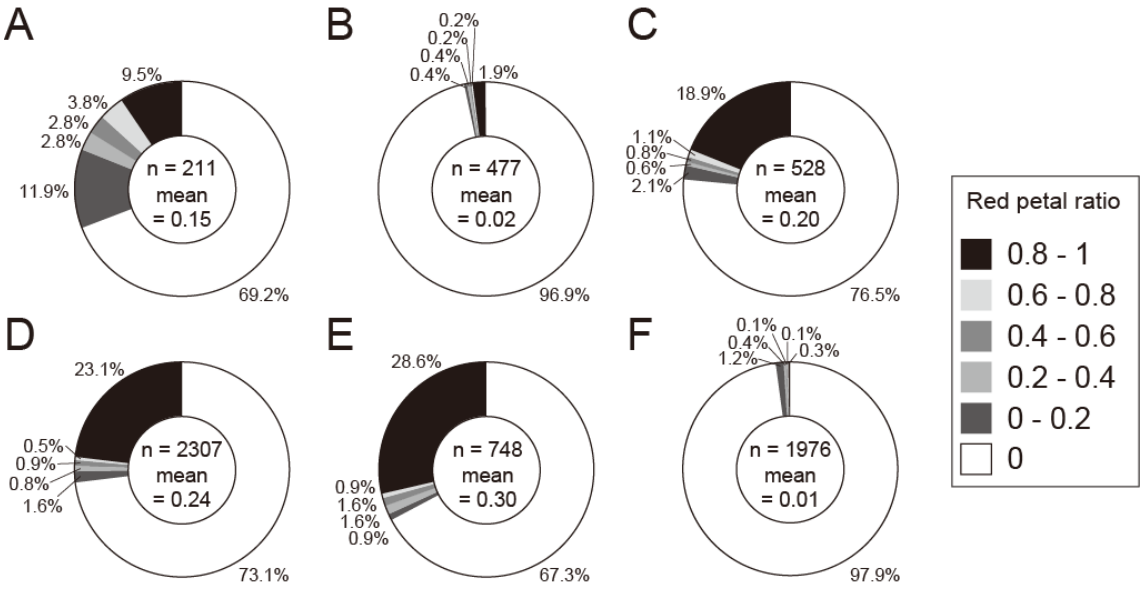

Fig. 4-2. Red petal ratio of inflorescences in field-grown plants in 2009 (A), 2010 (B), 2011 (C), 2012 (D), and 2013 (E) and greenhouse-grown plants in 2011–2012 (F).

The R-line tended to produce red petals

In the winter greenhouse cultivation of 2011–2012, while almost all cuttings maintained at 30°C until transplantation produced only bicolor petals, one plant consistently produced red petals at a high ratio. This plant scored the highest average red petal ratio of 0.57, while the average of all plants was 0.06 (Fig. 4-3). This plant was designated as the "R-line". To determine whether this characteristic of high red petal production was maintained through vegetative propagation, the R-line was propagated by cutting.

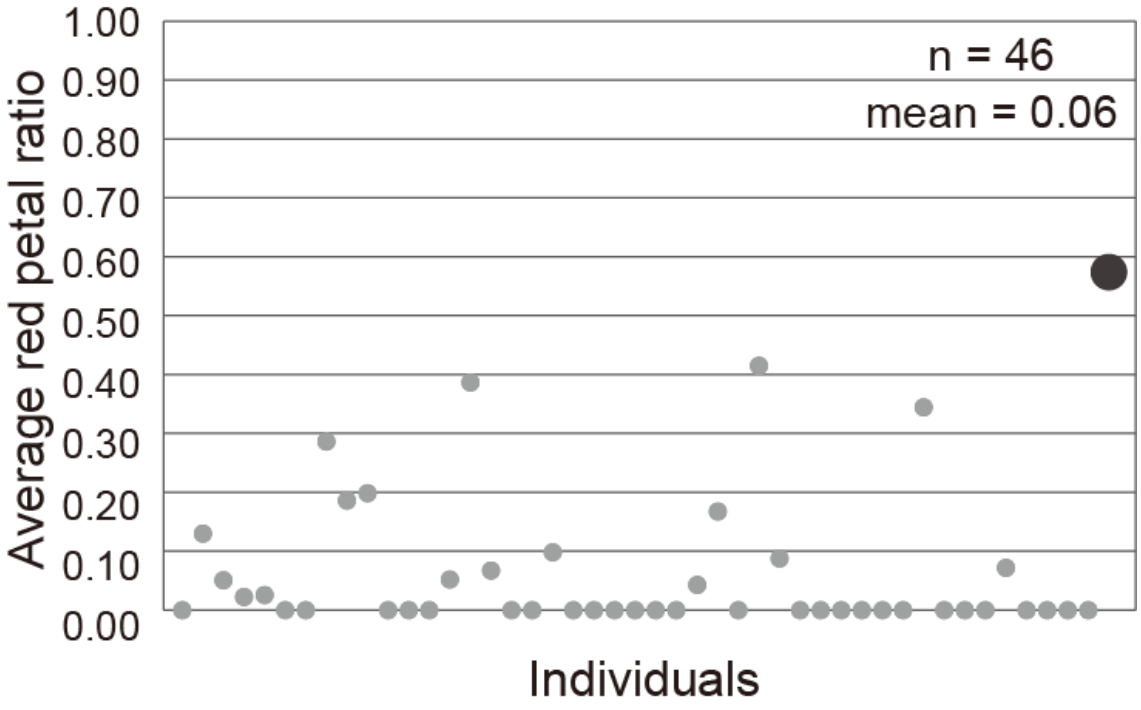

Fig. 4-3. Average red petal ratio of 30°C stored 09-line plants. One circle indicates the average red petal ratio of one plant. A big black circle of the highest average red petal ratio (0.57) indicates the R-line original plant.

When the R-line plants were grown in the field during the summer of 2013, 133 out of 135 inflorescences of all 23 plants had red petals. The average red petal ratio was 0.96 in the R-line, whereas 0.45 in the 12-line as a control (Fig. 4-4A). When the R-line plants were grown in a greenhouse during winter in 2013–2014, a much more marked result was obtained, where the average red petal ratio was 0.71 in the R-line and 0.05 in the 12-line (Fig. 4-4B). After the experience of the *in vitro* environment, the R-line showed a higher average red petal ratio (0.91) than the 12-line (0.69) and 11-line (0.03) (Fig. 4-4C).

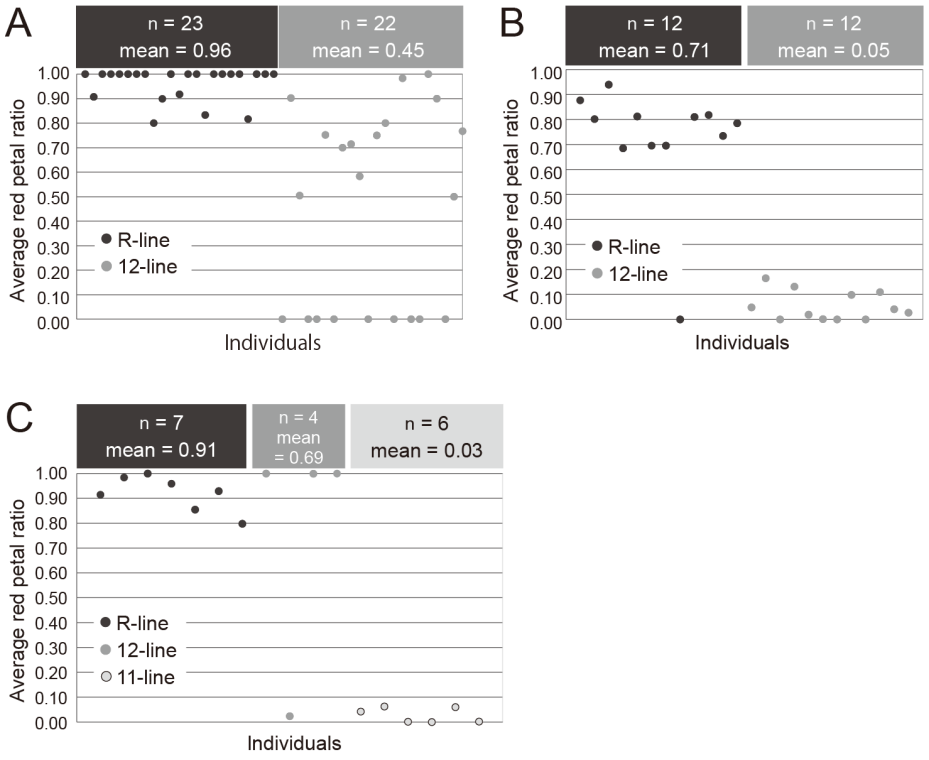

Fig. 4-4. Average red petal ratio after vegetative propagation in R-line plants. A, the field experiment during the 2013 summer. Total inflorescence number of R-line and 12-line were 135 and 143, respectively; B, the greenhouse experiment in 2013–2014 winter. Total inflorescence number of R-line and 12-line were 200 and 201, respectively; C, the greenhouse experiment in 2013–2014 winter using *in vitro* experienced plants. Total inflorescence number of R-line, 12-line, and 11-line were, 90, 57, and 108, respectively.

Relationship between petal colors and leaf flavonoid accumulation

In a mixed inflorescence, bicolor petals were located at an outer whorls (Fig. 4-1E) or sectorally (Fig. 4-1F) in an inflorescence. This indicated that red petals occurred in a similar fashion to a chimera or lateral mutant, and it was expected that some difference is observed not only in petal colors, but also in other characteristics of the shoot. Because the formation of a white tip in a petal is a result of loss of flavonoid synthetic capacity (Chapter1, 1.3), the relationship between inflorescence color and flavonoid accumulation in the uppermost leaves was analyzed. For this analysis, the score of ABS_{400}/ABS_{370} of leaf extracts was measured by a spectrophotometer. This score was used as an indicator of flavonoid accumulation, because absorbance at 400 nm is detected only from a flavonoid accumulating leaf (Fig. 4-5A), and not from a non-flavonoid accumulating leaf (Fig. 4-5B) using a photodiode array detector adjunct to HPLC. Most peaks detected only in the flavonoid accumulating leaves had a maximum absorbance at 368 nm (Table 4-4). These peaks were presumed to be derived from chalcone derivatives.

Among 185 field-grown individuals including 66 R-line plants, when an inflorescence had at least one red petal, the uppermost leaf accumulated flavonoids, whereas when an uppermost leaf did not accumulate flavonoids, the inflorescences inevitably were composed of all bicolor petals except for one plant (Table 4-5). The independent chi-square test indicated significant ($P < 0.001$) relationship between the uppermost leaf flavonoid accumulation and petal colors.

For further analysis, the relationship between petal color and flavonoid accumulation of whole plant leaves were analyzed. Among total 21 plants in the field experiment, eight plants including seven R-line plants produced at least one red petals, whereas thirteen plants including three R-line plants produced only bicolor petals (Fig. 4-6A). Scores of ABS_{400}/ABS_{370} in leaves among thirteen nodes from the bottom were higher in plants with red petals than in plants without red petals (Fig. 4-7A). Similarly, in the winter greenhouse experiment, the same tendency was observed, namely, all eight plants of R-3 with rich flavonoid accumulation produced red petals at the terminal

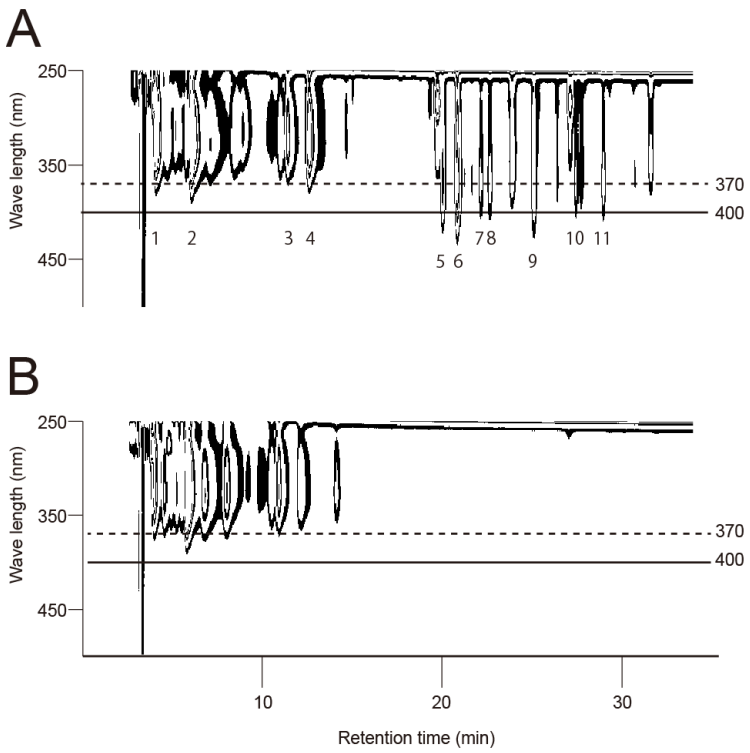

Fig. 4-5. Photo diode array detection in leaves. A, flavonoid accumulating leaf; B, non-flavonoid accumulating leaf. Only in flavonoid accumulating leaves, peaks which had absorbance spectrum to approximately 420 nm were detected. The number below the peaks are corresponded with the peak number in Table 4-4.

Table 4-4. HPLC photo diode array analysis of leaf extracts.

Peak number in Fig. 4-5A	Retention time (min)	Absorption maxima (nm)	Putative compound
1	4.1	328, 285, 241	Organic acid
2	6.0	329, 303sh, 245	Organic acid
3	11.4	326, 301sh, 239	Organic acid
4	12.6	328, 303sh, 239	Organic acid
5	20.0	368, 316sh	Chalcone
6	20.8	368, 316sh	Chalcone
7	22.1	368, 315sh	Chalcone
8	22.6	368, 317sh	Chalcone
9	25.1	381, 338, 300	Chalcone
10	27.5	370	Chalcone
11	29.0	369	Chalcone

Table 4-5. Relationship between petal colors in the terminal inflorescence and flavonoid accumulation in the uppermost leaf.

Uppermost leaf flavonoid accumulation	Petal colors		Chi-square test
	Inflorescence with only bicolor petals	Inflorescence with at least one red petal	
Rich	23 (5)	50 (40)	$P < 0.001$
Poor	111 (20)	1 (1)	

Flavonoid accumulation was determined by the score of ABS_{400}/ABS_{370} using a spectrophotometer and when the score excessed 0.8, the leaf was judges as a rich flavonoid accumulator.
Numbers in parentheses indicate the number for R-line plants.

inflorescence, whereas all ten plants of 12-2 and 09-2 with poor flavonoid accumulation produced completely bicolor petals in the terminal inflorescence (Fig. 4-6B). The scores of ABS_{400}/ABS_{370} in leaves among ten nodes from the bottom were higher in plants with red petals than in plants without red petals (Fig. 4-7B). Thus, these indicated that red-petal producing plants accumulated more abundant flavonoid in leaves than only bicolor-petal producing plants. Therefore, not only petal colors but also shoot phenotype differed between red-petal producing plants and bicolor-petal producing plants.

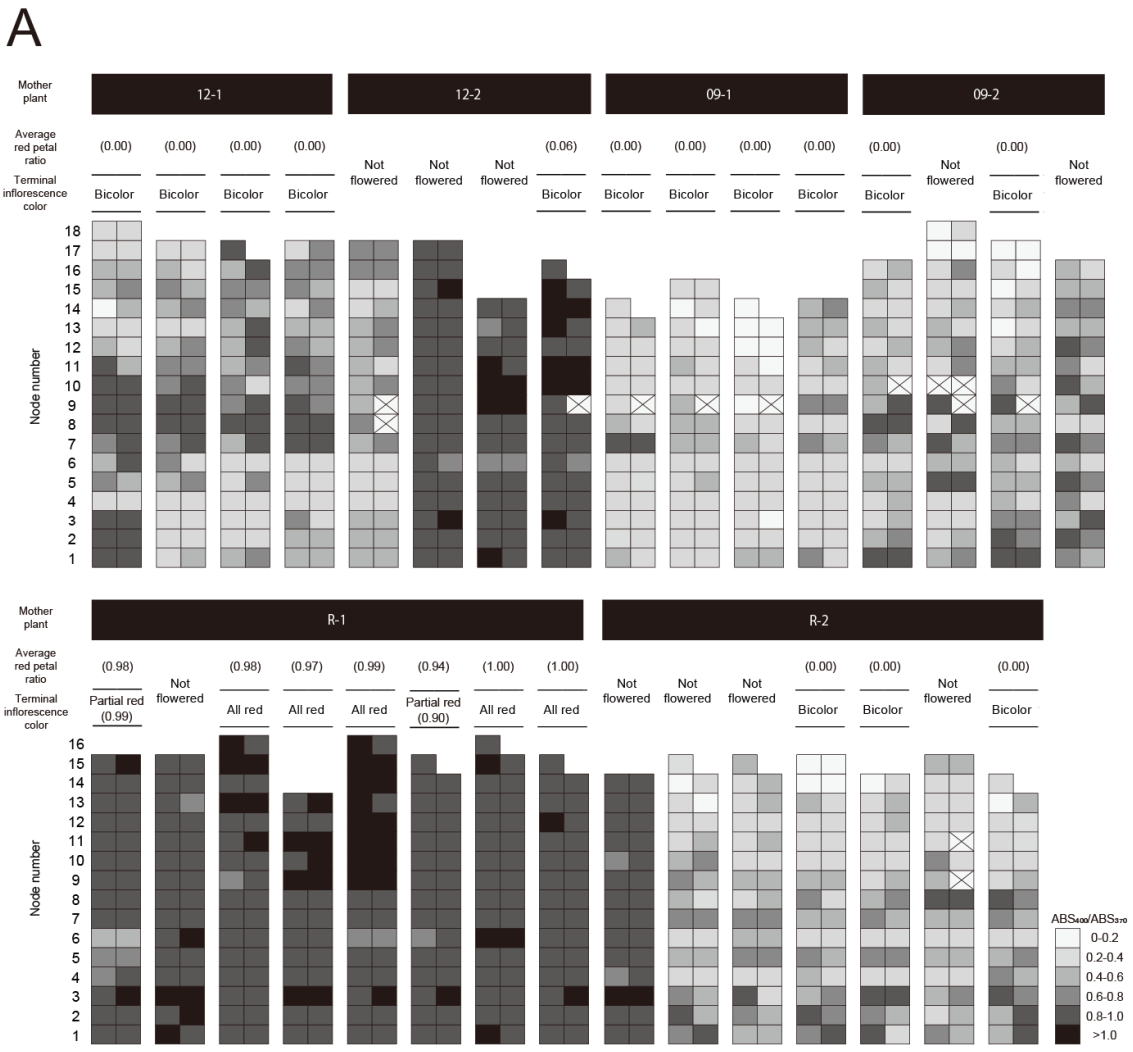

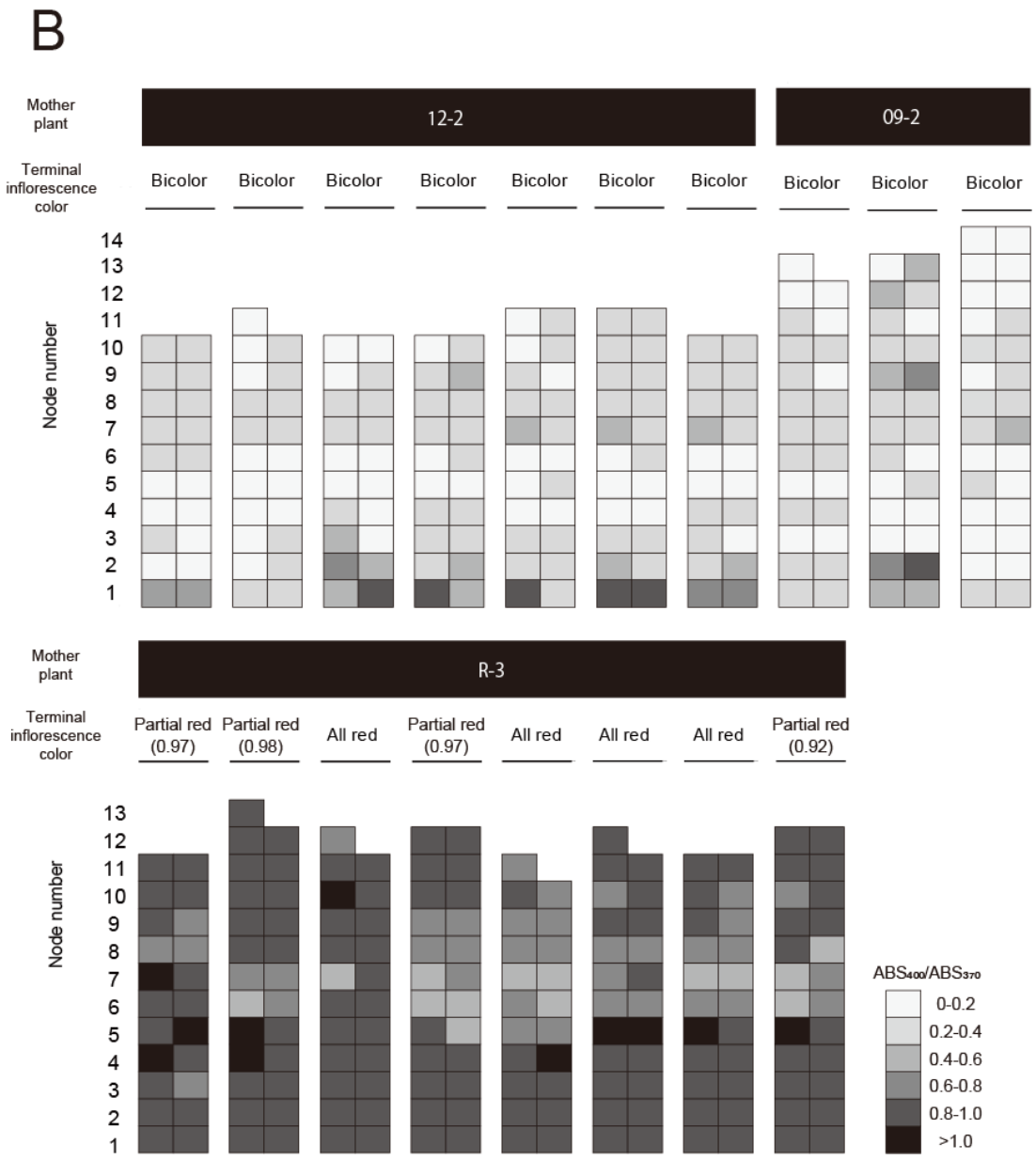

Fig. 4-6. Whole plant scores of ABS_{400}/ABS_{370} in leaf extracts by a spectrophotometer. A, the field experiment in 2014 summer to autumn; B, the greenhouse experiment in 2014-2015 winter to spring. Two columns in the same node number indicates two leaves from the same node. Cross indicates a leaf not measured. In the terminal inflorescence color, all red indicates that the inflorescence was composed of all red petals, bicolor indicates that inflorescence was composed of all bicolor petals, and partial red indicates that inflorescence was composed of both red and bicolor petals.

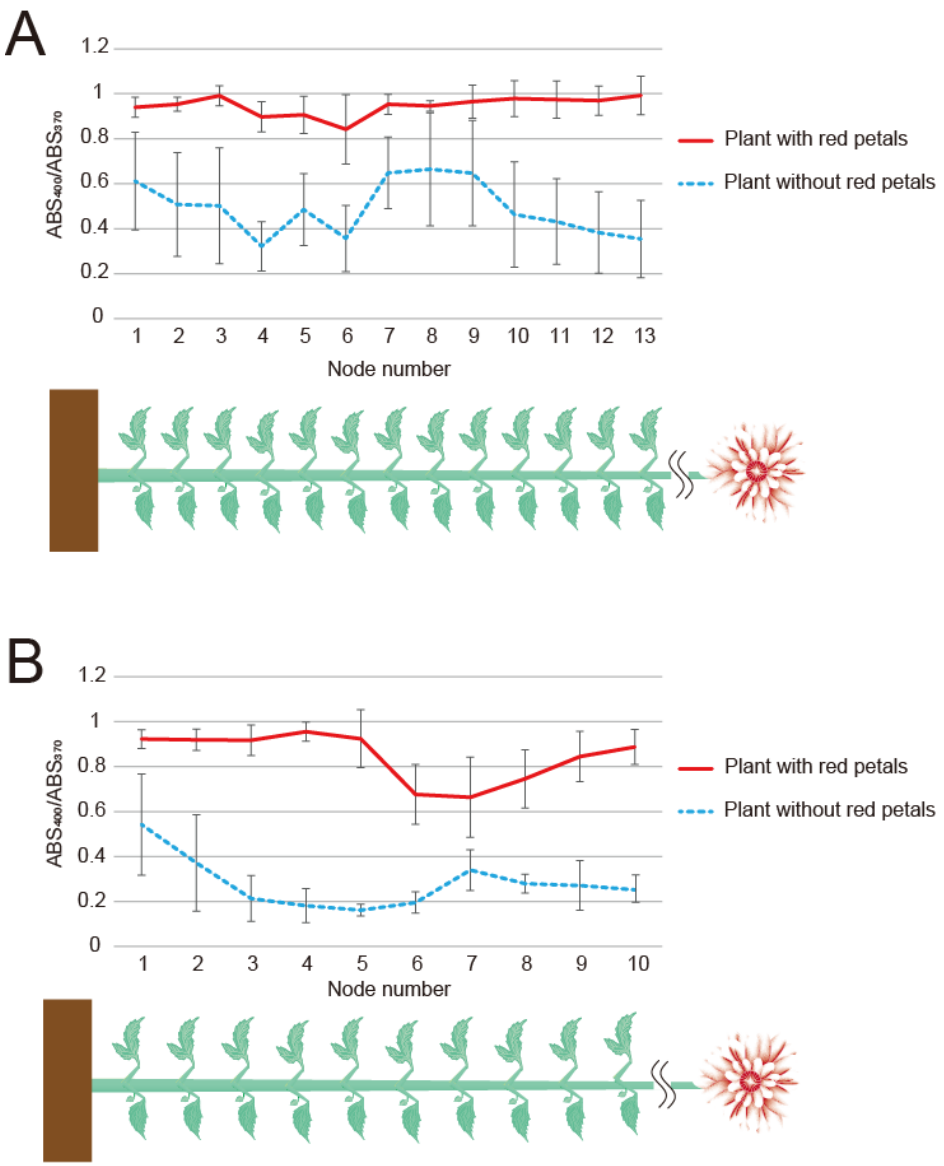

Fig. 4-7. The whole plant ABS_{400}/ABS_{370} scores of leaf extracts measured by a spectrophotometer in plants with red petals or without red petals. Scores of two leaves in the same node of each plant were averaged. A: Field experiment in 2014 summer to autumn. n = 8 for plants with red petals and n = 13 for plants without red petals. All flowered inflorescences were examined and plants with at least one red petal were classified into "plant with red petals". B: Greenhouse experiment in 2014-2015 winter to spring. n = 8 for plants with red petals and n = 10 for plants without red petals. Node numbers were given from the bottom. Vertical bars indicate standard deviations.

Difference in frequency of red petal occurrence in cutting siblings among mother plants

To assess the difference of mother plants in the red petal producing property, cuttings were obtained six times on different dates from the same six mother plants, composed of two 12-lines (12-1 and 12-2), two 09-lines (09-1 and 09-2), and two R-lines (R-1 and R-2) (Table 4-1), and the average red petal ratio was examined. These mother plants were selected based on flavonoid accumulation in leaves determined by thin layer chromatography (data not shown), and then confirmed by a spectrophotometer. The scores of ABS_{400}/ABS_{370} in leaves collected in March 2015 from the middle of the plant were 0.450, 0.976, 1.009, 0.457, 0.944, and 0.930 for 12-1, 12-2, 09-1, 09-2, R-1, and R-2, respectively. Namely, 12-2, 09-1, R-1, and R-2 did accumulate flavonoids in leaves, whereas 12-1 and 09-2 did not.

While only one plant produced red petals in cutting siblings of 12-1 (Fig. 4-8A), 18 out of 38 plants produced red petals in cutting siblings of 12-2 (Fig. 4-8B). Both 09-1 and 09-2 produced only bicolor petals (Fig. 4-8C and D). For R-line plants, 37 out of 42 plants produced red petals in R-1 cutting siblings (Fig. 4-8E), while 15 out of 40 plants produced red petals in R-2 cutting siblings (Fig. 4-8F). The average red petal ratio of 12-1, 12-2, 09-1, 09-2, R-1, and R-2 was 0.01, 0.18, 0.00, 0.00, 0.82, and 0.34, respectively. Therefore, the frequency of red petal occurrence differed among mother plants although in the same line.

DvCHSs expression and small RNA analysis in leaves

From the RNA-seq analysis, comparing with a flavonoid poor leaf, only two genes were significantly up-regulated and five genes were significantly down-regulated in a flavonoid rich leaf (Table 4-6). One of two up-regulated genes was *DvCHS2* (Table 4-6). The sequence was completely coincided with *DvCHS2-1*. From the real-time RT-PCR analysis, among four *DvCHS* genes, only *DvCHS2* was down-regulated in flavonoid poor leaves than flavonoid rich leaves (Fig. 4-9).

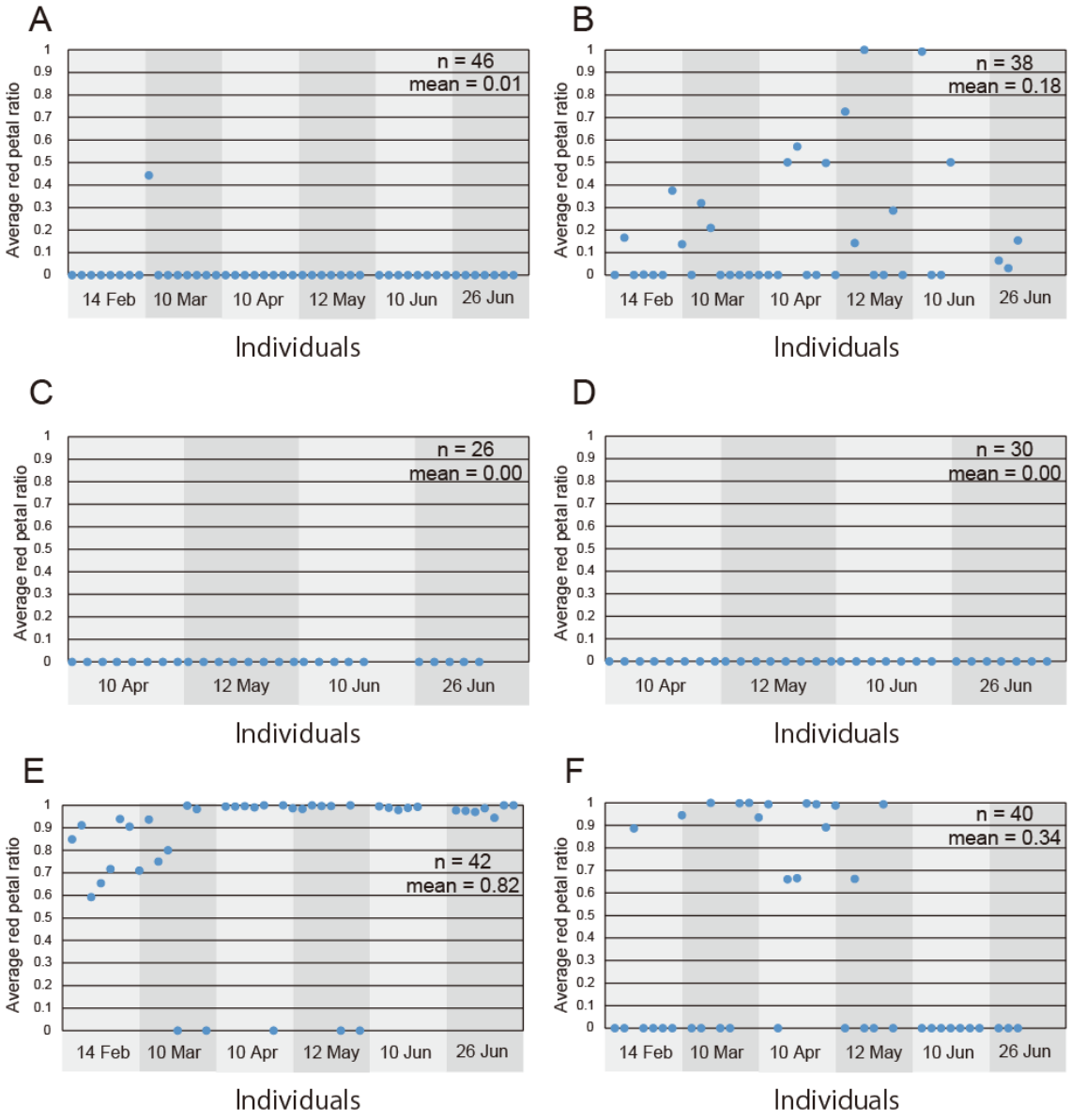

Fig. 4-8. Comparison of occurrence property of red petals among vegetatively propagated sibling from different mother plants. Average red petal ratio of cutting sibling from 12-1(A), 12-2 (B), 09-1 (C), 09-2 (D), R-1(E), and R-2 (F) mother plants are shown. Cutting plants were obtained on six dates from 12-1, 12-2, R-1, and R-2, and on four dates from 09-1 and 09-2. One plot indicates average red petal ratio of one cutting plant. The date under each graph indicates the date cuttings were obtained. Total inflorescence number measured for 12-1, 12-2, 09-1, 09-2, R-1, and R-2 lines were, 396, 340, 124, 122, 279, and 354, respectively.

Table 4-6. Genes showed significant difference in expression levels between a flavonoid-rich leaf and a flavonoid-poor leaf.

	logFC	logCPM	FDR	ID	Description by Blast2GO	Description by Blastx
Up regulated in flavonoid-rich leaf	4.10	10.08	0.001	c15993_g1	Chalcone synthase	Yuino CHS2-1 (*Dahlia pinnata*) (AB591825)
	3.65	6.19	0.031	c13892_g2	23 kda jasmonate-induced	PREDICTED: 23 kDa jasmonate-induced protein-like (*Malus domestica*)
Up regulated in flavonoid-poor leaf	-5.23	4.25	0.031	c15904_g1	BTB POZ and TAZ domain-containing protein 1-like	BTB and TAZ domain protein 1 (*Arabidopsis thaliana*) (NP201121)
	-4.33	4.77	0.031	c15650_g1	Transcription factor bHLH35	transcription factor bHLH35 (*Arabidopsis thaliana*) (NP568850)
	-4.23	7.01	0.002	c15638_g1	RESPONSE TO LOW SULFUR	RESPONSE TO LOW SULFUR 2 (*Arabidopsis thaliana*) (NP197854)
	-4.01	5.17	0.031	c15986_g1	Sugar transporter ERD6-like 16	sugar transporter ERD6-like 16 (*Arabidopsis thaliana*) (NP568367)
	-3.65	8.09	0.012	c19320_g2	5' -adenylylsulfate reductase chloroplastic-like	5'-adenylylsulfate reductase 1 (*Arabidopsis thaliana*) (NP192370)

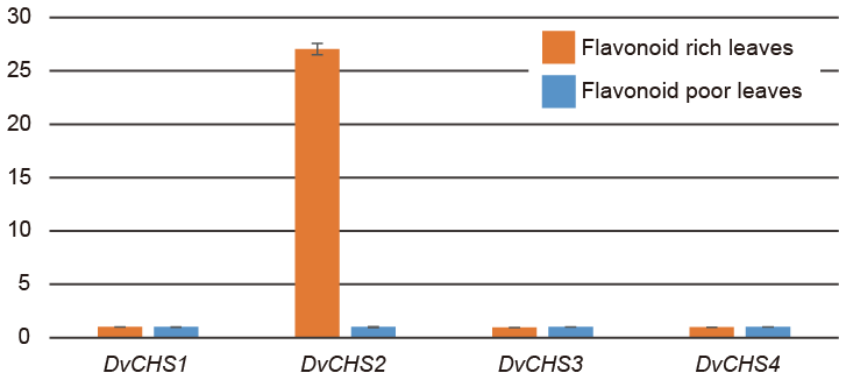

Fig. 4-9. Relative expression levels of *DvCHSs*, in flavonoid rich leaves and flavonoid poor leaves. Relative scores are calculated flavonoid poor leaves as one. The vertical bars indicate ±SE (n = 6).

To know whether this suppression of *DvCHS2* in flavonoid poor leaves was post-transcriptional, small RNA mapping analysis was performed. While only 122 of 12,046,092 reads were mapped on *DvCHS* genes in a flavonoid rich leaf (Fig. 4-10A), 21,507 of 11,465,948 reads were mapped on *DvCHS* genes in a flavonoid poor leaf (Fig. 4-10B). The 21,497 of 21,507 mapped reads in a flavonoid poor leaf was mainly derived from *DvCHS2* (Fig. 4-10B). Therefore, it was demonstrated that *DvCHS2* genes were silenced post-transcriptionally in a flavonoid poor leaf.

Genomic analysis of DvCHS2

DNA gel blot analysis was performed using *Bam*HI digested DNA, one intense bicolor cultivar specific band was detected when 3' or 5' coding region was used as a probe (Fig. 4-11A). For *Hin*dIII, one intense bicolor cultivar specific band was detected when 3' coding region was used as a probe (Fig. 4-11A). The sequence of this band was determined by inverse PCR and identified as *DvCHS2-1* allele in 'Yuino' (Fig. 4-11B). Inverse PCR using 'Michael J' genomic DNA identified two other alleles, *MJ-1* and *MJ-2* respectively, which was coincided with the two bands detected in DNA gel blot analysis

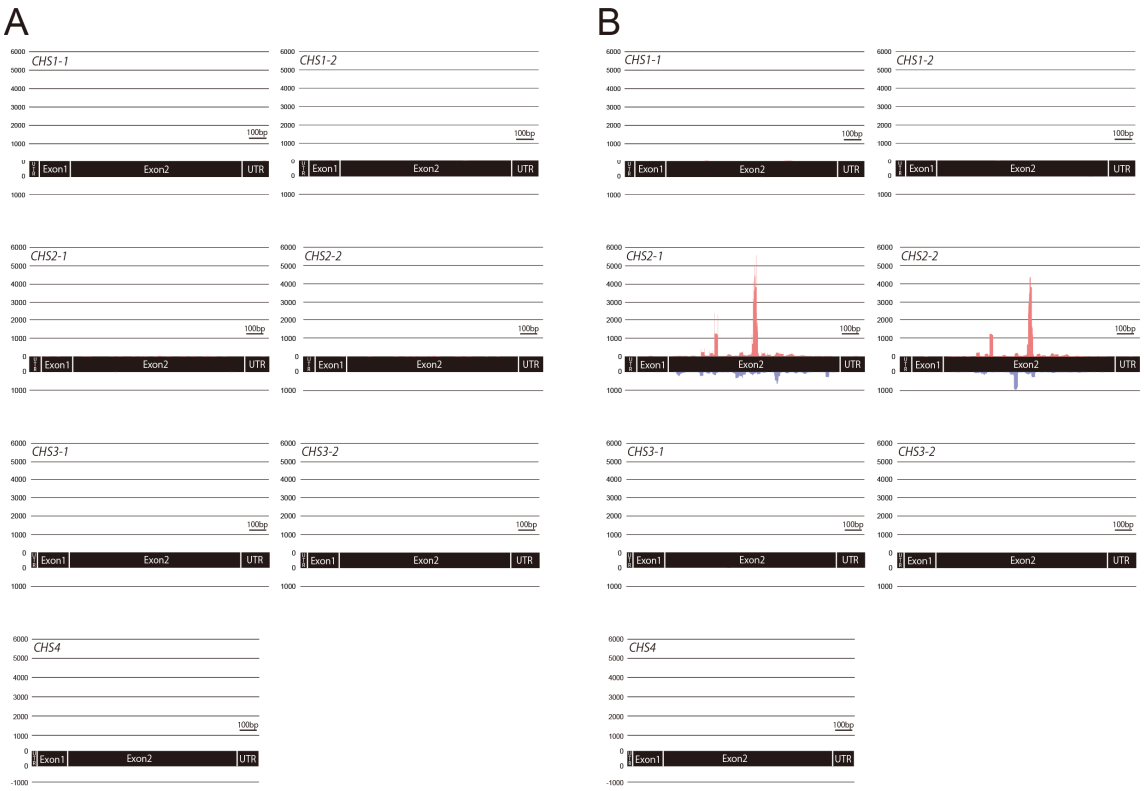

Fig. 4-10. Mapping of *CHS* small RNAs. A, a flavonoid rich leaf; B a flavonoid poor leaf. Small RNAs of 18–30 nt with 100% match to the *DvCHS1-1*, *DvCHS1-2*, *DvCHS2-1*, *DvCHS2-2*, *DvCHS3-1*, *DvCHS3-2* or *DvCHS4* genes were mapped on either the sense (pink: above the X-axis) or antisense (blue: below the X-axis) strand. The total reads of 18–30 nt were 12,046,092 for a flavonoid rich leaf, and 11,465,948 for a flavonoid poor leaf.

of *Hin*dIII using 3' probe in 'Michael J'. To confirm this results, genomic PCR was performed using each allele specific primers (Table 4-3). As with the DNA gel blot analysis, *DvCHS2-1* allele was detected from the tested six bicolor cultivars, but not from single-color cultivars (Fig. 4-11C). *MJ-1* and *MJ-2* alleles were detected from several cultivars, but no correlation between allele retention and flower color was detected (Fig. 4-11C).

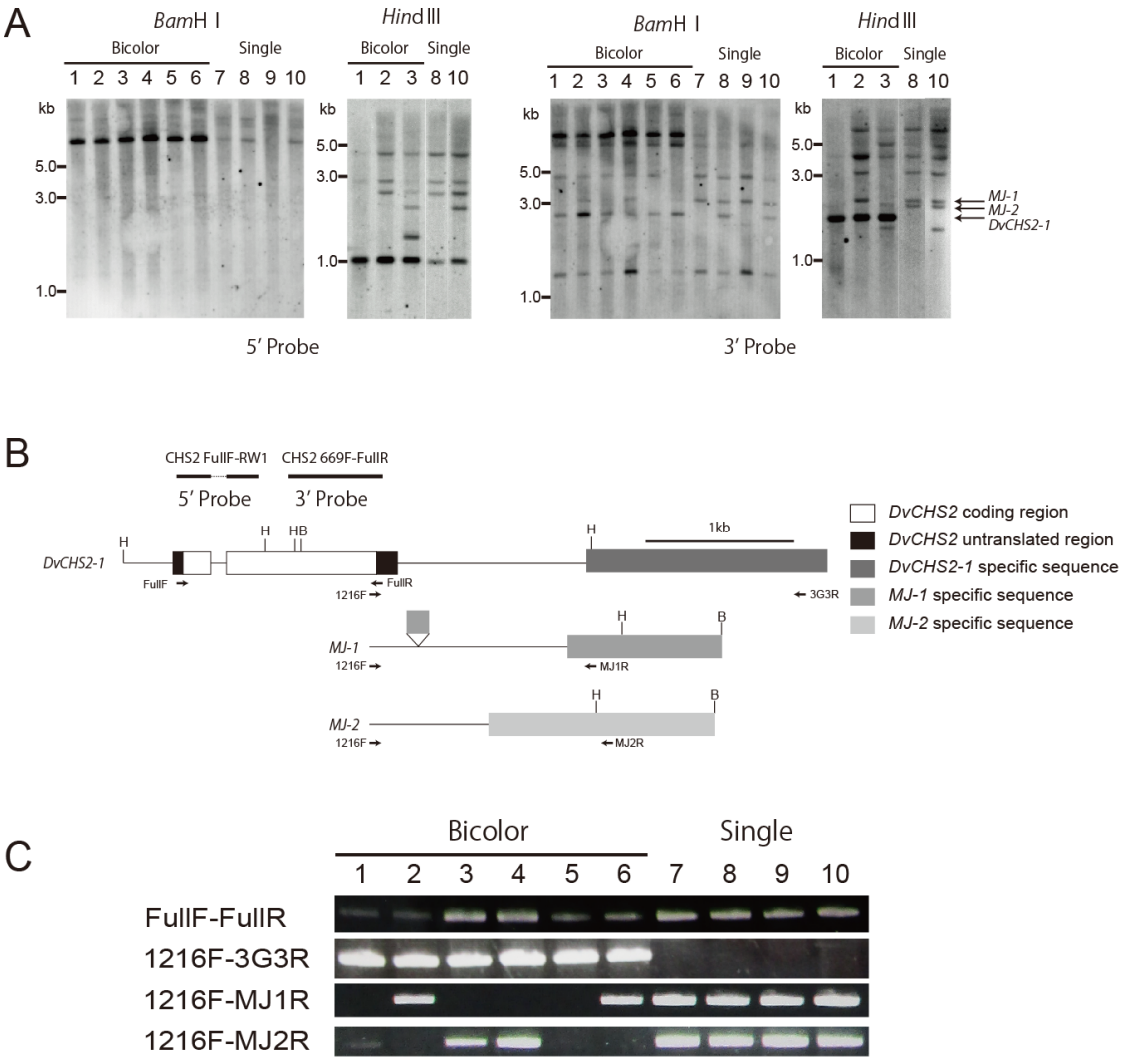

Fig. 4-11. Genomic structure of *DvCHS2*. A, DNA gel blot analysis of *DvCHS2*. The blot was hybridized with a 5' probe (left two panels) and a 3' probe (right two panels); B, physical map of *DvCHS2* genes in 'Yuino' and 'Michael J'. B and H indicate restriction enzyme recognition sites of *Bam*HI and *Hin*dIII. Arrows indicate the position of primers used in C; C, genomic PCR analysis of allele specific sequences in *DvCHS2* 3' flanking region. Numbers above the lanes indicate each cultivar: 1, 'Yuino'; 2, 'Matsuribayashi'; 3, 'Kazusa-shiranami'; 4, 'Santa Claus'; 5, 'OriW1'; 6, 'OriW2'; 7, 'Kokucho'; 8, 'Ms. Noir'; 9, 'Yukino' and 10, 'Michael J'.

Discussion

Petal color is associated with leaf flavonoid accumulation in a labile bicolor flowering dahlia 'Yuino'

Petal color lability is a common feature of bicolor dahlias, with the loss of the pure white tip from an original bicolor petal resulting in production of a single-colored petal. In some cases, all petals of an inflorescence develop into single color, and in other cases, partial petals of an inflorescence develop into single color. There are some species showing unstable flower color expression such as eustoma (Fukuta and Nakayama, 2008), but these cases of unstable flower color expression are obviously discriminated from petal color lability in bicolor dahlias. In other words, the case of eustoma is considered as a quantitative organ specific phenomenon, whereas the case of dahlia is considered as a qualitative phenomenon. Since petal color lability prevents uniform production and reduces the economic value of bicolor cultivars, a red–white bicolor cultivar 'Yuino' (Fig. 4-1C) was used to reveal the underlying mechanism. Similar to other bicolor flowering cultivars, 'Yuino' showed petal color lability (Fig. 4-2). The white tip in its petals (Fig. 4-1A) disappeared and single-colored petals (Fig. 4-1B) were formed entirely (Fig. 4-1D), or partially in an inflorescence (Fig. 4-1E, F).

I could identify particular features of red petals from the observation among > 10,000 inflorescences. One observation was that frequency of red petal occurrence was higher in the field experiment during spring to winter than in the greenhouse experiment during autumn to next summer (Figs 4-2 and 4-4). This indicates the involvement of environmental factor(s) in petal color lability. Another observation was the localization pattern of red petals in an inflorescence. When an inflorescence had more than 10 red petals, red petals occurred in the outer whorls and/or sectorally, and were not randomly arranged in an inflorescence in almost all cases (Fig. 4-1E, F). Red petals were never observed at the inner side of bicolor petals, coinciding with the results of the study by Tammes and Groeneveld-Huisman (1939). Not only petals (ray florets) but also disk

florets showed the specific localization. Lawrence (1931c) reported that when disk florets of 'Union Jack', a bicolor single flower cultivar, were fumed with ammonia, in many case of labile inflorescence, they were dark colored in the outer whorls and/or sectorally corresponded to petal colors. Here dark coloring by fuming with ammonia indicated accumulation of flavonoids. Thus, these results suggested that not only petals but the whole inflorescence itself was labile, and behaved in a similar fashion to a chimera or a lateral mutant. If so, it was assumed that some SAM state was labile, and that some characteristic(s) not only in an inflorescence but also at whole plant differed between red petal producing plants and bicolor petal producing plants. The difference between a bicolor petal and a single-colored petal was the presence or absence of the white area on the petals, where no flavonoids were accumulated. Therefore, it was expected that flavonoid accumulation in leaves should be a valuable indicator to reflect state of SAM, and I therefore further analyzed the relationship between petal colors and leaf flavonoid accumulation.

When an inflorescence had at least one red petal, all except for one plants accumulated flavonoids, presumably chalcones, in the uppermost leaf (Table 4-5). The ABS_{400}/ABS_{370} score of this exceptional plant was 0.708, suggesting that this plant accumulated a small amount of flavonoids. Regarding the contrapositive, when an uppermost leaf did not accumulate any flavonoids, the inflorescence inevitably had only bicolor petals (Table 4-5). Therefore, there was a distinct relationship between petal color and flavonoid accumulation in the uppermost leaf. This indicated the strong link of phenotypes between petal color and leaf flavonoid accumulation, suggesting petal color lability does not solely involve petal color change, but also SAM status change. From the results of whole plant analysis of leaf flavonoid accumulation, red-petal producing plants were rich flavonoid accumulator, while only bicolor-petal producing plants were poor or no flavonoid accumulator (Figs 4-6, 4-7). This suggested that leaf flavonoid synthetic potential was varied at whole plant level corresponding to petal colors. From these results, it is suggested that petal color lability of 'Yuino' results from a change in state of SAM in

flavonoid synthetic potential which is visualized as a petal color. This coincided with the interpretation by Jorgensen (1995) that multiple meristem states existed in a transgenic cosuppression petunia.

The R-line plant was selected from the plant which had the highest average red-petal ratio (Fig. 4-3). The feature of producing red petals with high frequency was maintained by cuttings or after an experience of *in vitro* environment (Fig. 4-4). Therefore, it was suggested that the high red frequency characteristic of the R-line was maintained by vegetative propagation. However, this does not mean that the R-line plant was a mutant incapable of producing bicolor petals, because some R-line plants still produced bicolor petals (Figs. 4-4 and 4-8) and interestingly, some R-line cutting siblings produced only bicolor petals. Not only R-line plants, but also three out of four *in vitro* 12-line plants produced red petals at a high frequency (Fig. 4-4C). This indicated that, although the underlying mechanism was unknown, as well as the R-line, other plants with a high red petal ratio could occur. Therefore, it is likely that propagation of these plants causes the increase of the frequency of single-colored petals.

Although in the same line, the 12-line and R-line plants showed clear difference in average red petal ratio of cutting siblings between mother plants (Fig. 4-8). The finding that 12-2 and R-1 plants clearly showed a higher average red petal ratio than 12-1 and R-2 plants, respectively, suggested that there was 'mother plant effect'. The 12-1 mother plant had been selected as a no leaf flavonoid accumulation plant and the 12-2 mother plant had been selected to show leaf flavonoid accumulation. The feature of leaf flavonoid synthesis was somewhat transferred to cutting siblings, with all four plants showing poor leaf flavonoid accumulation in 12-1, while three out of four showed rich flavonoid accumulation in 12-2 (data not shown). Therefore, the property of leaf flavonoid synthesis in a cutting sibling might be affected by the property of its mother plant.

PTGS of DvCHS2 *is associated with absence of leaf flavonoid accumulation*

In the current study, flavonoids accumulating leaves were putative chalcones

(Table 4-4). In *D. tenuicaulis*, 5, 7, 4'-trimethoxyflavanone, 5-hydroxy-7, 4'-dimethoxyflavanone, 2'-hydroxy-4, 4', 6'-trimethoxychalcone and 5, 7. 4'-trimethoxyflavan-4-ol were isolated from leaves (Lam and Wrang, 1975). Thus, it was expected that flavonoids in leaves might be subjected to modification such as methoxylation in *D. variabilis*. In flavonoid poor leaves, *DvCHS2* expression was lower than in flavonoid rich leaves (Table 4-6, Fig. 4-9). Small RNAs of a flavonoid poor leaf were mapped on *DvCHS2* genes (Fig. 4-10) indicating this suppression of *DvCHS2* was post-transcriptional. Therefore, PTGS of *DvCHS2* is associated with absence of leaf flavonoid accumulation and *DvCHS2* might be involved in leaf flavonoid biosynthesis.

Since CHS belongs to a member of multigene family, there are multiple paralogous CHS genes, and different paralogous genes function in different organs. In gerbera (*Gerbera hybrida*) *GhCHS1*, which is orthologous to *DvCHS2*, is associated with flavonoid biosynthesis in petals, while *GhCHS4*, which is orthologous to *DvCHS1*, is associated in vegetative tissues (Helariutta et al., 1995; Deng et al., 2013). However in dahlia, *DvCHS2* expressed in both petal and leaf tissues and the expression of this gene is completely coincided with flavonoid biosynthesis. Therefore, it was assumed that DvCHS2 protein might be the functional CHS enzyme in both petals and leaves.

Genomic background for PTGS of CHS genes

The specific structure of genomic sequence is reported as a causal factor for endogenous PTGS (Stam, 1997; Kusaba et al., 2003; Della Vedova et al., 2005; Kasai et al., 2007; Morita et al., 2012; Tsubokura et al., 2012). It is reported that two highly similar *glutelin* genes that form a tail-to-tail inverted repeat are a potent inducer of RNA silencing (Kusaba et al., 2003). With respect to *CHS* PTGS, inverted repeats of *CHS* in maize (Della Vedova et al., 2005) and soybean (Kasai et al., 2007) and a tandem repeat in petunia (Stam, 1997; Morita et al., 2012) are indicated as potent causes. In the case of dahlia, it could not confirm whether the silencing of *DvCHS1* and *DvCHS2* is interdependent, however, *CHS* siRNA was able to detect from the pure white area of OriW1 (Fig. 3-6), which did not

express *DvCHS1* in the petals (Figs. 3-3, 3-5). This demonstrates that the PTGS of *DvCHS2* can be induced without *DvCHS1* expression in OriW1. Thus, it was presumed that *DvCHS2* was a potential causal gene of the *CHS* PTGS in dahlia. DNA gel blot analysis suggested the existence of *DvCHS2* allele specific to bicolor flowering cultivars, which was identical to 'Yuino' *DvCHS2-1* (Fig. 4-11A). This allele was detected from only bicolor cultivars (Fig. 4-11C), suggesting *DvCHS2-1* allele is linked to silencing trigger locus.

There are some data to support this idea. The first is that the number of small RNAs matched to *DvCHS2-1* was higher than *DvCHS2-2* (Table 3-6), whereas no difference was observed between *DvCHS1-1* and *DvCHS1-2* (Table 3-5). The second is that, comparing with a flavonoid rich leaf, one of two down-regulated genes in a flavonoid poor leaf was completely coincided with *DvCHS2-1*. These data suggested that *DvCHS2-1* is more aggressively silenced than *DvCHS2-2* in petals and leaves. Therefore, *DvCHS2-1* allele might be linked with the causal gene of *CHS* PTGS.

Candidate mechanism behind petal color lability in bicolor flowering dahlias

A candidate mechanism controlling petal color lability in bicolor flowering dahlias is discussed here. Petal color was associated with leaf flavonoid accumulation (Table 4-5, Figs 4-6, 4-7), namely production of bicolor petals resulted from PTGS of *DvCHS1* and *DvCHS2* (Fig. 3-9) is tightly linked with flavonoid poor leaves resulted from PTGS of *DvCHS2* (Figs 4-9, 4-10). Causal gene of PTGS of *DvCHS* is presumed to be the *DvCHS2* (see above), thus, this petal color lability in bicolor dahlias could be interpreted as switching of *DvCHS2* PTGS. Since all shoot organs including petals and leaves are both differentiated from SAM, the location where switching occurs might be in the SAM.

A candidate model of SAM state for each flower coloration was proposed in Fig. 4-12. Here, an observation could be a strong clue that when red petals occurred in the outer whorls, red petals were located inevitably in the outer whorls rather than bicolor

petals (Fig. 4-1E), and the inverse pattern was never observed. This indicates an obvious direction for SAM state from red petal to bicolor petal. Considering a strong link between petal colors and leaf flavonoid accumulation (Table 4-5, Figs 4-6, 4-7), I could define SAM state of single-colored petal formation or a flavonoid accumulating leaf as "switch OFF" of *DvCHS2* PTGS, and SAM state of bicolor petal formation or a non-flavonoid accumulating leaf is "switch ON" of *DvCHS2* PTGS (Fig. 4-12A). Therefore, when the SAM maintains a "switch OFF" state, the inflorescence will be a single-color due to absence of *DvCHS2* PTGS, whereas when SAM maintains a "switch ON" state, inflorescence will be bicolor by *DvCHSs* PTGS. If the SAM maintains a "switch ON" state sectorally, inflorescence will be mixed with sectorial single-colored petals. If the switch of *DvCHSs* PTGS turns "ON" after the formation of outer whorl petals, the inflorescence color will be mixed with single-colored petals in the outer whorls (Fig. 4-12B). Original bicolor cultivars somewhere turn "switch ON" before the formation of inflorescence.

Above model can explain phenotypic relationship of petal color and leaf flavonoid accumulation, however another factor is required to explain the lability itself. Here, an endogenous factor is inferred to be involved in this switch control, perhaps an epigenetic factor such as DNA methylation. When the gene or locus which triggers *DvCHSs* PTGS is activated in SAM, an endogenous factor might fully or sectorally suppress the activation in SAM, resulting in petal color lability. To isolate the gene or locus which triggers *DvCHSs* PTGS would play an important role to elucidate the lability.

Selecting plants producing only bicolor petals

Vegetative propagation is convenient for mass propagation, and propagated plants are generally recognized as having the same property. However, propagated plants do not necessarily have the same property, and some kind of visible or invisible feature might have changed. In the case of 'Yuino', this might be the SAM state of *DvCHS2* PTGS. It was reported that PTGS of *CHS* in leaves caused phenotypic changes in

transgenic plant or viroid-infected plant (Dare et al., 2013; Füssy et al., 2013). However in dahlia, although flavonoid content was differed, almost no obvious changes was observed in appearance nor in gene expression (Table 4-6). This makes it difficult to discriminate the plants between potential single-colored petal producing plants and bicolor-only producing plants from the appearance.

However, my data suggested a method to regulate petal color lability. I could not identify red petal only plant line, but I could identify the bicolor petal only plant. Even if it was propagated by cutting from a mother plant with high single-colored petal frequency such as the R-line, poor or no flavonoid accumulating plants persisted and produced only bicolor petals (Figs. 4-6, 4-7). Thus, one candidate method for selecting bicolor flowering plants is to select and propagate from poor flavonoid accumulating plants where the switch of *DvCHS*s PTGS turns on. Although part of underlying mechanism still remains unknown, it might be possible to select plants producing only bicolor petals.

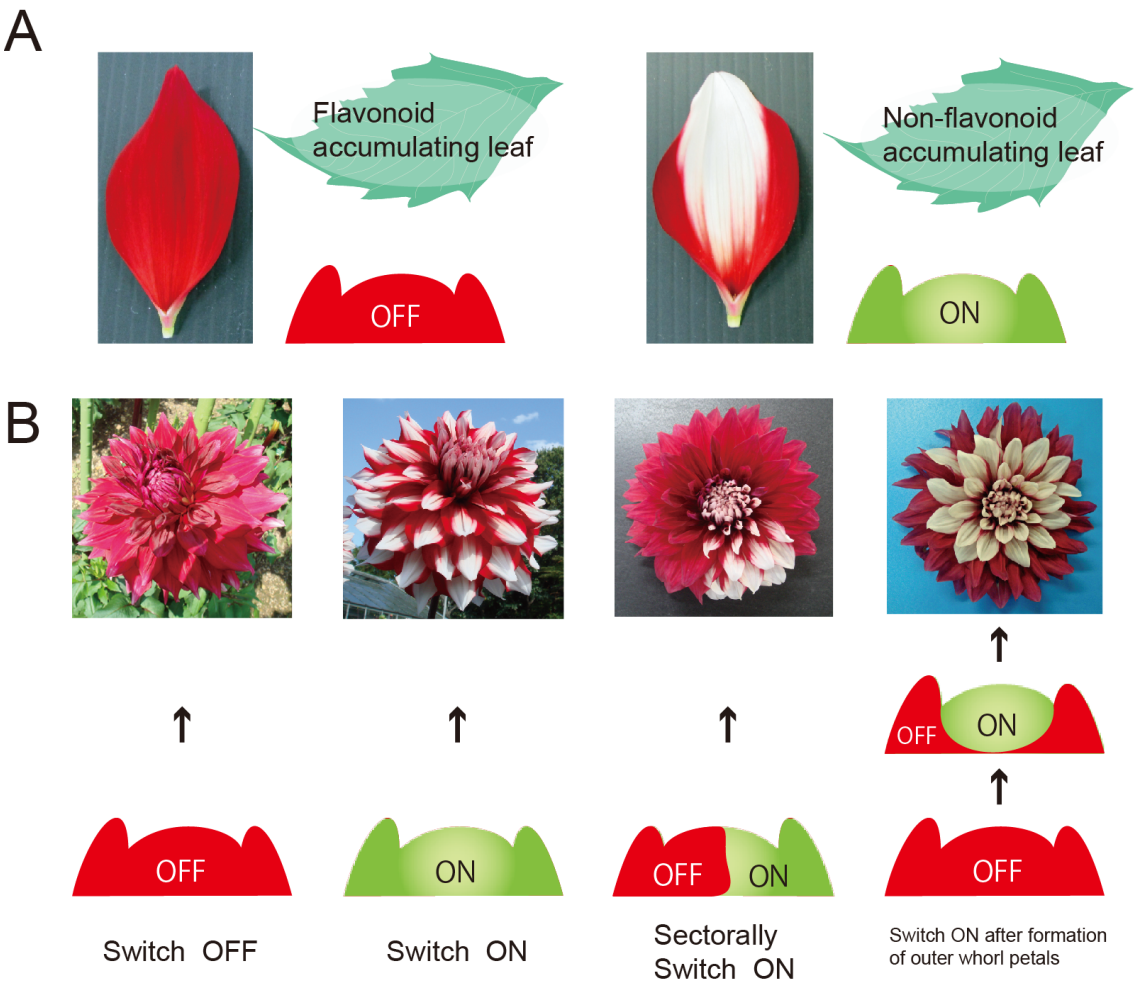

Fig. 4-12. A candidate model of SAM state for petal color lability in 'Yuino'. A, SAM state and petal coloration. SAM state is "OFF," single-colored petals are formed, and SAM state is "ON," bicolor petals are formed; B, SAM state and inflorescence coloration. SAM state is "OFF," inflorescences with only single-colored petals are formed, and SAM state is "ON," inflorescences with only bicolor colored petals are formed. When SAM state is sectorally "ON," mixed inflorescences with sectorial single-colored petals are formed. SAM state is switched from "OFF" to "ON" after formation of outer whorl petals, resulting in mixed inflorescences with outer whorl single-colored petals.

Abstract

Dahlias (*Dahlia variabilis*) are popular Asteraceae ornamental plants cultivated in many countries due to huge variation in flower shapes, sizes and colors. This wide variation is based onto complicated genetic background, namely dahlia is an autoallooctaploid with the chromosome number (2n = 8x = 64) having a large genome size. Dahlias exhibit a wide range of petal colors, such as ivory, yellow, pink, red, purple and black. In addition to huge color variation, there are flower color patterns such as variegation and bicolor. Pigments contributing to wide range of flower color in dahlia are flavonoids, mainly anthocyanin, butein, and flavone derivatives.

Polyploids are very common among plants. Polyploidy can be evolutionally advantageous in three points, i.e. heterosis, asexual reproduction and gene redundancy. In polyploids, complicated combination of alleles and/or loci can make for enormously huge variations in phenotype. However, it might be difficult that single loss of function mutation in biosynthetic pathway genes exhibit a phenotypic change, because of gene redundancy. Many horticultural plants are polyploids, therefore, how they diverse and regulate phenotypic characteristics is fascinating from the horticultural aspect.

In this study, I investigated the mechanisms controlling flower color and pattern diversity in *Dahlia*. Understanding the roles of genetic and epigenetic mechanisms controlling flower color and pattern diversity in dahlias provides useful information about not only the future breeding of dahlias, but also the regulation scheme of redundant genes in polyploid species.

In Chapter1, 1.1, the key factors for anthocyanin biosynthesis were analyzed using transposon tagging to MJOr and MJY, which are spontaneously occurring single-color bud mutants of the ‘Michael J’ that has orange variegation patterns on yellow petals.

MJOr produced completely red petals with anthocyanins, butein, and flavones, whereas MJY produced completely yellow petals with butein and flavones but without anthocyanins. Gene expression analysis revealed that six structural genes (*DvCHS1*, *DvF3H*, *DvDFR*, *DvANS*, *Dv3MT* and *DvGST*) in the anthocyanin synthesis pathway and a basic helix-loop-helix transcription factor *DvIVS* were downregulated in MJY. A CACTA superfamily transposable element was found in the *DvIVS* genomic region of MJY and was named *Tdv1*. These findings demonstrated that *DvIVS* is involved in the regulation of anthocyanin synthesis in dahlia flowers, and transposition of the *Tdv1* contributes to flower variegation patterning.

In Chapter1, 1.2, relationship between flower color intensities and *DvIVS* was analyzed using 12 cyanic cultivars with the petals of different color intensities. Flower color intensity was determined by the anthocyanin content and these cultivars were classified into four color groups depending on their anthocyanin content: deep purple cultivars (high anthocyanin content), purple cultivars (moderate anthocyanin content), pink cultivars (low anthocyanin content), and ivory white cultivars (no anthocyanin). In all these cultivars, a positive correlation was observed between the anthocyanin content and expression of some structural genes in the anthocyanin synthesis pathway that are regulated by *DvIVS*. A positive correlation was also found between anthocyanin content and *DvIVS* expression (r = 0.96), suggesting that quantitative expression of *DvIVS* determines flower color intensities in dahlia. Furthermore, *DvIVS* alleles were classified into at least six types on the basis of polymorphisms in the promoter and coding region. Correlations were also observed between flower color intensity and these *DvIVS* allelic types, indicating that *DvIVS* contributes to the diversity of flower color in dahlia by controlling the anthocyanin content.

In Chapter1, 1.3, the underlying mechanism controlling the formation of the white part in bicolor flowering dahlias was analyzed by comparing with ivory white cultivars. There were no flavonoids in the white part of bicolor petals, whereas flavone accumulated in petals of ivory white cultivars. Comparing expression levels of flavonoid biosynthetic genes between single-colored petals and the white part of bicolor petals, *DvCHS1* and *DvCHS2* were significantly lower in the white part of bicolor petals, while other flavonoid biosynthetic genes were almost the same. Comparing small RNA mapping profiles between a single-colored petal and the white part of a bicolor petal onto *CHS* genes, small RNAs from the white part of a bicolor petal were mapped onto two of four *CHSs*, *DvCHS1* and *DvCHS2*, while small RNAs from the single-colored red petal were not mapped onto all four *CHS*s. These results suggested that simultaneous post-transcriptional gene silencing (PTGS) of *CHS*s, mainly *DvCHS1* and *DvCHS2*, was a key factor for the white part formation in bicolor flowering dahlia.

In Chapter 2, petal color lability of bicolor flowering dahlias was analyzed. Bicolor flowering cultivars generally produce inflorescences with bicolor petals characterized by a colored basal part and a white tip; however, they frequently produce single-colored petals. This petal color lability prevents production of uniform cut or pot flowers of bicolor dahlias and reduces the economic value of bicolor cultivars. In this section, to reveal the underlying mechanism and to control color lability, the pattern of occurrence of single-colored petals was characterized in a red–white bicolor flowering cultivar ‘Yuino’. ‘Yuino’ produced inflorescences with bicolor petals, red petals, and both red and bicolor petals. Red petals occurred at the outer whorls or sectorally in a mixed inflorescence, similar to a chimera or a lateral mutant. There were strong relationships between the inflorescence color and the leaf phenotype; red petal-producing plants accumulated flavonoids in leaves, whereas only bicolor petal-producing plants tended not to accumulate flavonoids in leaves. This suggests that petal color of ‘Yuino’ is associated

with flavonoid synthetic potential in shoots. Therefore, a phenotypic difference is observed not only in petal colors but also at the whole plant level, and this phenotypic lability can be interpreted as flip of a switch of flavonoid biosynthesis in shoot apical meristem.

In flavonoid poor leaves, *DvCHS2* expression was lower than flavonoid rich leaves. Small RNAs in a flavonoid poor leaf were mapped on *DvCHS2* genes indicating this suppression of *DvCHS2* was post-transcriptional. Therefore, PTGS of *DvCHS2* is associated with flip of a switch of flavonoid biosynthesis in shoot apical meristem. The results that small RNAs in flavonoid poor leaves were poorly mapped on *DvCHS1*, and bicolor cultivars shared the specific *DvCHS2-1* allele, suggesting *DvCHS2-1* might be a trigger gene of *CHS* PTGS.

In conclusion, from genetic aspect, it was demonstrated that a bHLH transcription factor, *DvIVS* act as a regulator of anthocyanin biosynthesis, and diversify flower color intensity in dahlia. From epigenetic aspect, it was demonstrated that simultaneous silencing of multiple CHS genes is associated with bicolor pattern and petal color lability in bicolor cultivars. Because dahlias are polyploids, quantitative regulation by multiple alleles of the transcription factor, and PTGS that avoid gene redundancy play important roles to extend flower color and patterning.

Acknowledgements

I would like to express my sincere appreciation to Dr. Motoaki Doi (Kyoto University) for helpful suggestions and reviewing my work. Also, I would like to express my gratitude to Dr. Reiko Urade (Kyoto University) and Dr. Yutaka Okumoto (Kyoto University) for reviewing this thesis.

I would like to extend my appreciation to Dr. Susumu Yazawa (Kyoto University), Dr. Takahiro Hayashi (Kyoto University), Dr. Yoichi Mizuta (Kyoto University) and Dr. Munetaka Hosokawa (Kyoto University) for their advice. I am deeply grateful to Dr. Fumi Tatsuzawa (Iwate University) for his technical help on pigment analysis, Dr. Shigeru Iida (National Institute for Basic Biology), Dr. Atsushi Hoshino (National Institute for Basic Biology), Dr. Yasumasa Morita (National Institute for Basic Biology) and Dr. Kyeung-Il Park (National Institute for Basic Biology) for their technical help on molecular biology, Mr. Terufumi Naka (Nara Prefectural Agricultural Research and Development Center) and Mr. Yukihiro Fukuda for supplying plant materials. I express my sincere thanks to all the previous and present members of the laboratory of Vegetable and Ornamental Horticulture, Kyoto University, for their cheerful support. Finally, I would like to thank my friends and family for their continued support of my academic endeavors.

References

Azuma, A., Y. Udo, A. Sato, N. Mitani, A. Kono, Y. Ban, H. Yakushiji, Y. Koshita and S. Kobayashi. 2011. Haplotype composition at the color locus is a major genetic determinant of skin color variation in *Vitis* × *labruscana* grapes. Theor. Appl. Genet. 122: 1427–1438.

Bai, Y, S. Pattanaik, B. Patra, J. R. Werkman, C. H. Xie and L. Yuan. 2011. Flavonoid-related basic helix-loop-helix regulators, NtAn1a and NtAn1b, of tobacco have originated from two ancestors and are functionally active. Planta 234: 363–375.

Bate-Smith, E. C. and T. Swain. 1953. The isolation of 2, 4, 4'-trihydroxychalcone from yellow varieties of *Dahlia variabilis*. J. Chem. Soc. 2185–2187.

Bate-Smith, E. C., T. Swain and C. G. Nördstrom. 1955. Chemistry and inheritance of flower colour in the Dahlia. Nature 176: 1016–1018.

Bomati, E. K., M. B. Austin, M. E. Bowman, R. A. Dixon and J. P. Noel. 2005. Structural elucidation of chalcone reductase and implications for deoxychalcone biosynthesis. J. Biol. Chem. 280: 30496–30503.

Broertjes, C. and J. M. Ballego. 1967. Mutation breeding of *Dahlia variabilis*. Euphytica 16: 171–176.

Chopra, S., V. Brendel, J. Zhang, J. D. Axtell and T. Peterson. 1999. Molecular characterization of a mutable pigmentation phenotype and isolation of the first active transposable element from *Sorghum bicolor*. Proc. Natl. Acad. Sci. U. S. A. 96: 15330–15335.

Chuck, G., T. Robbins, C. Nijjar, E. Ralston, N. Courtney-Gutterson and H. K. Dooner. 1993. Tagging and cloning of a petunia flower color gene with the maize transposable element *Activator*. Plant Cell 5: 371–378.

Comai, L. 2005. The advantages and disadvantages of being polyploid. Nat. Rev. Gen. 6: 836–846.

Dare, A. P., S. Tomes, M. Jones, T. K. McGhie, D. E. Stevenson, R. A. Johnson, D. R. Greenwood and R. P. Hellens. 2013. Phenotypic changes associated with RNA interference silencing of chalcone synthase in apple (*Malus* × *domestica*). Plant J. 74: 398–410.

De Paoli, E., A. Dorantes-Acosta, Z. Jixian, M. Accerbi, D. H. Jeong, P. Sunhee, B. C. Meyers, R. A. Jorgensen and P. J. Green. 2009. Distinct extremely abundant siRNAs associated with cosuppression in petunia. RNA 15:1965–1970.

De Vetten, N., F. Quattrocchio, J. Mol and R. Koes. 1997. The *an11* locus controlling flower pigmentation in petunia encodes a novel WD-repeat protein conserved in yeast, plants, and animals. Genes Dev. 11: 1422–1434.

Della Vedova, C. B., R. Lorbiecke, H. Kirsch, M. B. Schulte, K. Scheets, L. M. Borchert, B. E. Scheffler, U. Wienand, K. C. Cone and J. A. Birchler. 2005. The dominant inhibitory chalcone synthase allele *C2-Idf* (*inhibitor diffuse*) from *Zea mays* (L.) acts via an endogenous RNA silencing mechanism. Genetics 170: 1989–2002.

Deng, X., H. Bashandy, M. Ainasoja, J. Kontturi, M. Pietiäinen, R. A. E. Laitinen, V. A. Albert, J. P. T. Valkonen, P. Elomaa and T. H. Teeri. 2014. Functional diversification of duplicated chalcone synthase genes in anthocyanin biosynthesis of *Gerbera hybrida*. New Phytol. 201: 1469–1483.

Dubos, C., J. Le Gourrierec, A. Baudry, G. Huep, E. Lanet, I. Debeaujon, J. M. Routaboul, A. Alboresi, B. Weisshaar and L. Lepiniec. 2008. MYBL2 is a new regulator of flavonoid biosynthesis in *Arabidopsis thaliana*. Plant J. 55: 940–953.

Fedoroff, N. V., D. B. Furtek and O. E. Nelson. 1984. Cloning of the *bronze* locus in maize by a simple and generalizable procedure using the transposable controlling element *Activator* (*Ac*). Proc. Natl. Acad. Sci. U. S. A. 81: 3825–3829.

Ferrer J. L., J. M. Jez, M. E. Bowman, R. A. Dixon and J. P. Noel. 1999. Structure of chalcone synthase and the molecular basis of plant polyketide biosynthesis. Nat. Struct. Biol. 6: 775–784.

Feschotte, C., N. Jiang and S. R. Wessler. 2002. Plant transposable elements: Where genetics meets genomics. Nat. Rev. Gen. 3: 329–341.

Fischer, D., K. Stich, L. Britsch, H. Grisebach. 1988. Purification and characterization of (+) dihydroflavonol (3-hydroxyflavanone) 4-reductase from flowers of *Dahlia variabilis*. Arch. Biochem. Biophys. 264: 40–47.

Fujioka, M., M. Kato, F. Kakihara and S. Tokumasu S. 1991. Anthocyanidin composition of petals in *Pelargonium* × *domesticum* Baiey. J. Japan. Soc. Hort. Sci. 59: 823–831.

Fukusaki, E. I., K. Kawasaki, S. Kajiyama, C. I. An, K. Suzuki, Y. Tanaka and A. Kobayashi. 2004. Flower color modulations of *Torenia hybrida* by downregulation of chalcone synthase genes with RNA interference. J. Biotechnol. 111: 229–240.

Fukuta, N. and M. Nakayama. 2008. Influence of temperature on the coloring area rate in picotee petals of *Eustoma grandiflorum* (Raf.) Shinn. Hort. Res. (Japan) 7: 531–536 (In Japanese with English abstract).

Füssy, Z., J. Patzak, J. Stehlík and J. Matoušek. 2013. Imbalance in expression of hop (*Humulus lupulus*) chalcone synthase H1 and its regulators during hop stunt viroid pathogenesis. J. Plant Physiol. 170: 688–695.

Gatt, M., H. Ding, K. Hammett and B. Murray. 1998. Polyploidy and evolution in wild and cultivated *Dahlia* species. Ann. Bot. 81: 647–656.

Ghildiyal, M. and P. D. Zamore. 2009. Small silencing RNAs: An expanding universe. Nat. Rev. Gen. 10: 94–108.

Gonzalez, A., M. Zhao, J. M. Leavitt and A. M. Lloyd. 2008. Regulation of the anthocyanin biosynthetic pathway by the TTG1/bHLH/Myb transcriptional complex in Arabidopsis seedlings. Plant J. 53: 814–827.

Grotewold, E. 2006. The genetics and biochemistry of floral pigments. Annu. Rev. Plant Biol. 57: 761–780.

Habu, Y., Y. Hisatomi and S. Iida. 1998. Molecular characterization of the mutable flaked allele for flower variegation in the common morning glory. Plant J. 16: 371–376.

Hamilton, A. J. and D. C. Baulcombe. 1999. A species of small antisense RNA in posttranscriptional gene silencing in plants. Science 286: 950–952.

Harborne, J. B. 1984. Phytochemical methods, second edition. Chapman and Hall, London.

Harborne, J. B., J. Greenham and J. Eagles. 1990. Malonylated chalcone glycosides in *Dahlia*. Phytochemistry 29: 2899–2900.

Hashimoto, F., M. Tanaka, H. Maeda, K. Shimizu and Y. Sakata. 2000. Characterization of cyanic flower color of *Delphinium* cultivars. J. Japan. Soc. Hort. Sci. 69: 428–434.

Helariutta, Y., P. Elomaa, M. Kotilainen, R. J. Griesbach, J. Schroder and T. H. Teeri. 1995. Chalcone synthase-like genes active during corolla development are differentially expressed and encode enzymes with different catalytic properties in *Gerbera hybrida* (Asteraceae). Plant Mol. Biol. 28: 47–60.

Hemleben, V., A. Dressel, B. Epping, R. Lukačin, S. Martens and M. B. Austin. 2004. Characterization and structural features of a chalcone synthase mutation in a white-flowering line of *Matthiola incana* R. Br. (Brassicaceae). Plant Mol. Biol. 55: 455–465.

Hichri, I., F. Barrieu, J. Bogs, C. Kappel, S. Delrot and V. Lauvergeat. 2011. Recent advances in the transcriptional regulation of the flavonoid biosynthetic pathway. J. Exp. Bot. 62: 2465–2483.

Hoshino, A., K. I. Park and S. Iida. 2009. Identification of *r* mutations conferring white flowers in the Japanese morning glory (*Ipomoea nil*). J. Plant Res. 122: 215–222.

Hosokawa, M., A. Otake, Y. Sugawara, T. Hayashi and S. Yazawa. 2004. Rescue of shoot apical meristems of chrysanthemum by culturing on root tips. Plant Cell Rep. 22: 443–448.

Inagaki, Y., Y. Hisatomi, T. Suzuki, K. Kasahara and S. Iida. 1994. Isolation of a *Suppressor-mutator*/*Enhancer*-like transposable element, *Tpn1*, from Japanese morning glory bearing variegated flowers. Plant Cell 6: 375–383.

Jiang, C. Z., J. C. Chen and M. Reid. 2011. Virus-induced gene silencing in ornamental plants. Methods Mol. Biol. 744: 81–96.

Jorgensen, R. A. 1995. Cosuppression, flower color patterns, and metastable gene expression states. Science 268: 686–691.

Kasai, A., K. Kasai, S. Yumoto and M. Senda. 2007. Structural features of *GmIRCHS*, candidate of the *I* gene inhibiting seed coat pigmentation in soybean: Implications for inducing endogenous RNA silencing of chalcone synthase genes. Plant Mol. Biol. 64: 467–479.

Kobayashi, S. 2009. Regulation of anthocyanin biosynthesis in grapes. J. Japan. Soc. Hort. Sci. 78: 387–393.

Kobayashi, S., N. Goto-Yamamoto and H. Hirochika. 2005. Association of VvmybA1 gene expression with anthocyanin production in grape (*Vitis vinifera*) skin-color mutants. J. Japan. Soc. Hort. Sci. 74: 196–203.

Kobayashi, S., M. Ishimaru, K. Hiraoka and C. Honda. 2002. Myb-related genes of the Kyoho grape (*Vitis labruscana*) regulate anthocyanin biosynthesis. Planta 215: 924–933.

Koes, R., W. Verweij and F. Quattrocchio. 2005. Flavonoids: A colorful model for the regulation and evolution of biochemical pathways. Trends Plant Sci. 10: 236–242.

Konishi, K. and K. Inaba. 1964. Studies on flowering control of dahlia. I. On optimum day-length. J. Japan. Soc. Hort. Sci. 33: 171–180 (In Japanese with English abstract).

Koseki, M., K. Goto, C. Masuta and A. Kanazawa. 2005. The star-type color pattern in *Petunia hybrida* 'Red Star' flowers is induced by sequence-specific degradation of *chalcone synthase* RNA. Plant Cell Physiol. 46: 1879–1883.

Kurauchi, T., T. Matsumoto, A. Taneda, T. Sano and M. Senda. 2009. Endogenous short interfering RNAs of chalcone synthase genes associated with inhibition of seed coat pigmentation in soybean. Breed. Sci. 59: 419–426.

Kusaba, M., K. Miyahara, S. Iida, H. Fukuoka, T. Takano, H. Sassa, M. Nishimura and T. Nishio. 2003. *Low glutelin content1*: A dominant mutation that suppresses the glutelin multigene family via RNA silencing in rice. Plant Cell 15: 1455–1467.

Laitinen, R. A. E., M. Ainasoja, S. K. Broholm, T. H. Teeri amd P. Elomaa. 2008. Identification of target genes for a MYB-type anthocyanin regulator in *Gerbera hybrida*. J. Exp. Bot. 59: 3691–3703.

Lam, J. and P. Wrang. 1975. Flavonoids and polyacetylenes in *Dahlia tenuicaulis*. Phytochemistry 14: 1621–1623.

Lawrence, R. J. and C. S. Pikaard. 2003. Transgene-induced RNA interference: A strategy for overcoming gene redundancy in polyploids to generate loss-of-function mutations. Plant J. 36: 114–121.

Lawrence, W. J. C. 1929. The genetics and cytology of Dahlia species. J. Genet. 21: 125–159.

Lawrence, W. J. C. 1931a. The secondary association of chromosomes. *Cytologia* 2: 352–384.

Lawrence, W. J. C. 1931b. The genetics and cytology of *Dahlia variabilis*. J. Genet. 24: 257–306.

Lawrence, W. J. C. 1931c. Mutation or segregation in the octoploid *Dahlia variabilis*. J. Genet. 24: 307–324.

Lawrence, W. J. C. and R. Scott-Honcrieff. 1935. The genetics and chemistry of flower colour in *Dahlia*: A new theory of specific pigmentation. J. Genet. 30: 155–226.

Ludwig, S. R., L. F. Habera, S. L. Dellaporta and S. R. Wessler. 1989. *Lc*, a member of the maize *R* gene family responsible for tissue-specific anthocyanin production,

encodes a protein similar to transcriptional activators and contains the *myc*-homology region. Proc. Natl. Acad. Sci. U. S. A. 86: 7092–7096.

Ma, L. Q., X. B. Pang, H. Y. Shen, G. B. Pu, H. H. Wang, C. Y. Lei, H. Wang, G. F. Li, B. Y. Liu and H. C. Ye. 2009. A novel type III polyketide synthase encoded by a three-intron gene from *Polygonum cuspidatum*. Planta 229: 457–469.

Marchler-Bauer, A., S. Lu, J. B. Anderson, F. Chitsaz, M. K. Derbyshire, C. DeWeese-Scott, J. H. Fong, L. Y. Geer, R. C. Geer, N. R. Gonzales, M. Gwadz, D. I. Hurwitz, J. D. Jackson, Z. Ke, C. J. Lanczycki, F. Lu, G. H. Marchler, M. Mullokandov, M. V. Omelchenko, C. L. Robertson, J. S. Song, N. Thanki, R. A. Yamashita, D. Zhang, N. Zhang, C. Zheng and S. H. Bryant. 2011. CDD: A Conserved Domain Database for the functional annotation of proteins. Nucleic Acids Res. 39: D225–D229.

Markham, K. R. and D. J. Ofman. 1993. Lisianthus flavonoid pigments and factors influencing their expression in flower colour. Phytochemistry 34: 679–685.

Martens, S. and A. Mithöfer. 2005. Flavones and flavone synthases. Phytochemistry 66: 2399–2407.

Martin, C., R. Carpenter, H. Sommer, H. Saedler and E. S. Coen. 1985. Molecular analysis of instability in flower pigmentation of *Antirrhinum majus*, following isolation of the *pallida* locus by transposon tagging. EMBO J. 4: 1625–1630.

Mato, M., T. Onozaki, Y. Ozeki, D. Higeta, Y. Itoh, T. Hisamatsu, H. Yoshida and M. Shibata. 2001. Flavonoid biosynthesis in pink-flowered cultivars derived from 'William Sim' carnation (*Dianthus caryophyllus*). J. Japan Soc. Hort. Sci. 70: 315–319.

Mato, M., T. Onozaki, Y. Ozeki, D. Higeta, Y. Itoh, Y. Yoshimoto, H. Ikeda, H. Yoshida and M. Shibata. 2000. Flavonoid biosynthesis in white-flowered Sim carnations (*Dianthus caryophyllus*). Sci. Hortic. 84: 333–347.

Matsui, K., Y. Umemura and M. Ohme-Takagi. 2008. AtMYBL2, a protein with a single MYB domain, acts as a negative regulator of anthocyanin biosynthesis in Arabidopsis. Plant J. 55: 954–967.

McClaren, M. 2009. *Dahlia*: history and species. p.161–166. In: B. McClaren, *Encyclopedia of dahlias*. Timber Press, Portland, OR.

Metzlaff, M., M. O'Dell, P. D. Cluster and R. B. Flavell. 1997. RNA-mediated RNA degradation and Chalcone Synthase A silencing in Petunia. Cell 88: 845–854.

Miura, A., S. Yonebayashi, K. Watanabe, T. Toyama, H. Shimada and T. Kakutani. 2001. Mobilization of transposons by a mutation abolishing full DNA methylation in Arabidopsis. Nature 411: 212–214.

Mol, J., E. Grofewold and R. Koes. 1998. How genes paint flowers and seeds. Trends Plant Sci. 3: 212–217.

Morita, Y., R. Saito, Y. Ban, N. Tanikawa, K. Kuchitsu, T. Ando, M. Yoshikawa, Y. Habu, Y. Ozeki and M. Nakayama. 2012. Tandemly arranged *chalcone synthase A* genes contribute to the spatially regulated expression of siRNA and the natural bicolor floral phenotype in *Petunia hybrida*. Plant J. 70: 739–749.

Morita, Y., M. Saitoh, A. Hoshino, E. Nitasaka and S. Iida. 2006. Isolation of cDNAs for R2R3-MYB, bHLH and WDR transcriptional regulators and identification of *c* and *ca* mutations conferring white flowers in the Japanese morning glory. Plant Cell Physiol. 47: 457–470.

Motohashi, R., E. Ohtsubo and H. Ohtsubo. 1996. Identification of *Tnr3*, a *Suppressor-Mutator*/*Enhancer*-like transposable element from rice. Mol. Gen. Genet. 250: 148–152.

Murashige, T. and F. Skoog. 1962. A revised medium for rapid growth and bioassays with tobacco tissue cultures. Physiol. Plant. 15: 473–497.

Murray, M. G. and W. F. Thompson. 1980. Rapid isolation of high molecular weight plant DNA. Nucleic Acids Res. 8: 4321–4325.

Nacken, W. K. F., R. Piotrowiak, H. Saedler and H. Sommer. 1991. The transposable element *Tam1* from *Antirrhinum majus* shows structural homology to the maize transposon *En*/*Spm* and has no sequence specificity of insertion. Mol. Gen. Genet. 228: 201–208.

Naka, T., S. Maeda and Y. Sumikawa. 2007. Tuberous root production of dahlia (*Dahlia* × *cultorum*) by cuttage from apical meristem culture plants. Bull. Nara Agr. Exp. Sta. 38: 23–30 (In Japanese with English abstract).

Nakatsuka, T., K. S. Haruta, C. Pitaksutheepong, Y. Abe, Y. Kakizaki, K. Yamamoto, N. Shimada, S. Yamamura and M. Nishihara. 2008. Identification and characterization of R2R3-MYB and bHLH transcription factors regulating anthocyanin biosynthesis in gentian flowers. Plant Cell Physiol. 49: 1818–1829.

Nakatsuka, T., M. Nishihara, K. Mishiba and S. Yamamura. 2005. Two different mutations are involved in the formation of white-flowered gentian plants. Plant Sci. 169: 949–958.

Napoli, C., C. Lemieux and R. Jorgensen. 1990. Introduction of a chimeric chalcone synthase gene into petunia results in reversible co-suppression of homologous genes *in trans*. Plant Cell 2: 279–289.

Nesi, N., I. Debeaujon, C. Jond, G. Pelletier, M. Caboche and L. Lepiniec. 2000. The TT8 gene encodes a basic helix-loop-helix domain protein required for expression of DFR and BAN genes in Arabidopsis siliques. Plant Cell 12: 1863–1878.

Noda, K. I., B. J. Glover, P. Linstead and C. Martin. 1994. Flower colour intensity depends on specialized cell shape controlled by a Myb-related transcription factor. Nature 369: 661–664.

Nordström, C. G. and T. Swain. 1953. The flavonoid glycosides of *Dahlia variabilis*. Part I. General introduction. Cyanidin, apigenin, and luteolin glycosides from the variety "Dandy". J. Chem. Soc. 2764–2773.

Nordström, C. G. and T. Swain. 1956. The flavonoid glycosides of *Dahlia variabilis*. II. Glycosides of yellow varieties Pius IX and Coton. Arch. Biochem. Biophys. 60: 329–344.

Nordström, C. G. and T. Swain. 1958. The flavonoid glycosides of *Dahlia variabilis*. III. Glycosides from white varieties. Arch. Biochem. Biophys. 73: 220–223.

Ogata, J., T. Sakamoto, M. A. Yamaguchi, S. Kawanobu and K. Yoshitama. 2001. Isolation and characterization of anthocyanin 5-*O*-glucosyltransferase from flowers of *Dahlia variabilis*. J. Plant Physiol. 158: 709–714.

Onozaki, T., M. Mato, M. Shibata and H. Ikeda. 1999. Differences in flower color and pigment composition among white carnation (*Dianthus caryophyllus* L.) cultivars. Sci. Hortic. 82: 103–111.

Ozeki, Y., E. Davies and J. Takeda. 1997. Somatic variation during long term subculturing of plant cells caused by insertion of a transposable element in a phenylalanine ammonia-lyase (PAL) gene. Mol. Gen. Genet. 254: 407–416.

Park, K. I., J. D. Choi, A. Hoshino, Y. Morita and S. Iida. 2004. An intragenic tandem duplication in a transcriptional regulatory gene for anthocyanin biosynthesis confers pale-colored flowers and seeds with fine spots in *Ipomoea tricolor*. Plant J. 38: 840–849.

Park, K. I., N. Ishikawa, Y. Morita, J. D. Choi, A. Hoshino and S. Iida. 2007. A bHLH regulatory gene in the common morning glory, Ipomoea purpurea, controls anthocyanin biosynthesis in flowers, proanthocyanidin and phytomelanin pigmentation in seeds, and seed trichome formation. Plant J. 49: 641–654.

Pattanaik, S., Q. Kong, D. Zaitlin, J. R. Werkman, C. H. Xie, B. Patra and L. Yuan. 2010. Isolation and functional characterization of a floral tissue-specific R2R3 MYB regulator from tobacco. Planta 231: 1061–1076.

Payne, C. T., F. Zhang and A. M. Lloyd. 2000. *GL3* encodes a bHLH protein that regulates trichome development in arabidopsis through interaction with GL1 and TTG1. Genetics 156: 1349–1362.

Pereira, A., H. Cuypers, A. Gierl, Z. Schwarz-Sommer and H. Saedler. 1986. Molecular analysis of the *En*/*Spm* transposable element system of *Zea mays*. EMBO J. 5: 835–841.

Price, J. R. 1939. The yellow colouring matter of *Dahlia variabilis*. J. Chem. Soc. 1017–1018.

Quattrocchio, F., W. Verweij, A. Kroon, C. Spelt, J. Mol and R. Koes. 2006. PH4 of petunia is an R2R3 MYB protein that activates vacuolar acidification through interactions with basic-helix-loop-helix transcription factors of the anthocyanin pathway. Plant Cell 18: 1274–1291.

Quattrocchio, F., J. F. Wing, H. T. C. Leppen, J. N. M. Moland R. E. Koes. 1993. Regulatory genes controlling anthocyanin pigmentation are functionally conserved among plant species and have distinct sets of target genes. Plant Cell 5: 1497–1512.

Quattrocchio, F., J. F. Wing, K. Van der Woude, J. N. M. Mol and R. Koes. 1998. Analysis of bHLH and MYB domain proteins: Species-specific regulatory differences are caused by divergent evolution of target anthocyanin genes. Plant J. 13: 475–488.

Robinson, M. D., D. J. McCarthy and G. K. Smyth. 2010. edgeR: a Bioconductor package for differential expression analysis of digital gene expression data. Bioinformatics 26: 139–140.

Saito, N., K. Ishizuka and Y. Osawa. 1970. Paper-choromatographic identification of flavonoids from a scarlet-flowering dahlia and crystallization of pelargonidin and butein. Botanical Magazine Tokyo 83: 229–232.

Saito N., J. Cheng, M. Ichimura, M. Yokoi, Y. Abe and T. Honda. 1994. Flavonoids in the acyanic flowers of *Pharbits nil*. Phytochemistry 35:687–691.

Saito, R., N. Fukuta, A. Ohmiya, Y. Itoh, Y. Ozeki, K. Kuchitsu and M. Nakayama. 2006. Regulation of anthocyanin biosynthesis involved in the formation of marginal picotee petals in *Petunia*. Plant Sci. 170: 828–834.

Schlangen, K., S. Miosic and H. Halbwirth. 2010a. Allelic variants from *Dahlia variabilis* encode flavonoid 3′-hydroxylases with functional differences in chalcone 3-hydroxylase activity. Arch. Biochem. Biophys. 494: 40–45.

Schlangen, K., S. Miosic, J. Thill and H. Halbwirth. 2010b. Cloning, functional expression, and characterization of a chalcone 3-hydroxylase from *Cosmos sulphureus*. J. Exp. Bot. 61: 3451–3459.

Schlangen, K., S. Miosic, F. Topuz, G. Muster, T. Marosits, C. Seitz and H. Halbwirth. 2009. Chalcone 3-hydroxylation is not a general property of flavonoid 3′-hydroxylase. Plant Sci. 177: 97–102.

Senda, M., A. Jumonji, S. Yumoto, R. Ishikawa, T. Harada, M. Niizeki and S. Akada. 2002. Analysis of the duplicated *CHS1* gene related to the suppression of the seed coat pigmentation in yellow soybeans. Theor. Appl. Genet. 104: 1086–1091.

Shirsat, A. H. 1988. A transposon-like structure in the 5′ flanking sequence of a legumin gene from *Pisum sativum*. Mol. Gen. Genet. 212: 129–133.

Singh, J. P., R. S. Arora, S. R. Dohare and K. Sengupta. 1970. A spontaneous mutant for flower colour and shape in a white flowering dahlia. Euphytica 19: 261–262.

Slotkin, R. K. and R. Martienssen. 2007. Transposable elements and the epigenetic regulation of the genome. Nat. Rev. Genet. 8: 272–285.

Snowden, K. C. and C. A. Napoli. 1998. *Psl*: A novel *Spm*-like transposable element from *Petunia hybrida*. Plant J. 14: 43–54.

Spelt, C., F. Quattrocchio, J. Mol and R. Koes. 2002. ANTHOCYANIN1 of petunia controls pigment synthesis, vacuolar pH, and seed coat development by genetically distinct mechanisms. Plant Cell 14: 2121–2135.

Spelt, C., F. Quattrocchio, J. N. M. Mol and R. Koes. 2000. *anthocyanin1* of Petunia encodes a basic helix-loop-helix protein that directly activates transcription of structural anthocyanin genes. Plant Cell 12: 1619–1631.

Spribille, R. and G. Forkmann. 1982. Genetic control of chalcone synthase activity in flowers of *Antirrhinum majus*. Phytochemistry 21: 2231–2234.

Stam, M. 1997. Post-transcriptional silencing of flower pigmentation genes in *Petunia hybrida* by (trans)gene repeats. PhD thesis, Vrije Universiteit.

Suzuki, H., T. Nakayama, K. Yonekura-Sakakibara, Y. Fukui, N. Nakamura, M. A. Yamaguchi, Y. Tanaka, T. Kusumi and T. Nishino. 2002. cDNA cloning, heterologous expressions, and functional characterization of malonyl-coenzyme A:anthocyanidin 3-*O*-glucoside-6′-*O*-malonyltransferase from dahlia flowers. Plant Physiol. 130: 2142–2151.

Takeda, K., J. B. Harborne and R. Self. 1986. Identification and distribution of malonated anthocyanins in plants of the compositae. Phytochemistry 25: 1337–1342.

Tammes, T. and A. F. Groeneveld-Huisman. 1939. Local pigment suppression in the flowers of *Dahlia variabilis* Desf. Genetica 21: 301–324.

Tanaka, Y., N. Sasaki and A. Ohmiya. 2008. Biosynthesis of plant pigments: Anthocyanins, betalains and carotenoids. Plant J. 54: 733–749.

Temsch, E. M., J. Greilhuber, K. R. W. Hammett and B. G. Murray. 2008. Genome size in *Dahlia* Cav. (Asteraceae-Coreopsideae). Plant Syst. Evol. 276: 157–166.

Tian, P. F. 2006. Progress in plant CACTA elements. Acta Genet. Sinica 33: 765–774.

Toledo-Ortiz, G., E. Huq and P. H. Quail. 2003. The Arabidopsis basic/helix-loop-helix transcription factor family. Plant Cell 15: 1749–1770.

Tsubokura, Y., M. Hajika, H. Kanamori, Z. Xia, S. Watanabe, A. Kaga, Y. Katayose, M. Ishimoto and K. Harada. 2012. The β-conglycinin deficiency in wild soybean is

associated with the tail-to-tail inverted repeat of the α-subunit genes. Plant Mol. Biol. 78: 301–309.

Tuteja, J. H., G. Zabala, K. Varala, M. Hudson and L. O. Vodkin. 2009. Endogenous, tissue-specific short interfering RNAs silence the chalcone synthase gene family in *Glycine max* seed coats. Plant Cell 21: 3063–3077.

Uddin, A. F. M. J., F. Hashimoto, T. Miwa, K. Ohbo, Y. Sakata. 2004. Seasonal variation in pigmentation and anthocyanidin phenetics in commercial Eustoma flowers. Sci Hortic. 100: 103–115.

Van Der Krol, A. R., L. A. Mur, M. Beld, J. N. M. Mol and A. R. Stuitje. 1990. Flavonoid genes in petunia: Addition of a limited number of gene copies may lead to a suppression of gene expression. Plant Cell 2: 291–299.

Vodkin, L. O., P. R. Rhodes, R. B. Goldberg. 1983. Ca lectin gene insertion has the structural features of a transposable element. Cell 34: 1023–1031.

Wimmer, G., H. Halbwirth, F. Wurst, G. Forkmann and K. Stich. 1998. Enzymatic hydroxylation of 6'-deoxychalcones with protein preparations from petals of *Dahlia variabilis*. Phytochemistry 47: 1013–1016.

Winkel-Shirley, B. 2001. Flavonoid biosynthesis. A colorful model for genetics, biochemistry, cell biology, and biotechnology. Plant Physiol. 126: 485–493.

Xu, M., H. K. Brar, S. Grosic, R. G. Palmer and M. K. Bhattacharyya. 2010. Excision of an active CACTA-like transposable element from *DFR2* causes variegated flowers in soybean [*Glycine max* (L.) Merr.]. Genetics 184: 53–63.

Yamagishi, M., Y. Yoshida and M. Nakayama. 2012. The transcription factor LhMYB12 determines anthocyanin pigmentation in the tepals of Asiatic hybrid lilies (*Lilium* spp.) and regulates pigment quantity. Mol. Breed. 30: 913–925.

Yamaguchi, M. A., N. Oshida, M. Nakayama, M. Koshioka, Y. Yamaguchi and I. Ino. 1999. Anthocyanidin 3-glucoside malonyltransferase from *Dahlia variabilis*. Phytochemistry 52: 15–18.

Yamasaki, H., H. Uefuji and Y. Sakihama. 1996. Bleaching of the red anthocyanin induced by superoxide radical. Arch. Biochem. Biophys. 332: 183–186.

Yoshida, K., T. Kondo, Y. Okazaki and K. Katou. 1995. Cause of blue petal colour. Nature 373: 291.

Zabala, G. and L. Vodkin. 2008. A putative autonomous 20.5 kb-CACTA transposon insertion in an *F3'H* allele identifies a new CACTA transposon subfamily in *Glycine max*. BMC Plant Biol. 8: 124.

Zhang, F., A. Gonzalez, M. Zhao, C. T. Payne and A. Lloyd. 2003. A network of redundant bHLH proteins functions in all TTG1-dependent pathways of *Arabidopsis*. Development 130: 4859–4869.

Zheng, D., G. Schröder, J. Schröder and G. Hrazdina. 2001. Molecular and biochemical characterization of three aromatic polyketide synthase genes from *Rubus idaeus*. Plant Mol. Biol. 46: 1–15.

Zhu, H. F., K. Fitzsimmons, A. Khandelwal and R. G. Kranz. 2009. CPC, a single-repeat R3 MYB, is a negative regulator of anthocyanin biosynthesis in *Arabidopsis*. Mol. Plant 2: 790–802.